Article

Current Biology

ISP1-Anchored Polarization of GCβ/CDC50A Complex Initiates Malaria Ookinete Gliding Motility

Graphical Abstract

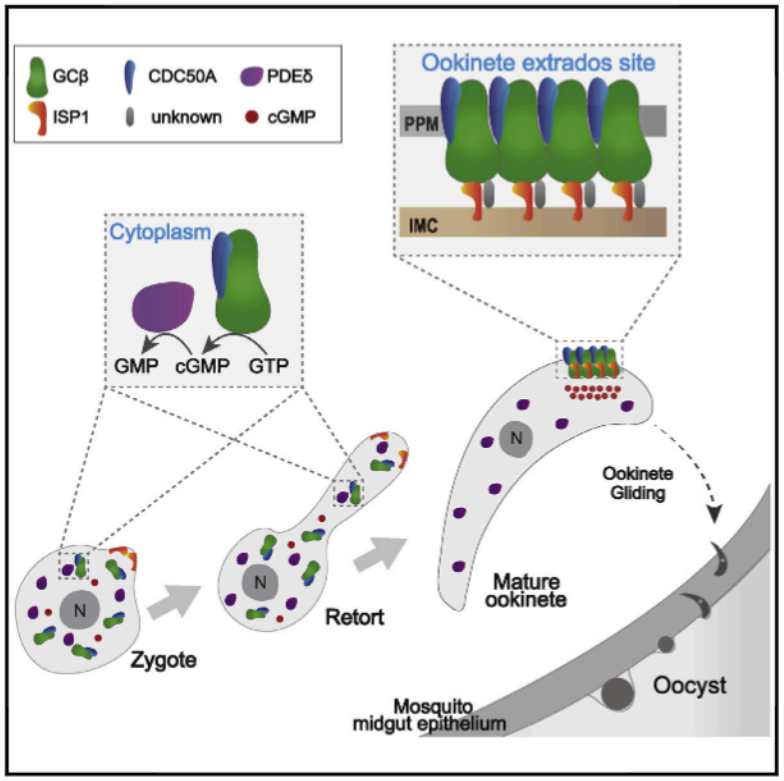

Authors

Han Gao, Zhenke Yang, Xu Wang, ..., Xin-zhuan Su, Huiting Cui, Jing Yuan

Correspondence

yuanjing@xmu.edu.cn

In Brief

The upstream mechanism of how the malaria parasites activate cGMP signaling for ookinete gliding remains unknown. Gao et al. reveal that *Plasmodium* GCβ polarization at "ookinete extrados site" in a precise spatial-temporal manner is the trigger for elevating cGMP level and activating PKG signaling for initiating ookinete gliding motility.

Highlights

- GCβ polarization coincides with gliding initiation of mature ookinete
- GCβ polarization elevates cGMP level and activates PKG signaling
- CDC50A binds to and stabilizes GCβ during ookinete development
- Polarization of GCβ/CDC50A complex is anchored by ISP1 at the IMC

Gao et al., 2018, Current Biology 28, 2763–2776
September 10, 2018
https://doi.org/10.1016/j.cub.2018.06.069

CellPress

Current Biology
Article

ISP1-Anchored Polarization of GCβ/CDC50A Complex Initiates Malaria Ookinete Gliding Motility

Han Gao,[1,3] Zhenke Yang,[1,3] Xu Wang,[1,3] Pengge Qian,[1] Renjie Hong,[1] Xin Chen,[1] Xin-zhuan Su,[2] Huiting Cui,[1] and Jing Yuan[1,4,*]

[1]State Key Laboratory of Cellular Stress Biology, Innovation Center for Cell Signal Network, School of Life Sciences, Xiamen University, Xiamen, Fujian 361102, China

[2]Laboratory of Malaria and Vector Research, National Institute of Allergy and Infectious Diseases, NIH, Bethesda, MD 20892, USA

[3]These authors contributed equally

[4]Lead Contact

*Correspondence: yuanjing@xmu.edu.cn

https://doi.org/10.1016/j.cub.2018.06.069

SUMMARY

Ookinete gliding motility is essential for penetration of the mosquito midgut wall and transmission of malaria parasites. Cyclic guanosine monophosphate (cGMP) signaling has been implicated in ookinete gliding. However, the upstream mechanism of how the parasites activate cGMP signaling and thus initiate ookinete gliding remains unknown. Using real-time imaging to visualize *Plasmodium yoelii* guanylate cyclase β (GCβ), we show that cytoplasmic GCβ translocates and polarizes to the parasite plasma membrane at "ookinete extrados site" (OES) during zygote-to-ookinete differentiation. The polarization of enzymatic active GCβ at OES initiates gliding of matured ookinete. Both the P4-ATPase-like domain and guanylate cyclase domain are required for GCβ polarization and ookinete gliding. CDC50A, a co-factor of P4-ATPase, binds to and stabilizes GCβ during ookinete development. Screening of inner membrane complex proteins identifies ISP1 as a key molecule that anchors GCβ/CDC50A complex at the OES of mature ookinetes. This study defines a spatial-temporal mechanism for the initiation of ookinete gliding, where GCβ polarization likely elevates local cGMP levels and activates cGMP-dependent protein kinase signaling.

INTRODUCTION

The spread of a malaria parasite relies on its successful development in a mosquito vector. Upon entering the mosquito midgut from a blood meal, gametocytes are activated to gametes that fertilize to form round-shaped immotile zygotes. Within 12–20 hr, the zygotes further differentiate into crescent-shaped motile ookinetes that penetrate the midgut epithelium and develop into oocysts, each containing hundreds of sporozoites. Mature sporozoites then invade the salivary glands and infect a new vertebrate host when the mosquito bites again [1]. Gliding motility of malaria parasites is essential for ookinete penetration of mosquito midgut wall and sporozoite migration to salivary gland for transmission from mosquito to vertebrate host. Ookinete gliding is achieved via a multiple-component protein complex called the glideosome located between parasite plasma membrane (PPM) and the underside of the inner membrane complex (IMC) [2, 3]. The IMC complex consists of flattened vesicles underlying the plasma membrane interconnected with the cytoskeleton and is known to play roles in motility and cytokinesis [2, 3]. A secreted transmembrane adhesion protein, CTRP, connected to actin, serves as an anchor for host cell ligand or extracellular matrix [4]. Mechanical force produced by the actomyosin motor is converted to backward movement of CTRP, generating forward gliding motility that acts as a driving force for invasion of host cells [5]. 3′–5′-cyclic guanosine monophosphate (cGMP), cGMP-dependent protein kinase G (PKG), phosphodiesterase delta (PDEδ), and guanylate cyclase beta (GCβ) have been shown to be crucial for ookinete motility in the rodent malaria parasite *Plasmodium berghei* [6–8]. Coordinated activities of GCβ (synthesizes cGMP) and PDEδ (hydrolyzes cGMP) regulate cGMP levels that activate PKG, leading to phospholipase C (PLC)/inositol triphosphate (IP_3)-mediated Ca^{2+} release, phosphorylation of multiple proteins in the glideosome, and initiation of ookinete gliding [7–9]. However, how the parasite initiates cGMP signaling upstream of PKG and regulates ookinete gliding remains unknown.

The *Plasmodium yoelii* parasite encodes two large guanylate cyclases (GCα, 3,850 amino acids [aas] and GCβ, 3,015 aas; Figure S1A) that contain 22 transmembrane (TM) helixes spanning an N-terminal P4-ATPase-like domain (ALD) and a C-terminal guanylate cyclase domain (GCD) [10–12]. The GC enzymes possessing this ALD/GCD structure are observed in many protozoan species (Figure S1B). Whereas the GCD is responsible for cGMP synthesis, the function of the ALD is still obscure [12].

In this study, we show that GCβ is expressed in ookinetes, and its polarization at the ookinete extrados site (OES) is essential for ookinete gliding. Both ALD and GCD are indispensable for GCβ polarization. We also identify a co-factor (CDC50A) that shows OES polarization and may function to stabilize GCβ during ookinete development and gliding. Screening of IMC-related proteins identifies another protein (IMC sub-compartment protein 1 [ISP1]) that anchors GCβ at the OES. This study defines a spatial-temporal mechanism for the initiation of ookinete gliding motility.

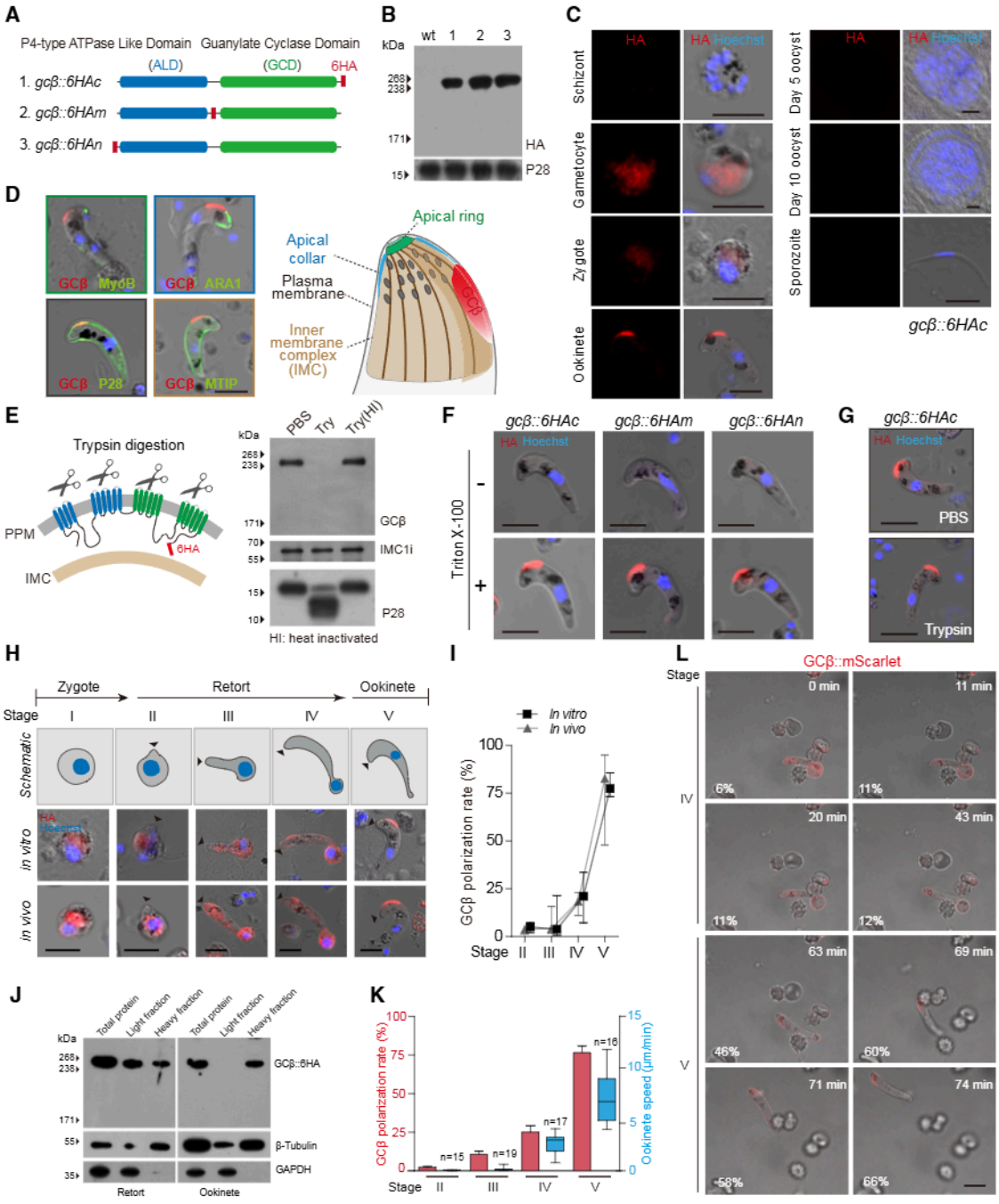

Figure 1. Dynamics of GCβ Polarization to a Unique OES and Initiation of Ookinete Gliding

(A) Diagrams of GCβ tagged with a sextuple HA epitope (6HA) (red) at three different locations. GCβ possesses a P4-type ATPase-like domain (ALD) (blue) and a guanylate cyclase domain (GCD) (green). The 6HA is inserted at the C terminus (*gcβ::6HAc*), between ALD and GCD (*gcβ::6HAm*), and at the N terminus (*gcβ::6HAn*), respectively.

(B) Western blotting of tagged GCβ protein in ookinetes. P28 protein as loading control is shown.

(C) IFA detection of GCβ during the life cycle of the *gcβ::6HAc* parasite. Nuclei are labeled with Hoechst 33342. The scale bars represent 5 μm.

(D) Co-localization of GCβ with proteins of known cellular localizations in ookinetes. ARA1 (apical collar), apical ring associated protein 1; MTIP (glideosome), myosin A tail domain interacting protein; MyoB (apical ring), myosin B; P28, ookinete plasma membrane protein. The scale bar represents 5 μm. The right panel shows the diagram of apical structure of *Plasmodium* ookinete.

(E) Western blotting of GCβ, P28, and IMC1i (inner membrane complex protein 1i) proteins of the *gcβ::6HA/imc1i::4Myc* ookinetes treated with PBS, trypsin (Try), or heat-inactivated (HI) trypsin. The left panel shows the predicted topology of GCβ.

(F) IFA of GCβ in ookinetes of three tagged parasite lines with or without Triton X-100 permeabilization. The scale bars represent 5 μm.

(G) IFA of GCβ protein in the ookinete treated with PBS or trypsin. The scale bars represent 5 μm.

(legend continued on next page)

RESULTS

GCβ Is Polarized at a Unique Extrados Site in Mature Ookinetes

To dissect the roles of GC proteins in ookinete gliding, we first investigated the expression of GCα and GCβ in ookinetes. We tagged both GCα and GCβ with a sextuple hemagglutinin (HA) epitope (6HA) (Data S1), using the Cas9 method described previously [13]. GCα was expressed in asexual blood stages and gametocytes, but not in ookinetes, and was not pursued further in this study (Figures S1C and S1D). We tagged GCβ with 6HA at the C or N terminus as well as at the region between the ALD and GCD domains (Figure 1A). Successful tagging was confirmed by both genotypic PCR (Data S1) and western blotting (Figure 1B). All of the *gcβ::6HA* parasites showed normal progression throughout the life cycle (Table S1). Immunofluorescence assay (IFA) indicated that GCβ protein was expressed in gametocytes, zygotes, and ookinetes and could not be detected in asexual blood stage parasites (Figure 1C). Interestingly, GCβ was localized in the cytoplasm of both gametocytes and zygotes but was concentrated at a site posterior to the apical structure in mature ookinetes (Figure 1D). Because of its unique location in ookinetes, we designate the specific location as OES.

To further investigate GCβ localization in ookinetes relative to proteins known to be expressed within specific organelles or locations, we engineered parasite clones with additional proteins tagged with quadruple Myc epitope (4Myc) from the *gcβ::6HAc* parasite (Data S1). These proteins included MTIP (glideosome) [14], IMC1i (IMC) [2], ARA1 (apical collar) [15], myosin B (apical ring) [16], and DHHC10 (crystalloid body) [17] (Figures S1E and S1F). GCβ was localized at the extrados area behind the apical collar defined by ARA1 (Figure 1D). Only P28 (plasma membrane) and MTIP showed overlapping localization with GCβ in mature ookinete (Figure 1D). Additionally, GCβ did not co-localize with proteins in cellular organelles, including endoplasmic reticulum (ER), Golgi apparatus, and apicoplast through double staining using antisera targeting BiP, ERD2, and ACP proteins, respectively (Figure S1G). These data show that GCβ is expressed in the cytoplasm of gametocytes and zygotes but is polarized at a unique position in mature ookinetes.

GCβ Is Expressed on the PPM of Mature Ookinete with N and C Termini Facing the IMC

The ALD and GCD domains, as well as the inter-domain linker, are predicted to be intracellular (Figure S1A). However, whether GCβ is localized at PPM or IMC remains to be determined. We treated the *gcβ::6HA/imc1i::4Myc* ookinetes with trypsin to digest the extracellular parts of GCβ if it was localized on the PPM surface. Western blotting analysis detected a protein band of ~240 kDa from PBS- or heat-inactivated trypsin-treated ookinetes, but not in trypsin-treated ookinetes, suggesting surface exposure (Figure 1E). As a control, we also detected digestion of the PPM protein P28, but not the IMC protein IMC1i (Figure 1E). These results indicate that GCβ is localized on the PPM. Additionally, all three 6HA-tagged GCβ could be detected using the anti-HA antibody only after Triton X-100 treatment (Figure 1F), which supports the predicted topology of GCβ (Figure 1E). Interestingly, trypsin treatment did not alter GCβ polarization (Figure 1G), suggesting the existence of other proteins or structures acting to stabilize GCβ at OES.

GCβ Polarization at OES Coincides with Initiation of Ookinete Gliding

The round-shaped immotile zygotes undergo significant morphological changes (stages I–V) to differentiate into crescent-shaped motile ookinetes (Figure 1H, upper panel). To investigate the GCβ's localization dynamics during ookinete maturation and its relationship with ookinete gliding, we analyzed GCβ expression from zygote to mature ookinete using *in-vitro*-cultured *gcβ::6HAc* parasites. GCβ was distributed in the cytoplasm and localized with BiP from zygote (stage I) to retort (stage III; Figure S1H), started to cluster at OES in stage IV retort, and completely polarized to OES of mature ookinetes (stages V; Figure 1H, middle panel). We also isolated parasites from infected mosquito midguts and observed a similar dynamic distribution of GCβ (Figure 1H, lower panel), confirming the *in vitro* observations. Indeed, the rates of GCβ polarization at OES were almost identical in ookinetes either from mosquitoes or *in vitro* cultures (Figure 1I). We next isolated the heavy (including plasma membrane and cytoskeleton) and light (including cytoplasm) fractions from extracts of retort and mature ookinetes after hypotonic lysis and showed that GCβ could be detected in both fractions of the retorts but only in heavy fraction of mature ookinetes (Figure 1J), supporting GCβ association with plasma membrane in mature ookinetes.

We next quantified GCβ polarization level by calculating fluorescent signals at OES over the whole cell at different stages of ookinete development (Figure S1I) and measured ookinete gliding using a Matrigel-based assay [7, 18]. We showed that ookinete gliding was highly correlated with GCβ polarization at OES (Figure 1K). No stage II and III retorts had gliding motility; stage IV retorts showed some motility (1–3 μm/min) and initial GCβ

(H) IFA showing GCβ localization during ookinete development *in vitro* and *in vivo*. (Upper panel) Diagrams depicting morphological changes from zygote (stage I) to crescent-shaped mature ookinete (stage V) are shown. IFA images of tagged-GCβ expression from *in-vitro*-cultured parasites (middle panel) or *in-vivo*-infected mosquito midgut (bottom panel) are shown. Black arrow indicates the apical of ookinetes. The scale bars represent 5 μm.

(I) Quantification of GCβ polarization level at the OES during ookinete development obtained from mosquitoes or *in vitro* culture as in (H). Polarization rates are means ± SEM of at least 30 ookinetes in each group.

(J) Western blotting of GCβ from the isolated cellular fractions (total protein, light fraction, and heavy fraction) of retorts and ookinetes.

(K) Relationship of GCβ polarization rate (red) at OES and gliding speed (blue) of ookinetes in different stages. Polarization rates are means ± SEM of at least 30 ookinetes. The range of whisker plots for ookinete gliding speeds indicates the 2.5 and 97.5 percentiles, the box includes 50% of all values, and the horizontal line shows median values obtained for the tested number (n) of ookinetes in each group.

(L) Real-time capturing of fluorescent signals with mScarlet-tagged GCβ in developing ookinete and initiation of gliding motility. Percentage number (lower left) is the GCβ polarization rate (signal at the OES over signal from the whole cell). Note, at 69 min or 60%, the parasite started moving as reference to the nearby cells. The scale bar represents 5 μm.

See also Figures S1 and S2, Tables S1 and S2, and Video S1.

polarization; and mature ookinetes (stage V) with clear GCβ polarization had acquired normal gliding (5–12 μm/min; Figure 1K).

To capture the dynamics of GCβ polarization and the timing of ookinete gliding initiation, we generated a parasite, *gcβ::mScarlet* (Data S1), with GCβ C-terminally tagged with mScarlet that had enhanced red fluorescence [19] and allowed tracking GCβ expression in real time. The mScarlet-tagged protein was expressed at OES of mature ookinetes (Figure S2A), and the tagging modification did not affect ookinete gliding (Figure S2B). Real-time tracking the GCβ::mScarlet signals of the developing retorts and ookinetes showed cytoplasmic distribution of GCβ in both the protrusion and the zygote remnant of an immotile stage IV retort (Figure 1L; Video S1). Strikingly, as soon as the majority (~60%) of the GCβ were polarized at OES of mature ookinete, the parasites started gliding (Figure 1L; Video S1), suggesting that accumulation of GCβ to a required level at the OES is the trigger for gliding. Additionally, GCβ polarization at OES was always present as long as an ookinete was moving spirally (Figures S2C and S2D). These observations directly link GCβ polarization at the OES to initiation of ookinete gliding.

Ookinete Gliding Depends on cGMP Synthesis Activity of GCβ Polarized at OES

We disrupted the *gcβ* gene in wild-type (WT) and the *gcβ::6HAc* parasites (Figures S3A–S3C). Parasites without GCβ could develop into ookinetes with normal morphology (Figure S3D) but lost gliding (Figure S3E), oocyst and sporozoite formation in the mosquito, and infectivity to mouse (Figures S3F and S3G). These results confirm that GCβ is essential for ookinete gliding and mosquito transmission, which is consistent with findings in *gcβ* disrupted *P. berghei* parasites [6, 8].

To test whether cGMP synthesis activity of polarized GCβ at OES is required for ookinete gliding, we generated GCβ mutant parasites that maintained GCβ OES polarization but lost the ability to synthesize cGMP. Sequences analysis reveal the conserved residues Asn-Thr-Ala-Ser-Arg (NTASR) in the α4 helix of catalytic domain 1 (C1) of GC, which are likely critical for the cyclase to bind its substrate guanosine triphosphate (GTP) [20], and mutations in these residues may reduce or abolish the cyclase activity (Figure S3H). Accordingly, we introduced mutations by replacing "NTASR" with "NKASR" or "AKASA" in the *gcβ::6HA* parasite, generating *GCDm1* and *GCDm2* parasites, respectively (Figure S3I). Both mutants showed normal GCβ polarization and expression levels similar to that of *gcβ::6HA* parasite (Figures 2A and 2B) but had severely impaired ookinete motility (Figure 2C), resembling the phenotype of *gcβ* disruption (Figure S3E). To further test whether the GC activity for cGMP synthesis results in a loss in ookinetes of these mutants, we utilized a recently developed probe (Green cGull) that emits EGFP fluorescence when binding to cGMP [21]. We episomally expressed a plasmid containing the gene encoding Green cGull protein and observed basal levels of fluorescent signal in the cytoplasm of WT, Δ*gcβ*, and *GCDm2* ookinetes when treated with DMSO (Figures 2D and 2E). The fluorescent signals in WT ookinetes significantly increased after a 20-min treatment with zaprinast, an inhibitor active against *Plasmodium* PDEs, which degrade cGMP [7], but not in Δ*gcβ* and *GCDm2* ookinetes (Figures 2D and 2E). These data not only demonstrate loss of cGMP synthesis activity in mature ookinetes of the Δ*gcβ* and *GCDm2* parasites but also show that ookinete gliding depends on the cGMP synthesis activity of GCβ enriched at the OES.

GCβ Polarization Elevates cGMP Levels and Activates PKG Signaling

cGMP signals in malaria parasites exert their function via directly binding and activating the master effector, PKG, and thus transducing signaling downstream [7, 22]. We tagged the endogenous PKG protein with 4Myc and found that PKG maintains evenly cytoplasmic distribution during zygote to ookinete development of both single-tagged *pkg::4myc* and double-tagged *gcβ::6HA/pkg::4myc* parasites (Figures 2F and S3J). To test whether PKG is required for GCβ polarization and ookinete gliding, we treated the *gcβ::6HA* ookinetes with a potent *Plasmodium* PKG inhibitor, compound 2 (C2) [7]. As expected, C2 treatment completely inhibited ookinete gliding (Figure 2G), confirming the essential role of PKG in ookinete gliding as previously reported in *P. berghei* [7]. However, C2 treatment had no influence on GCβ polarization in mature ookinetes (Figure 2H).

Balanced activities of GCβ and PDEδ are critical for maintaining appropriate cGMP concentration, and changes in protein expression or localization in one of them may affect cGMP levels and downstream PKG signaling. To investigate PDEδ expression and localization relative to GCβ, we tagged PDEδ with 4Myc to generate *pdeδ::4myc* parasite (Table S1) and observed the cytoplasmic distribution of PDEδ during the zygote to ookinete differentiation (Figure S3J). Furthermore, we generated a doubly tagged parasite, *gcβ::6HA/pdeδ::4myc*, by tagging the endogenous PDEδ with 4Myc in the *gcβ::6HAc* parasite (Data S1). At zygote and retort stages, both proteins were distributed at both zygote remnant and protrusion and mostly co-localized (Figure 2I). In mature ookinetes, PDEδ remained relatively evenly distributed throughout the cytoplasm, whereas GCβ polarized at the OES (Figure 3I). The re-distribution of these two proteins led to local enrichment of GCβ, with higher levels of GCβ over PDEδ at OES (Figure 2J), which could probably create an elevated cGMP level at the OES and drive PKG activation locally (Figure 2K).

Both ALD and GCD Domains Are Required for GCβ Polarization

To analyze the role of ALD in GCβ expression or localization, we generated a modified parasite, *gcβ::T2A*, by introducing the "ribosome skip" T2A peptide (EGRGSLLTCGDVEENPGP) into the middle linker region in the *gcβ::6HAc* parasite (Figure 3A). The T2A peptide allows expression of the ALD (residues 1–1,248) and GCD peptides (residues 1,249–3,015) separately. Western blotting detected a protein band (GCD::6HA) smaller than the full-length protein (Figure 3B), indicating separated ALD and GCD expression in the *gcβ::T2A* ookinetes. Notably, the GCD lost OES polarization with cytoplasmic distribution (Figures 3C and 3D). As expected, this parasite had severely impaired gliding (Figure 3E). As a control, we replaced a key proline at position 17 of the T2A peptide with arginine to abrogate its function (Figure 3A). The resulting *gcβ::T2Am* parasite expressed a full-length protein with a molecular weight comparable to that of GCβ::6HA protein (Figure 3B). The *gcβ::T2Am* ookinetes also maintained GCβ polarization (Figures 3C and 3D)

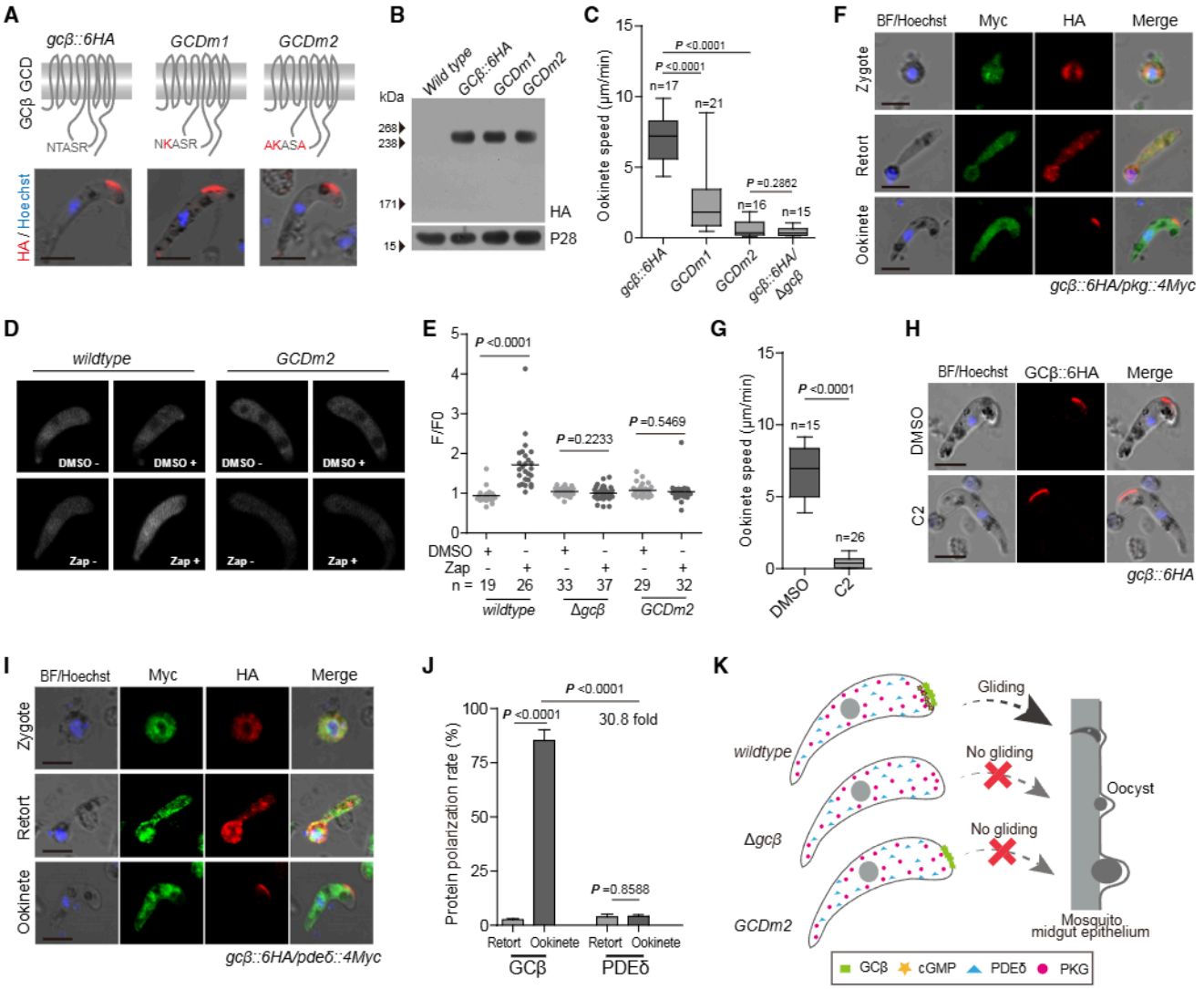

Figure 2. GCβ Polarization Elevates cGMP Levels and Activates PKG

(A) IFA analysis of GCβ in mature ookinetes of the *GCDm1* and *GCDm2* parasites. The upper panel shows the mutations (red) introduced in the GCD. The scale bars represent 5 μm.

(B) Western blotting of GCβ expression in ookinetes of the *GCDm1* and *GCDm2*.

(C) Gliding motility of the *GCDm1* and *GCDm2* ookinetes. n is the number of ookinetes tested in each group.

(D) Detection of endogenous cGMP in ookinetes of wild-type and *GCDm2* parasites expressing the Green cGull probe reporter. The fluorescent signals were microscopically monitored in ookinetes without treatment (−) or with DMSO or Zap treatment (+) for 20 min.

(E) Quantification of the fluorescent intensity change (F/F_0) in (D). n is the number of ookinetes tested in each group. The horizontal line shows the mean values.

(F) Two-colored IFA analysis of GCβ and PKG proteins during ookinete development of the *gcβ::6HA/pkg::4Myc* parasite. The scale bars represent 5 μm.

(G) Ookinete gliding motility of wild-type parasites treated with DMSO or a potent *Plasmodium* PKG inhibitor, compound 2 (C2).

(H) IFA analysis of GCβ proteins in mature ookinete of the *gcβ::6HA* parasites treated with DMSO or C2. The scale bars represent 5 μm.

(I) Two-colored IFA analysis of GCβ and PDEδ proteins during ookinete development of the *gcβ::6HA/pdeδ::4Myc* parasite. The scale bars represent 5 μm.

(J) Protein polarization rate of GCβ and PDEδ at OES of retort and ookinete in (I).

(K) A proposed model of GCβ polarization at OES and initiation of cGMP and PKG-dependent ookinete gliding. In mature ookinetes, GCβ polarizes at OES, and PDEδ remains in the cytoplasm, which breaks cGMP synthesis-hydrolysis balance and increases cGMP levels, activates PKG, and initiates ookinete gliding.

See also Figure S3 and Tables S1 and S2.

and normal gliding (Figure 3E). To further confirm the T2A-mediated separation of ALD and GCD, we generated another parasite *gcβ::T2An* (Figure S4A), in which ALD and GCD were tagged with the triple V5 epitope (3V5) and 6HA, respectively. Separate expression of ALD and GCD was confirmed on western blot using anti-V5 and anti-HA antibodies, respectively (Figure S4B). IFA analysis revealed cytoplasmic distribution for both ALD and GCD with little co-localization (Figure S4C). Like *gcβ::T2A*, this *gcβ::T2An* also displayed a defect in ookinete gliding (Figure S4D). Together, these results show that expression of both ALD and GCD together in a single protein is required for GCβ polarization and ookinete gliding.

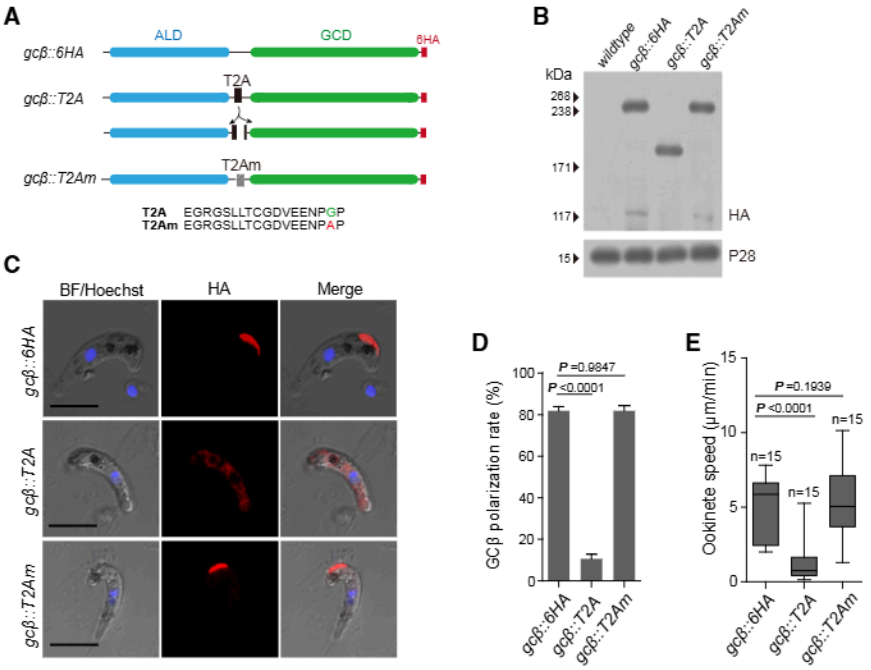

Figure 3. Expression of ALD and GCD in a Single Peptide Is Required for GCβ Polarization and Ookinete Gliding

(A) Diagrams of the endogenous GCβ protein modification. The viral "ribosome skip" T2A peptide was inserted into the region between the ALD and GCD domains in the *gcβ::T2A* parasite, leading to expression of the two domains separately. In the *gcβ::T2Am* parasite, replacing a proline with arginine in the T2A abrogated the peptide function, resulting in expression of both ALD and GCD in one peptide.

(B) Western blotting of GCβ protein using anti-HA antibody in the modified strains.

(C) IFA analysis of labeled GCβ proteins in ookinetes of modified strains. The scale bars represent 5 μm.

(D) Quantification of GCβ polarization rate at OES of the ookinetes in (C).

(E) Gliding motility of ookinetes from different modified strains.

See also Figure S4 and Tables S1 and S2.

P4-ATPase Co-factor CDC50A Co-localizes and Interacts with GCβ

The ALD of GCβ is structurally related to the P4-ATPase proteins, which function as flippase translocating phospholipids, such as phosphatidylserine (PS) from exofacial to cytofacial leaflets of membranes in eukaryotic cells [23, 24]. However, sequence analysis revealed that ALD contains mutations in several conserved functional motifs (Figure S4E), including the critical DKTGT motif, suggesting a pseudo P4-ATPase. To investigate whether PS is enriched at OES and thus mediates GCβ polarization, we stained the living WT ookinetes with the annexin V-fluorescein isothiocyanate (FITC) probe and detected no enrichment of PS molecule at either exofacial or cytofacial leaflets of plasma membranes at the OES (Figures S4F–S4H). In addition, saponin treatment, which is expected to impair the PS-lipid component in the membrane via depleting cholesterol [25], did not affect GCβ polarization (Figure S4I). These data suggest that PS-lipid is unlikely the mediator for GCβ polarization.

P4-ATPase interacts with the co-factor protein, CDC50, which is required for trafficking of the complex from ER to plasma membrane and for flippase activity [26] (Figure 4A). A search of the *Plasmodium* genomes identified three paralogs of *cdc50* genes: *cdc50a* (PY17X_0619700); *cdc50b* (PY17X_0916600); and *cdc50c* (PY17X_0514500; Figure S5A). To determine which CDC50 associates with GCβ, we generated parasites with individual CDC50 protein tagged with 6HA: *cdc50a::6HA*; *cdc50b::6HA*; and *cdc50c::6HA* (Figure 4B). Of the three proteins, only CDC50A has polarization at OES similar to GCβ in mature ookinetes (Figure 4B). Notably, CDC50A is exclusively expressed in gametocytes, zygotes, and ookinetes during the parasite life cycle (Figures S5B and S5C) and, similar to GCβ, polarized at OES during zygote to ookinete development (Figure S5D). These observations were reproduced in another independent mScarlet-tagged parasite, *50a::mScarlet* (Figure S5E). Next, we generated two doubly tagged parasites, *gcβ::6HA/50a::mCherry* and *gcβ::6HA/50a::3V5*, from the *gcβ::6HA* parasite (Table S1). Results from these parasites show that GCβ and CDC50A were completely co-localized at the cytoplasm of female gametocytes, zygotes, and retorts and at ookinete OES (Figures 4C and 4D). Furthermore, results from immunoprecipitation using anti-HA antibody indicate that GCβ binds to CDC50A in ookinetes lysate of the *gcβ::6HA/cdc50a::mCherry* parasite (Figure 4E). These data demonstrate that CDC50A co-localizes and binds to GCβ during ookinete development.

Deletion of CDC50A Phenocopies GCβ Deficiency in Ookinete Gliding

We next genetically disrupted the *cdc50a* gene and showed that, similar to *gcβ* disruption, Δ*cdc50a* parasites displayed normal asexual blood stage growth, gametocyte formation, and ookinete differentiation (Figures S6A–S6D) but had severe defect in ookinete gliding (Figure 4F). Parasites with gliding defect cannot penetrate the mosquito midgut and produce no oocysts; indeed, no midgut oocyst (day 7) or salivary gland sporozoite (day 14) was detected in the mosquitoes infected with Δ*gcβ* or Δ*cdc50a* parasites (Figures 4G and 4H). To further confirm the phenotype, we deleted *gcβ* or *cdc50a* gene in a parasite strain expressing mCherry-labeled P28, 17XNL/P28mCh [27], to investigate early oocyst development (Table S1). Again, these mutant parasites lost ookinete gliding (Figure S6E) and produced no oocyst in mosquitoes (Figure S6F). In mosquitoes infected with these parasites, no early midgut parasites were observed at as early as 36 hr post-blood feeding (Figure S6G). To rule out that the phenotype defects were caused by Cas9 off-target effects, we re-introduced a *cdc50a* gene with sequence encoding an N-terminal Flag tag back to the endogenous *cdc50a* locus in the Δ*cdc50a* parasite (Data S1). This complemented parasite (Δ*50a/50a*) showed proper CDC50A protein expression driven

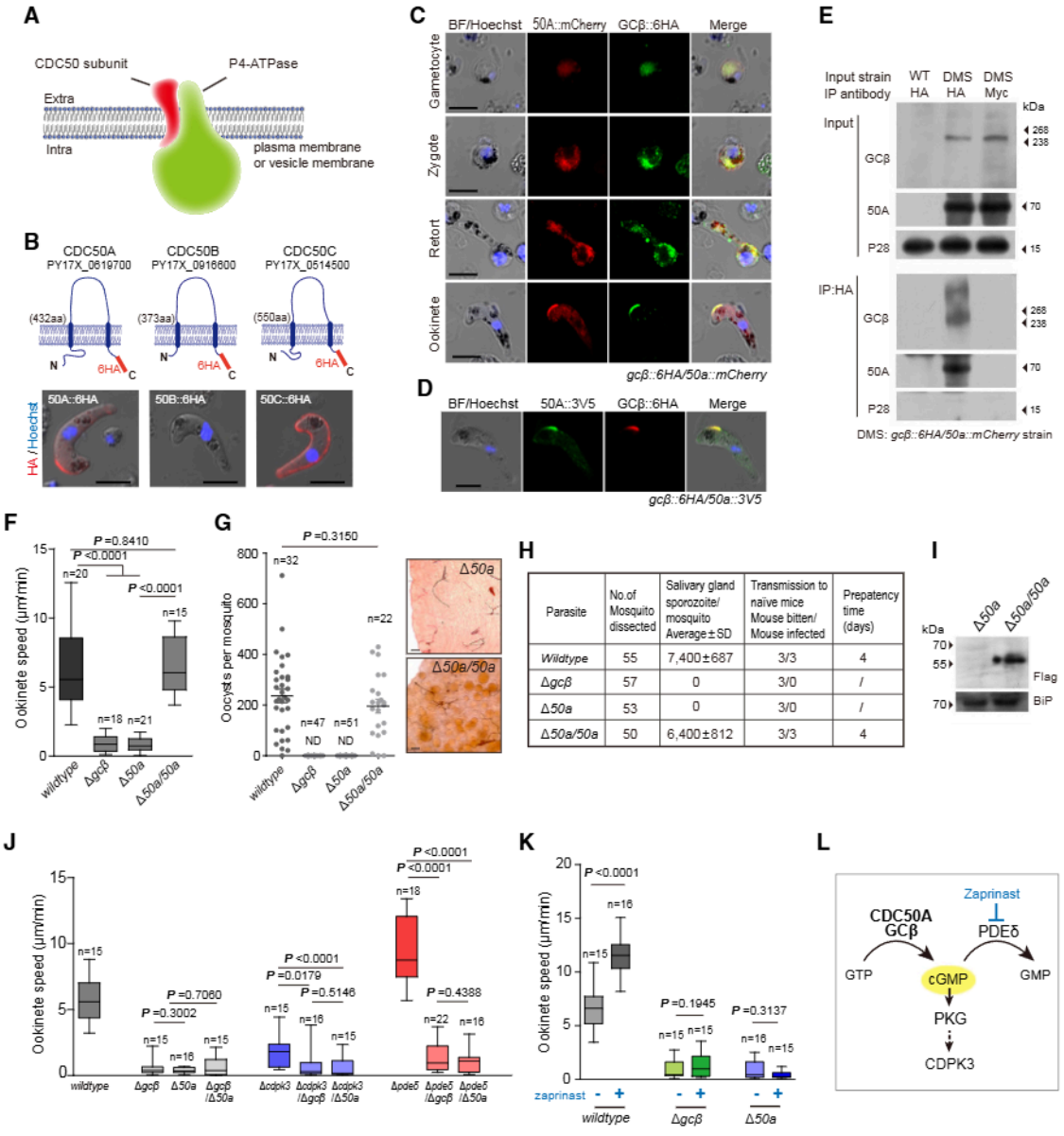

Parasite	No.of Mosquito dissected	Salivary gland sporozoite/ mosquito Average±SD	Transmission to naïve mice Mouse bitten/ Mouse infected	Prepatency time (days)
Wildtype	55	7,400±687	3/3	4
Δgcβ	57	0	3/0	/
Δ50a	53	0	3/0	/
Δ50a/50a	50	6,400±812	3/3	4

Figure 4. CDC50A Mimics GCβ Function in Ookinete Gliding

(A) Diagram of P4-ATPase (green) and CDC50 (red) protein complex in eukaryotes.

(B) Topology and IFA analysis of three CDC50 proteins in ookinetes of *P. yoelii*: CDC50A (50A); CDC50B (50B); and CDC50C (50C). These endogenous proteins were tagged with a 6HA tag (red rectangle) C-terminally. The scale bars represent 5 μm.

(C) Two-colored IFA analysis of CDC50A and GCβ proteins during gametocyte to ookinete development of the double-tagged *gcβ::6HA/cdc50a::mCherry* parasite using anti-HA and anti-mCherry antibodies. The scale bars represent 5 μm.

(D) Two-colored IFA analysis of CDC50A and GCβ proteins in ookinete of the double-tagged *gcβ::6HA/cdc50a::3V5* parasite. The scale bar represents 5 μm.

(E) Co-immunoprecipitation assay of GCβ and CDC50A proteins in ookinetes of the *gcβ::6HA/cdc50a::mCherry* strain (double modified strain [DMS]).

(F) Ookinete gliding motility of the wild-type, Δ*gcβ*, Δ*50a*, and the complemented Δ*50a/50a* parasites.

(G) Number of oocysts in mosquito midgut 8 days post-blood feeding. n is the number of mosquitoes tested in each group. The horizontal line shows the mean value of each group. Right panel shows the dissected mosquito midguts stained with 0.5% mercurochrome. The scale bars represent 50 μm.

(H) Formation and infectivity to mouse of salivary gland sporozoites in the mosquitoes 14 days post-blood feeding. In each group, ten mosquitoes were fed on one mouse and the prepatent time was measured.

(I) Western blot of the Flag-tagged CDC50A expression in ookinetes of the complemented Δ*50a/50a* parasite.

(J) Ookinete gliding motility of the parasites with various combinations of double deletions of *gcβ*, *50a*, *pdeδ*, and *cdpk3* genes.

(K) Ookinete gliding motility of the parasites with or without the *Plasmodium* PDE inhibitor zaprinast (Zap) (100 μM) treatment.

(L) A proposed model depicting positions of GCβ and CDC50A in cGMP signaling for ookinete gliding.

See also Figures S5 and S6 and Tables S1 and S2.

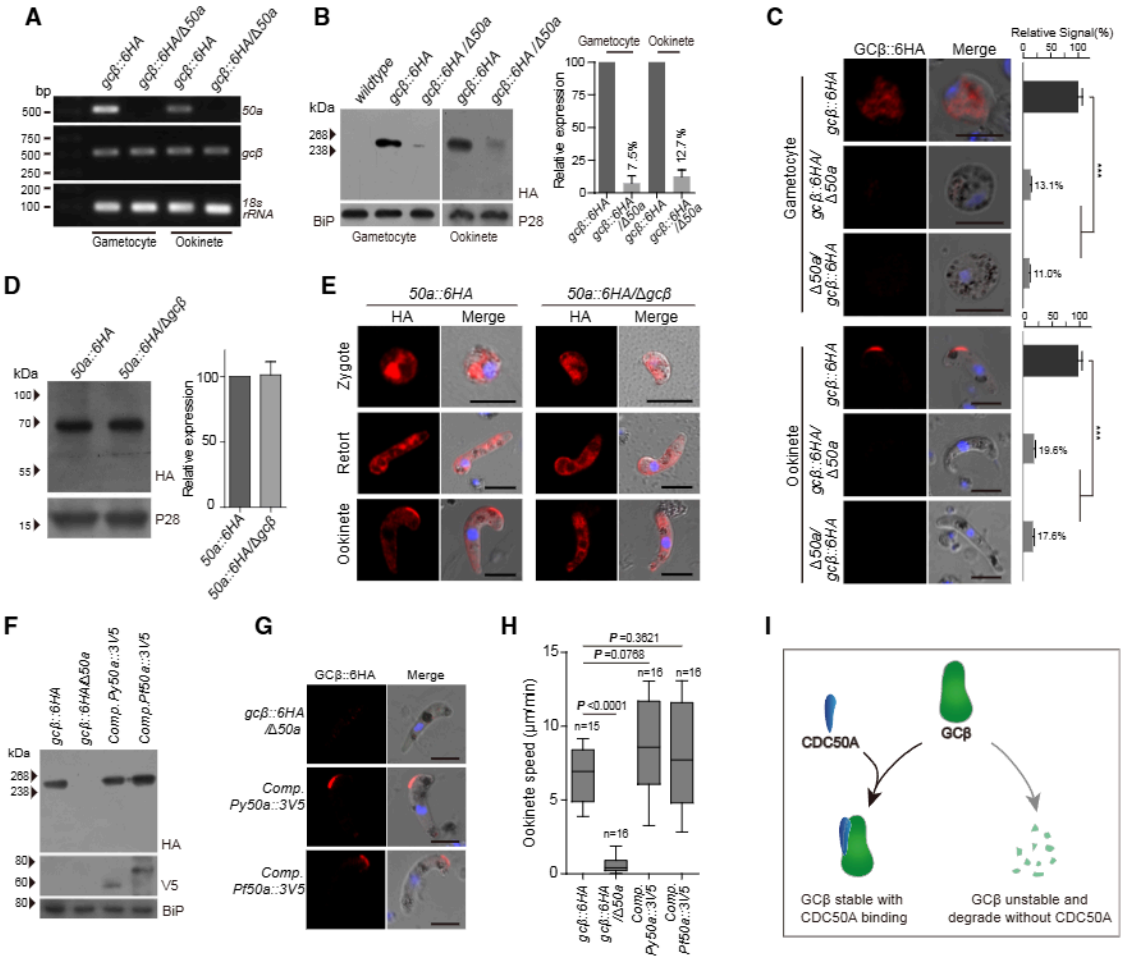

Figure 5. CDC50A Stabilizes GCβ during Sexual Development

(A) RT-PCR analysis of *gcβ* and *50a* transcripts in gametocytes and ookinetes of the *gcβ::6HA* and *gcβ::6HA/Δ50a* parasites. *18 s rRNA* gene as control is shown.

(B) Western blot of GCβ expression in gametocytes and ookinetes of the *gcβ::6HA* and *gcβ::6HA/Δ50a* parasites. The right panel is the quantifications of GCβ band intensity in the blot from three independent experiments.

(C) IFA analysis of GCβ protein in gametocyte (left) and ookinete (right) of the *gcβ::6HA* and *50a*-deleted parasites. Two independent modified strains, *gcβ::6HA/Δ50a* and *Δ50a/gcβ::6HA*, were tested. The right panel is quantifications of the fluorescent signal of GCβ.

(D) Western blot of 50A expression in the *50a::6HA* and *50a::6HA/Δgcβ* parasites. Right panel is the quantification of the results from three independent experiments.

(E) IFA of 50A protein during *in vitro* ookinete development of *50a::6HA* and *50a::6HA/Δgcβ* parasites.

(F) Western blot of GCβ and 50A proteins in ookinete of the *gcβ::6HA/Δ50a* parasite complemented with 3V5-tagged *50a* gene from either *P. yoelii* or *P. falciparum*.

(G) IFA analysis of GCβ proteins in ookinete of complemented parasites.

(H) Ookinete gliding motility of the complemented parasites.

(I) A proposed model of CDC50A binding and stabilizing GCβ.

In (C), (E), and (G), scale bars represent 5 μm. See also Tables S1 and S2.

by the endogenous promoter (Figure 4I) and displayed normal ookinete gliding (Figure 4F), oocyst counts (Figure 4G), and infectivity of mice (Figure 4H). Together, these results confirm that loss of the CDC50A protein causes ookinete gliding defect and mosquito transmission blocking.

Four genes (*gcβ*, *cdc50a*, *pdeδ*, and *cdpk3*) have been shown to affect ookinete gliding. To further investigate the functional relationships of these genes, we generated double knockout (DKO) parasites of *gcβ/50a*, *gcβ/cdpk3*, *50a/cdpk3*, *gcβ/pdeδ*, and *50a/pdeδ* (Table S1) and compared the effects of these DKOs on ookinete motility with single-gene deletion. The *gcβ/50a* DKO displayed the similar level of gliding defect with single gene deletion (Figure 4J). Both *gcβ/cdpk3* and *50a/cdpk3* DKO showed slight reductions in gliding than the Δ*cdpk3* (Figure 5J). The Δ*pdeδ* had higher gliding than that of WT, probably due to increased motility with elevated cGMP level; however, DKO parasites (*gcβ/pdeδ* and *50a/pdeδ*) almost completely abolished ookinete gliding (Figure 4J), suggesting that GCβ and CDC50A may function similarly in the signaling upstream of cGMP (without cGMP synthesis, there will be no cGMP for hydrolysis).

Consistent with these observations, zaprinast (Zap) treatment boosted gliding of WT ookinetes, but not with either *Δgcβ* or *Δcdc50a* parasite (Figure 4K). Together, these results show that CDC50A serves as a GCβ co-factor, having a similar expression pattern and deletion phenotype to those of GCβ, to regulate cGMP levels in ookinete gliding (Figure 4L).

CDC50A Stabilizes GCβ during Ookinete Development

To investigate how CDC50A regulates GCβ, we deleted the *cdc50a* gene in the *gcβ::6HA* parasite and generated the *gcβ::6HA/Δ50a* parasite (Data S1). CDC50A depletion did not affect *gcβ* mRNA levels in either gametocytes or ookinetes (Figure 5A), ruling out an effect of CDC50A on *gcβ* transcription. However, an approximately 90% reduction in GCβ protein abundance was observed in both gametocytes and ookinetes of the *gcβ::6HA/Δ50a*, compared to the parental line in both IFA and western blotting analyses (Figures 5B and 5C). As expected, no OES polarization of GCβ occurred in these parasites (Figure 5C). In addition, we generated another parasite, *Δ50a/gcβ::6HA*, by tagging GCβ in the *Δcdc50a* parasite (Data S1) and observed the same results (Figure 5C). In contrast, deleting *gcβ* had no impact on CDC50A protein abundance in gametocytes or ookinetes of the *50a::6HA/Δgcβ* line (Figure 5D). Interestingly, CDC50A protein alone did not polarize at OES in the *50a::6HA/Δgcβ* ookinete (Figure 5E). These data indicate that CDC50A stabilizes GCβ during gametocyte-zygote-ookinete development, which may explain the similar phenotypic defects in *Δgcβ* and *Δcdc50a* parasites but does not carry the signal for directing the protein complex to the OES. Instead, the polarization signal is likely within GCβ as shown above.

CDC50A amino acid sequences display high homology (75% identity) between *P. yoelii* and human malaria parasite *P. falciparum*, suggesting conserved functions. To test this, we complemented the *gcβ::6HA/Δ50a* parasite with the *cdc50a* gene from the *P. falciparum* (*Pfcdc50a*) or *P. yoelii* (*Pycdc50a* as control) by episomal expression of the *Pfcdc50a* or *Pycdc50a*. CDC50A protein expression was detected in ookinetes of the parasites complemented with either *Pfcdc50a* or *Pycdc50a* C-terminally tagged with 3V5 (Figure 5F). Importantly, both proteins successfully restored GCβ expression and polarization in ookinetes (Figures 5F and 5G) and ookinete gliding comparable to that of WT parasite (Figure 5H). Together, these data show that CDC50A may stabilize GCβ protein or play a role in the translation of GCβ mRNA during sexual development and its functions are evolutionarily conserved between *P. yoelii* and *P. falciparum* (Figure 5I).

ISP1 Polarizes and Interacts with GCβ at OES of Mature Ookinete

GCβ is likely anchored by the molecules at the IMC of mature ookinetes because (1) GCβ polarizes at a curved region of the ookinete (Figure 1D) that is mostly maintained by the IMC [28, 29] and (2) PPM-residing GCβ remains polarized at OES even after trypsin digestion (Figure 1G). Therefore, we searched putative IMC proteins expressed in ookinetes identified previously [30] and selected 10 genes for protein localization analyses by tagging the protein with 6HA or 4Myc (Figure S7A). Out of 10 proteins, only the ISP1 displayed OES polarization as well as some distribution along the cell periphery in the *isp1::6HA* ookinete (Figure 6A). We observed the same location of ISP1 in the ookinetes of another tagged parasite—*isp1::3V5* (Figure S7B). ISP3, another member of the ISP proteins, distributes along the periphery of ookinete (Figure 6A).

We generated doubly tagged *gcβ::6HA/isp1::3V5* parasites by tagging endogenous *isp1* with 3V5 in the *gcβ::6HA* parasite to investigate GCβ and ISP1 expression in the same parasite (Figure 6B; Table S1). ISP1 was expressed and polarized as an elongated dot in early zygotes, became two branches lining the future apical in the retort, and polarized at the OES in mature ookinete (Figure 6B), which is consistent with the observations in *P. berghei* [31]. Using stochastic optical reconstruction microscopy (STORM), we overlaid GCβ and ISP1 signals at OES and observed overlapping signals at the middle (Figure 6C). Furthermore, we detected the interaction between GCβ and ISP1 in ookinete lysates of the *gcβ::6HA/isp1::3V5* parasite using immunoprecipitation (Figure 6D), indicating that GCβ and ISP1 interact with each other.

GCβ Polarization Is Maintained by ISP1 at the IMC

ISP1 was reported as an essential gene refractory to deletion in *P. berghei* asexual blood stages [31]. However, we were able to disrupt the *isp1* gene in *P. yoelii* 17XNL using the Cas9 method and obtained three mutant clones from two independent transfections (Data S1). *Δisp1* parasites showed normal asexual blood stages and gametocyte development in mouse, male gametocyte activation, and mature ookinetes with normal morphology (Figures S7C–S7F). However, *isp1* disruption caused a slight decrease in conversion rate to mature ookinete (25% in *Δisp1*; 51% in WT; Figure S7G). Importantly, the *Δisp1* ookinetes with normal morphology showed significantly reduced ookinete gliding (Figure 7A) and oocyst counts in mosquito (Figure 7B).

ISP1 may play a role in anchoring GCβ at the OES. To test this, we deleted the *isp1* gene in the *gcβ::6HA* parasite generating the *gcβ::6HA/Δisp1* parasite (Data S1). ISP1 depletion did not affect GCβ protein abundance (Figure S7H) but disrupted GCβ polarization in ~93% of the ookinetes (Figures 7C and 7D); GCβ appeared to be randomly distributed in cytoplasm, at cell periphery, or at the apical region (Figure 7C). Indeed, *gcβ::6HA/Δisp1* ookinetes also displayed a severe defect in gliding compared with those of parental *gcβ::6HA* (Figure 7E). To further confirm the defect, we performed complementation to rescue the defect of the *gcβ::6HA/Δisp1* parasite by episomal expression of the 3V5-tagged PyISP1 (from *P. yoelii*) and PfISP1 (from *P. falciparum*; Data S1). Both tagged PyISP1 and PfISP1 protein expression were detected in ookinetes of the complemented parasites (Figure 7F), and these complementations successfully restored GCβ polarization (Figures 7D, 7G, and 7H) and ookinete gliding to the *gcβ::6HA/Δisp1* ookinetes (Figure 7E), consistent with the high homology (90% identity) in ISP1 protein sequence between *P. falciparum* and *P. yoelii* (Figure S7I). In contrast, GCβ depletion in the *isp1::3V5* parasite had no impact on the ISP1 dynamic localization and final OES polarization during ookinete differentiation (Figure 7I), suggesting that ISP1 itself contains a GCβ-independent signal for OES polarization at mature ookinete.

The ISP1 protein bears two N-terminal cysteine residues for palmitoyl-transferase-mediated palmitoylation modification

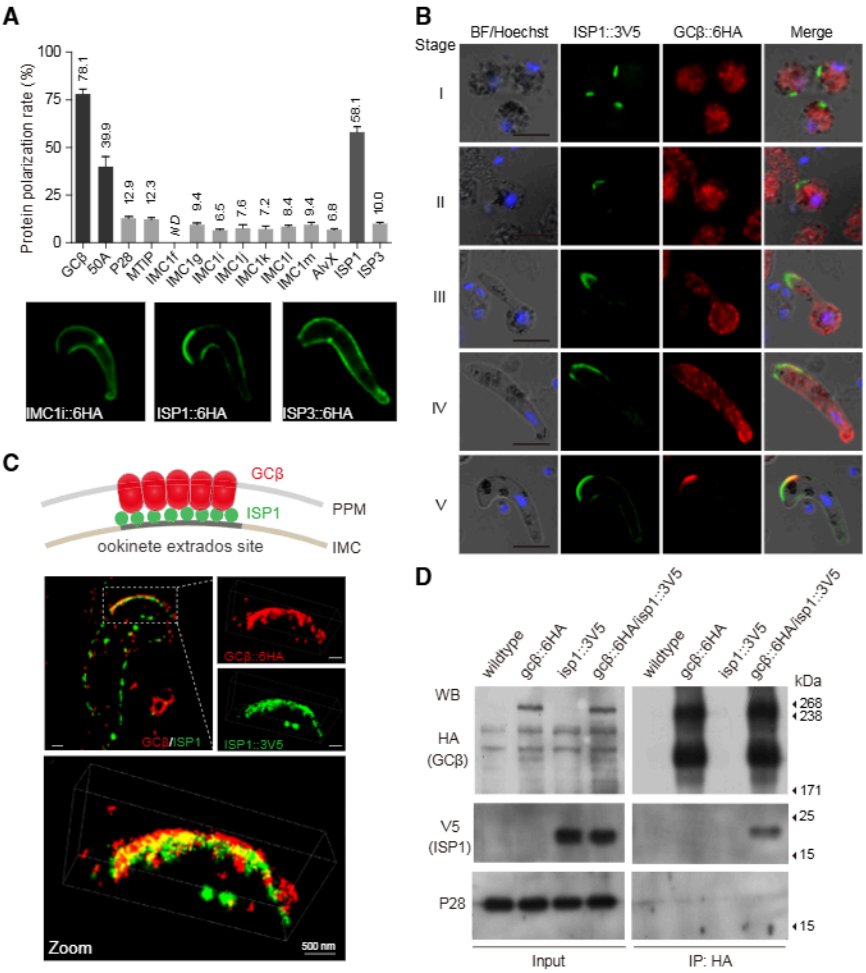

Figure 6. ISP1 Polarizes and Interacts with GCβ at OES of Mature Ookinete

(A) Protein polarization levels at OES based on IFA signals for IMC-related proteins in mature ookinetes. The localization of the tested proteins is indicated in Figure S7A. Polarization rates are means ± SEM of at least 30 cells and indicated at the top of each column. Lower panel is the IFA images of three selected proteins: IMC1i and IMC sub-compartment proteins 1 and 3 (ISP1 and ISP3, respectively).

(B) IFA analysis of ISP1 and GCβ proteins from zygote to ookinete development in the parasite *gcβ::6HA/isp1::3V5*. The scale bars represent 5 μm.

(C) Stochastic optical reconstruction microscopy (STORM) imaging of GCβ and ISP1 proteins in mature ookinete. The scale bars represent 0.5 μm.

(D) Co-immunoprecipitation assay of GCβ and ISP1 proteins in ookinetes of the *gcβ::6HA/isp1::3V5* parasite.

See also Figure S7 and Tables S1 and S2.

By real-time capturing mScarlet-tagged GCβ signals, we clearly showed that ookinetes start to move only when the majority (>60%) of GCβ is clustered at the OES (Figure 1L), providing a mechanism for the initiation of ookinete gliding motility. In addition, we demonstrated that CDC50A, an essential component of P4-ATPase trafficking and activity in other organisms [26], plays an important role in GCβ protein expression and ISP1, an IMC protein, contributes to anchoring GCβ at OES of mature ookinetes.

(Figure S7I), which is critical for its docking to the IMC [32]. We attempted to complement the *gcβ::6HA/Δisp1* parasite by episomal expression of the 3V5-tagged ISP1-bearing C7A/C8A mutations (cysteine changed to alanine in both amino acid 7 and 8 positions). The ISP1$^{C7A/C8A}$::3V5 protein lost palmitoylation modification compared with ISP1^{WT}::3V5 protein (Figure 7J). Consistently, ISP1$^{C7A/C8A}$::3V5 localized evenly at cytoplasm instead of polarizing at OES (Figure 7K) and failed to rescue the GCβ polarization in the ookinetes of complemented *gcβ::6HA/Δisp1* parasite (Figure 7L). Furthermore, treating the developing ookinete of the *gcβ::6HA/isp1::3V5* parasite with 2-BMP, a potent inhibitor of protein palmitoylation [33], impaired ookinete differentiation and maturation (Figure S7J) as well as OES localization of both ISP1 and GCβ in ookinetes with abnormal morphology (Figure S7K). Again, these abnormal ookinetes displayed no gliding (Figure S7L). Together, these data indicate that ISP1, with signal for tracking to OES and residing at the IMC, could anchor GCβ at the OES of mature ookinetes (Figure 7M).

DISCUSSION

Using *P. yoelii* as a model, here, we show that GCβ polarization at the ookinete OES is essential for the initiation of ookinete gliding.

Why does the GCβ polarization occur only after ookinete maturation? A previous study showed that PDEδ deletion led to a defect in ookinete development and gliding, which could be rescued by additional GCβ disruption or PKG inhibition in *P. berghei* [8]. Premature activation of cGMP and PKG signal caused by PDEδ disruption before ookinete maturation could interfere with the programmed development of ookinetes. These observations not only suggest both GCβ and PDEδ are constitutively active for synthesizing and hydrolyzing cGMP, respectively, during the ookinete development but also suggest that strictly spatial-temporal regulation of cGMP and PKG signaling is required for coordinating ookinete development and gliding. Consistent with this speculation, our results showed that both GCβ and PDEδ were distributed in cytoplasmic membrane structures (mostly ER) and largely co-localized in zygotes and retorts, which likely allow maintenance of a balanced and low level of cGMP throughout the cytoplasm, assuming that all the enzymes are constitutively active. In mature ookinetes, GCβ is polarized at OES but PDEδ remains cytoplasmic. GCβ polarization generates a higher protein ratio of GCβ over PDEδ at OES and likely a higher rate of cGMP synthesis than hydrolysis locally. This locally elevated cGMP may activate the PKG signaling and then initiate the ookinete gliding. The sequential events in this process are supported by direct observations of GCβ polarization at OES

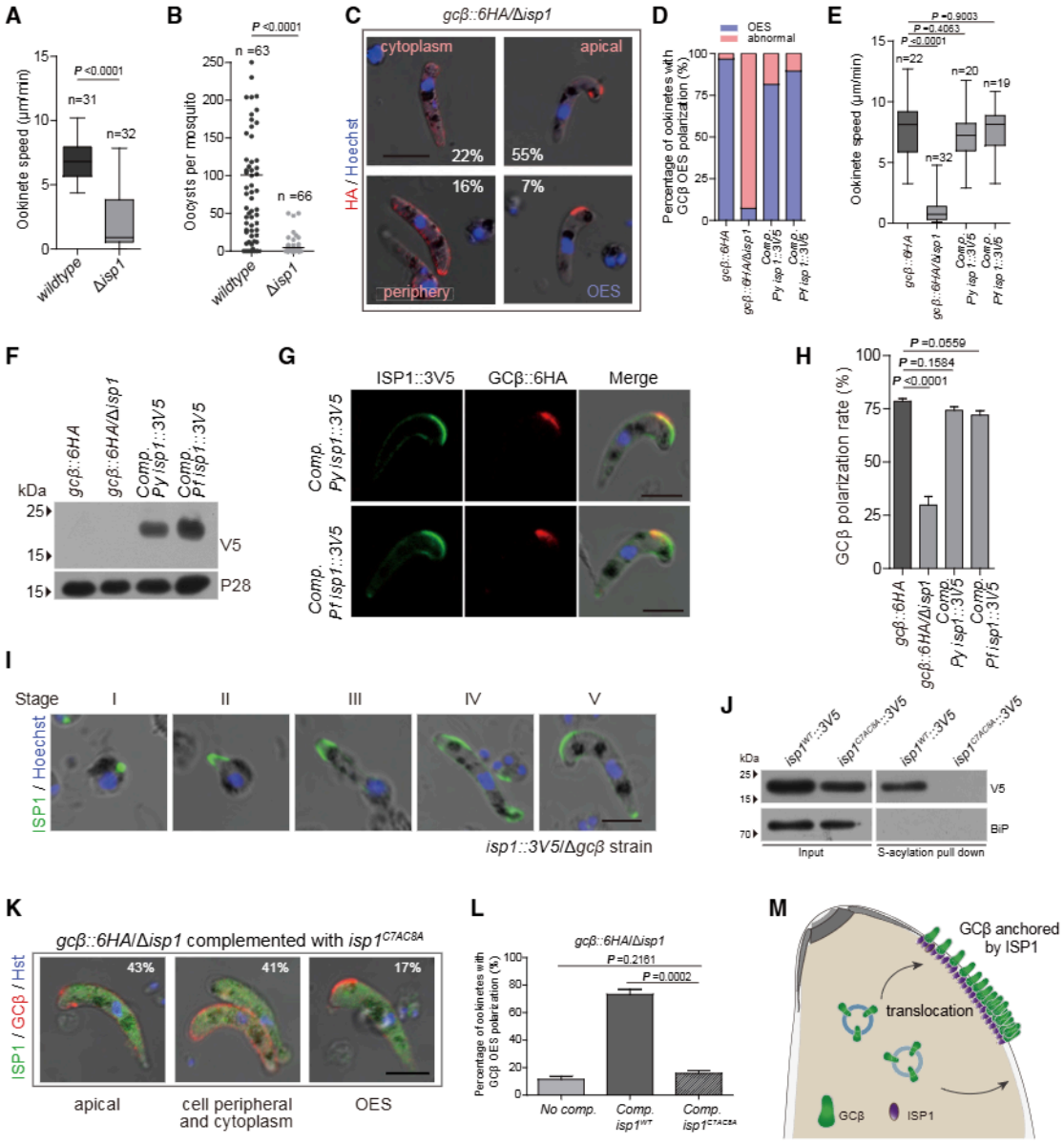

Figure 7. GCβ Polarization Is Maintained by ISP1 at the IMC

(A) Ookinete gliding motility of wild-type and Δ*isp1* parasites.

(B) Number of oocysts in the mosquito midguts 7 days post-blood feeding.

(C) IFA analysis of GCβ localization in ookinetes of the *gcβ::6HA/Δisp1* parasite. The scale bar represents 5 μm.

(D) Percentage of ookinete types showing different localization of GCβ in (C). More than 100 ookinetes were analyzed in each group from three independent tests.

(E) Ookinete gliding motility of *gcβ::6HA*, *gcβ::6HA/Δisp1*, and the complemented parasites: *Pyisp1::3V5* (*P. yoelii isp1*) and *Pfisp1::3V5* (*P. falciparum isp1*).

(F) Western blot detecting the 3V5-tagged PyISP1 or PfISP1 proteins expression in the complemented parasites.

(G) IFA analysis of GCβ and ISP1 proteins in ookinetes of the complemented parasites. The scale bars represent 5 μm.

(H) Quantification of GCβ polarization rate at OES of ookinetes in (G).

(I) IFA analysis of ISP1 protein from zygote to ookinete development of the *isp1::3V5/Δgcβ* parasites. The scale bar represents 5 μm.

(J) Western blot detection of expression and palmitoylation of ISP1 in the *gcβ::6HA/Δisp1* parasite complemented with the 3V5-tagged wild-type ISP1 ($ISP1^{WT}$::3V5) or ISP1 bearing C7A/C8A mutations ($ISP1^{C7A/C8A}$::3V5). BiP as the loading control is shown.

(K) Two-colored IFA analysis of ISP1 and GCβ proteins in ookinetes of the *gcβ::6HA/Δisp1* parasite complemented with $ISP1^{C7A/C8A}$::3V5. The scale bar represents 5 μm.

(L) Percentage of ookinetes with GCβ polarization at OES from the *gcβ::6HA/Δisp1* parasites complemented with $ISP1^{WT}$::3V5 or $ISP1^{C7A/C8A}$::3V5. The value is means ± SEM of three independent tests analyzing more than 150 ookinetes. Two-tailed t test was used.

(M) A proposed model of the IMC-residing protein ISP1 in anchoring GCβ at OES of mature ookinetes.

See also Figure S7 and Tables S1 and S2.

and the initiation of ookinete gliding (Figure 1L), although we were not able to detect elevated level of cGMP at OES directly using a cGMP probe reporter Green cGull developed recently [21]. This is likely due to either the extremely fast diffusion property of cytoplasmic cGMP inside the ookinete [34, 35] or limited sensitivity of the probe in detecting cGMP. Further investigation using more sensitive methods is necessary to prove that locally elevated cGMP concentration drives ookinete gliding motility.

In many organisms, from yeast to mammals, CDC50 is a cofactor or chaperon of P4-ATPase proteins that mediates the complex's cellular trafficking [36]. Disruption of *cdc50a* dramatically reduced GCβ protein levels in gametocytes and ookinetes and abolished ookinete gliding. Interestingly, the CDC50A protein level is not affected after GCβ deletion, and it alone cannot polarize to OES. These results imply that CDC50A may not contain the signal for trafficking the complex to OES, as reported in other organisms [36, 37]; instead, it may function as a chaperon stabilizing GCβ in *Plasmodium*, although we cannot rule out that CDC50A could also regulate GCβ at the translational level.

IMC-residing protein ISP1 co-localizes and interacts with GCβ at OES of mature ookinetes, with GCβ distributed at the PPM and ISP1 at the IMC, functioning as an anchor pulling the GCβ complex to OES in mature ookinetes. Consistently, the majority (93%) of ookinetes lost GCβ polarization after ISP1 depletion. However, approximately 7% of ookinetes still maintained GCβ OES polarization, suggesting that other proteins may participate in anchoring GCβ/CDC50A complex at OES. It is still unknown how the GCβ is "pulled" to ISP1 at OES of mature ookinete, although ISP1 already polarizes in zygote stage (Figure 6B); it is possible that some specific proteins are expressed and direct GCβ/CDC50A to OES when ookinete is mature or about to mature. Previous studies have shown that biogenesis of the IMC is dependent on vesicular transport by the alveolate-specific GTPase protein, Rab11A and Rab11B, in apicomplexans [38, 39]. Whether Rab11A and Rab11B play a role in translocating the GCβ/CDC50A to the OES requires further investigation.

We propose a model for GCβ polarization-directed cGMP signaling and the initiation of ookinete gliding. (1) From zygote to retort stages, cytoplasmic-distributed GCβ/CDC50A complex and PDEδ maintain a sub-threshold cGMP level precluding PKG activation in the cytoplasm throughout the whole cell, assuming that all the enzymes are constitutively active. (2) Upon ookinete maturation, the GCβ/CDC50A complex translocates to the PPM and is anchored by the IMC-residing ISP1 at OES. (3) The GCβ polarization presumably increases the local cGMP concentration that drives PKG activation and initiates ookinetes gliding. Mosquito midgut traversal by ookinetes is a critical limiting step during the malaria transmission, and elucidating the mechanism involved in ookinete gliding could assist the development of interventions for blocking disease transmission.

STAR★METHODS

Detailed methods are provided in the online version of this paper and include the following:

- KEY RESOURCES TABLE
- CONTACT FOR REAGENT AND RESOURCE SHARING
- EXPERIMENTAL MODEL AND SUBJECT DETAILS
  - Mouse usage and ethics statement
  - Genotypic analysis of transgenic parasites
  - Housing conditions of mosquitos
  - Culture conditions for *in vitro* systems
- METHOD DETAILS
  - Plasmid construction and parasite transfection
  - Parasite negative selection with 5-Fluorouracil
  - Gametocyte induction in mouse
  - *In vitro* ookinete culture and purification
  - Mosquito feeding and transmission assay
  - Ookinete motility assay
  - Chemical treatment of ookinetes and gliding motility
  - Plasmid transfection for protein transient expression in ookinetes
  - Antibodies and antiserum
  - Immunofluorescence assays
  - Imaging of live ookinetes using confocal fluorescence microscopy
  - Cellular cGMP detection in ookinetes
  - Cellular phosphatidylserine detection in ookinetes
  - Protein extraction and western blotting
  - Cellular fractionation
  - Immunoprecipitation
  - Detection of protein palmitoylation
  - Bioinformatic searches and tools
- QUANTIFICATION AND STATISTICAL ANALYSIS

SUPPLEMENTAL INFORMATION

Supplemental Information includes seven figures, two tables, one video, and one data file and can be found with this article online at https://doi.org/10.1016/j.cub.2018.06.069.

ACKNOWLEDGMENTS

We thank Dr. David Baker (London School of Hygiene and Tropical Medicine) for his comments on this manuscript. This work was supported by the National Natural Science Foundation of China (81522027, 31772443, and 31501912), the Fundamental Research Funds for the Central Universities (20720160069, 20720150165, and 2013121033), the China's 1000 Young Talents Program, the "111" Project of the Ministration of Education of China (B06016), and the Division of Intramural Research, National Institute of Allergy and Infectious Diseases (NIAID), NIH (X.S.). The authors thank Cindy Clark, NIH Library Writing Center, for manuscript editing assistance.

AUTHOR CONTRIBUTIONS

H.G. and J.Y. designed the study. H.G., Z.Y., and X.W. generated the modified parasites and conducted the phenotype analysis, IFA assay, image analysis, mosquito experiments, ookinete motility assay, and biochemical experiments. R.H. and P.Q. generated the modified parasites. X.C. performed the STORM imaging. J.Y. and H.C. supervised the work. X.S., H.G., and J.Y. analyzed the data and wrote the manuscript.

DECLARATION OF INTERESTS

The authors declare no competing interests.

Received: April 4, 2018
Revised: May 28, 2018
Accepted: June 26, 2018
Published: August 23, 2018

REFERENCES

1. Bennink, S., Kiesow, M.J., and Pradel, G. (2016). The development of malaria parasites in the mosquito midgut. Cell. Microbiol. *18*, 905–918.
2. Al-Khattaf, F.S., Tremp, A.Z., and Dessens, J.T. (2015). Plasmodium alveolins possess distinct but structurally and functionally related multi-repeat domains. Parasitol. Res. *114*, 631–639.
3. Keeley, A., and Soldati, D. (2004). The glideosome: a molecular machine powering motility and host-cell invasion by Apicomplexa. Trends Cell Biol. *14*, 528–532.
4. Dessens, J.T., Beetsma, A.L., Dimopoulos, G., Wengelnik, K., Crisanti, A., Kafatos, F.C., and Sinden, R.E. (1999). CTRP is essential for mosquito infection by malaria ookinetes. EMBO J. *18*, 6221–6227.
5. Boucher, L.E., and Bosch, J. (2015). The apicomplexan glideosome and adhesins - Structures and function. J. Struct. Biol. *190*, 93–114.
6. Hirai, M., Arai, M., Kawai, S., and Matsuoka, H. (2006). PbGCbeta is essential for Plasmodium ookinete motility to invade midgut cell and for successful completion of parasite life cycle in mosquitoes. J. Biochem. *140*, 747–757.
7. Brochet, M., Collins, M.O., Smith, T.K., Thompson, E., Sebastian, S., Volkmann, K., Schwach, F., Chappell, L., Gomes, A.R., Berriman, M., et al. (2014). Phosphoinositide metabolism links cGMP-dependent protein kinase G to essential Ca^{2+} signals at key decision points in the life cycle of malaria parasites. PLoS Biol. *12*, e1001806.
8. Moon, R.W., Taylor, C.J., Bex, C., Schepers, R., Goulding, D., Janse, C.J., Waters, A.P., Baker, D.A., and Billker, O. (2009). A cyclic GMP signalling module that regulates gliding motility in a malaria parasite. PLoS Pathog. *5*, e1000599.
9. Ishino, T., Orito, Y., Chinzei, Y., and Yuda, M. (2006). A calcium-dependent protein kinase regulates Plasmodium ookinete access to the midgut epithelial cell. Mol. Microbiol. *59*, 1175–1184.
10. Linder, J.U., Engel, P., Reimer, A., Krüger, T., Plattner, H., Schultz, A., and Schultz, J.E. (1999). Guanylyl cyclases with the topology of mammalian adenylyl cyclases and an N-terminal P-type ATPase-like domain in Paramecium, Tetrahymena and Plasmodium. EMBO J. *18*, 4222–4232.
11. Baker, D.A., Drought, L.G., Flueck, C., Nofal, S.D., Patel, A., Penzo, M., and Walker, E.M. (2017). Cyclic nucleotide signalling in malaria parasites. Open Biol. *7*, 170213.
12. Carucci, D.J., Witney, A.A., Muhia, D.K., Warhurst, D.C., Schaap, P., Meima, M., Li, J.L., Taylor, M.C., Kelly, J.M., and Baker, D.A. (2000). Guanylyl cyclase activity associated with putative bifunctional integral membrane proteins in Plasmodium falciparum. J. Biol. Chem. *275*, 22147–22156.
13. Zhang, C., Xiao, B., Jiang, Y., Zhao, Y., Li, Z., Gao, H., Ling, Y., Wei, J., Li, S., Lu, M., et al. (2014). Efficient editing of malaria parasite genome using the CRISPR/Cas9 system. MBio *5*, e01414-14.
14. Bergman, L.W., Kaiser, K., Fujioka, H., Coppens, I., Daly, T.M., Fox, S., Matuschewski, K., Nussenzweig, V., and Kappe, S.H. (2003). Myosin A tail domain interacting protein (MTIP) localizes to the inner membrane complex of Plasmodium sporozoites. J. Cell Sci. *116*, 39–49.
15. Kaneko, I., Iwanaga, S., Kato, T., Kobayashi, I., and Yuda, M. (2015). Genome-wide identification of the target genes of AP2-O, a Plasmodium AP2-family transcription factor. PLoS Pathog. *11*, e1004905.
16. Yusuf, N.A., Green, J.L., Wall, R.J., Knuepfer, E., Moon, R.W., Schulte-Huxel, C., Stanway, R.R., Martin, S.R., Howell, S.A., Douse, C.H., et al. (2015). The Plasmodium class XIV myosin, MyoB, has a distinct subcellular location in invasive and motile stages of the malaria parasite and an unusual light chain. J. Biol. Chem. *290*, 12147–12164.
17. Santos, J.M., Duarte, N., Kehrer, J., Ramesar, J., Avramut, M.C., Koster, A.J., Dessens, J.T., Frischknecht, F., Chevalley-Maurel, S., Janse, C.J., et al. (2016). Maternally supplied S-acyl-transferase is required for crystalloid organelle formation and transmission of the malaria parasite. Proc. Natl. Acad. Sci. USA *113*, 7183–7188.
18. Frénal, K., Dubremetz, J.F., Lebrun, M., and Soldati-Favre, D. (2017). Gliding motility powers invasion and egress in Apicomplexa. Nat. Rev. Microbiol. *15*, 645–660.
19. Bindels, D.S., Haarbosch, L., van Weeren, L., Postma, M., Wiese, K.E., Mastop, M., Aumonier, S., Gotthard, G., Royant, A., Hink, M.A., and Gadella, T.W., Jr. (2017). mScarlet: a bright monomeric red fluorescent protein for cellular imaging. Nat. Methods *14*, 53–56.
20. Winger, J.A., Derbyshire, E.R., Lamers, M.H., Marletta, M.A., and Kuriyan, J. (2008). The crystal structure of the catalytic domain of a eukaryotic guanylate cyclase. BMC Struct. Biol. *8*, 42.
21. Matsuda, S., Harada, K., Ito, M., Takizawa, M., Wongso, D., Tsuboi, T., and Kitaguchi, T. (2017). Generation of a cGMP indicator with an expanded dynamic range by optimization of amino acid linkers between a fluorescent protein and PDE5α. ACS Sens. *2*, 46–51.
22. Deng, W., and Baker, D.A. (2002). A novel cyclic GMP-dependent protein kinase is expressed in the ring stage of the Plasmodium falciparum life cycle. Mol. Microbiol. *44*, 1141–1151.
23. Andersen, J.P., Vestergaard, A.L., Mikkelsen, S.A., Mogensen, L.S., Chalat, M., and Molday, R.S. (2016). P4-ATPases as phospholipid flippases-structure, function, and enigmas. Front. Physiol. *7*, 275.
24. Lopez-Marques, R.L., Theorin, L., Palmgren, M.G., and Pomorski, T.G. (2014). P4-ATPases: lipid flippases in cell membranes. Pflugers Arch. *466*, 1227–1240.
25. Raghupathy, R., Anilkumar, A.A., Polley, A., Singh, P.P., Yadav, M., Johnson, C., Suryawanshi, S., Saikam, V., Sawant, S.D., Panda, A., et al. (2015). Transbilayer lipid interactions mediate nanoclustering of lipid-anchored proteins. Cell *161*, 581–594.
26. Paulusma, C.C., Folmer, D.E., Ho-Mok, K.S., de Waart, D.R., Hilarius, P.M., Verhoeven, A.J., and Oude Elferink, R.P. (2008). ATP8B1 requires an accessory protein for endoplasmic reticulum exit and plasma membrane lipid flippase activity. Hepatology *47*, 268–278.
27. Zhang, C., Gao, H., Yang, Z., Jiang, Y., Li, Z., Wang, X., Xiao, B., Su, X.Z., Cui, H., and Yuan, J. (2017). CRISPR/Cas9 mediated sequential editing of genes critical for ookinete motility in Plasmodium yoelii. Mol. Biochem. Parasitol. *212*, 1–8.
28. Raibaud, A., Lupetti, P., Paul, R.E., Mercati, D., Brey, P.T., Sinden, R.E., Heuser, J.E., and Dallai, R. (2001). Cryofracture electron microscopy of the ookinete pellicle of Plasmodium gallinaceum reveals the existence of novel pores in the alveolar membranes. J. Struct. Biol. *135*, 47–57.
29. Morrissette, N.S., and Sibley, L.D. (2002). Cytoskeleton of apicomplexan parasites. Microbiol. Mol. Biol. Rev. *66*, 21–38.
30. Kono, M., Herrmann, S., Loughran, N.B., Cabrera, A., Engelberg, K., Lehmann, C., Sinha, D., Prinz, B., Ruch, U., Heussler, V., et al. (2012). Evolution and architecture of the inner membrane complex in asexual and sexual stages of the malaria parasite. Mol. Biol. Evol. *29*, 2113–2132.
31. Poulin, B., Patzewitz, E.M., Brady, D., Silvie, O., Wright, M.H., Ferguson, D.J., Wall, R.J., Whipple, S., Guttery, D.S., Tate, E.W., et al. (2013). Unique apicomplexan IMC sub-compartment proteins are early markers for apical polarity in the malaria parasite. Biol. Open *2*, 1160–1170.
32. Fung, C., Beck, J.R., Robertson, S.D., Gubbels, M.J., and Bradley, P.J. (2012). Toxoplasma ISP4 is a central IMC sub-compartment protein whose localization depends on palmitoylation but not myristoylation. Mol. Biochem. Parasitol. *184*, 99–108.
33. Jennings, B.C., Nadolski, M.J., Ling, Y., Baker, M.B., Harrison, M.L., Deschenes, R.J., and Linder, M.E. (2009). 2-Bromopalmitate and 2-(2-hydroxy-5-nitro-benzylidene)-benzo[b]thiophen-3-one inhibit DHHC-mediated palmitoylation in vitro. J. Lipid Res. *50*, 233–242.
34. Allbritton, N.L., Meyer, T., and Stryer, L. (1992). Range of messenger action of calcium ion and inositol 1,4,5-trisphosphate. Science *258*, 1812–1815.
35. Chen, C., Nakamura, T., and Koutalos, Y. (1999). Cyclic AMP diffusion coefficient in frog olfactory cilia. Biophys. J. *76*, 2861–2867.
36. Azouaoui, H., Montigny, C., Jacquot, A., Barry, R., Champeil, P., and Lenoir, G. (2016). Coordinated overexpression in yeast of a P4-ATPase

and its associated Cdc50 subunit: the case of the Drs2p/Cdc50p lipid flippase complex. Methods Mol. Biol. *1377*, 37–55.

37. Bryde, S., Hennrich, H., Verhulst, P.M., Devaux, P.F., Lenoir, G., and Holthuis, J.C. (2010). CDC50 proteins are critical components of the human class-1 P4-ATPase transport machinery. J. Biol. Chem. *285*, 40562–40572.

38. Agop-Nersesian, C., Egarter, S., Langsley, G., Foth, B.J., Ferguson, D.J., and Meissner, M. (2010). Biogenesis of the inner membrane complex is dependent on vesicular transport by the alveolate specific GTPase Rab11B. PLoS Pathog. *6*, e1001029.

39. Agop-Nersesian, C., Naissant, B., Ben Rached, F., Rauch, M., Kretzschmar, A., Thiberge, S., Menard, R., Ferguson, D.J., Meissner, M., and Langsley, G. (2009). Rab11A-controlled assembly of the inner membrane complex is required for completion of apicomplexan cytokinesis. PLoS Pathog. *5*, e1000270.

40. Wright, D.A., Thibodeau-Beganny, S., Sander, J.D., Winfrey, R.J., Hirsh, A.S., Eichtinger, M., Fu, F., Porteus, M.H., Dobbs, D., Voytas, D.F., and Joung, J.K. (2006). Standardized reagents and protocols for engineering zinc finger nucleases by modular assembly. Nat. Protoc. *1*, 1637–1652.

41. Bernsel, A., Viklund, H., Hennerdal, A., and Elofsson, A. (2009). TOPCONS: consensus prediction of membrane protein topology. Nucleic Acids Res. *37*, W465–W468.

42. Zhang, Y., Zhuang, Y.L., Nie, X.M., Liu, Y., Song, Y.H., Wang, G.C., and Zhu, C.F. (2012). [Analysis of HLA-A, B, and DRB1 polymorphism and genetic distance in Han population living in Yantai and Weihai regions of Shandong province]. Zhonghua Yi Xue Yi Chuan Xue Za Zhi *29*, 229–233.

43. Schindelin, J., Arganda-Carreras, I., Frise, E., Kaynig, V., Longair, M., Pietzsch, T., Preibisch, S., Rueden, C., Saalfeld, S., Schmid, B., et al. (2012). Fiji: an open-source platform for biological-image analysis. Nat. Methods *9*, 676–682.

44. Abou-Zeid, K.A., Yoon, K.S., Oscar, T.P., Schwarz, J.G., Hashem, F.M., and Whiting, R.C. (2007). Survival and growth of Listeria monocytogenes in broth as a function of temperature, pH, and potassium lactate and sodium diacetate concentrations. J. Food Prot. *70*, 2620–2625.

45. Billker, O., Dechamps, S., Tewari, R., Wenig, G., Franke-Fayard, B., and Brinkmann, V. (2004). Calcium and a calcium-dependent protein kinase regulate gamete formation and mosquito transmission in a malaria parasite. Cell *117*, 503–514.

46. Rodríguez, M.C., Margos, G., Compton, H., Ku, M., Lanz, H., Rodríguez, M.H., and Sinden, R.E. (2002). Plasmodium berghei: routine production of pure gametocytes, extracellular gametes, zygotes, and ookinetes. Exp. Parasitol. *101*, 73–76.

47. Harris, L.A., Shew, T.M., Skinner, J.R., and Wolins, N.E. (2012). A single centrifugation method for isolating fat droplets from cells and tissues. J. Lipid Res. *53*, 1021–1025.

48. Howie, J., Reilly, L., Fraser, N.J., Vlachaki Walker, J.M., Wypijewski, K.J., Ashford, M.L., Calaghan, S.C., McClafferty, H., Tian, L., Shipston, M.J., et al. (2014). Substrate recognition by the cell surface palmitoyl transferase DHHC5. Proc. Natl. Acad. Sci. USA *111*, 17534–17539.

STAR★METHODS

KEY RESOURCES TABLE

REAGENT or RESOURCE	SOURCE	IDENTIFIER
Antibodies		
Rabbit anti-Flag	Sigma-Aldrich	cat# F2555; RRID:AB_796202
Rabbit anti-HA	Cell Signaling Technology	cat#3724S; RRID:AB_1549585
Mouse anti-HA	Cell Signaling Technology	cat#2367S; RRID:AB_10691311
Rabbit anti-Myc	Cell Signaling Technology	cat#2272S; RRID:AB_10692100
Mouse anti-Myc	Cell Signaling Technology	cat#2276S; RRID:AB_331783
Rabbit anti-mCherry	Abcam	cat# ab183628; RRID:AB_2650480
Mouse anti-α Tubulin II	Sigma-Aldrich	cat#T6199; RRID:AB_477583
Mouse anti-V5	Genescript	cat#A01724-100
Alexa 488 conjugated goat anti-mouse IgG antibody	ThermoFisher Scientific	cat#A11001; RRID:AB_2534069
Alexa 488 conjugated goat anti-rabbit IgG antibody	ThermoFisher Scientific	cat# A31566; RRID:AB_10374301
Alexa 555 conjugated goat anti-mouse IgG antibody	ThermoFisher Scientific	cat#A21422; RRID:AB_141822
Alexa 555 conjugated goat anti-rabbit IgG antibody	ThermoFisher Scientific	cat#A21428; RRID:AB_141784
Alexa 555 conjugated goat anti-rat IgG antibody	ThermoFisher Scientific	cat#A21434; RRID:AB_141733
Goat anti-mouse IgG HRP-conjugated	Abcam	cat#ab6789; RRID:AB_955439
Goat anti-rabbit IgG HRP-conjugated	Abcam	cat#ab6721; RRID:AB_955447
Rabbit anti-P28 serum	Prepared in our lab [27]	N/A
Rabbit anti-BiP serum	Prepared in our lab	N/A
Rabbit anti-ERD2 serum	Prepared in our lab	N/A
Rat anti-ACP serum	Prepared in our lab	N/A
Rabbit anti-Hep17 serum	Prepared in our lab	N/A
Experimental models: parasite strains		
P.yoelii 17XNL strain	[13]	N/A
P.yoelii 17XNL/P28M strain	[27]	N/A
Plasmids and vectors		
pYCm Cas9 plasmid	[27]	N/A
PL0019	Malaria Research and Reference Reagent Resource Center	Cat#MRA-788
PL0019-Pysoap-mScarlet	This manuscript	N/A
PL0019-Pysoap-BeCyClope::mScarlet	This manuscript	N/A
PL0019-Pysoap-AnnexinV::mScarlet	This manuscript	N/A
PL0019-Pycdc50a::3V5 rescue	This manuscript	N/A
PL0019-Pyisp1::3V5 rescue	This manuscript	N/A
PL0019-Pfisp1::3V5 rescue	This manuscript	N/A
PL0019-Pysoap-GreencGull	This manuscript	N/A
Chemicals, Peptides, and Recombinant Proteins		
RPMI 1640 medium liquid	Hyclone	cat#SH30809.01B
Fetal Bovine Serum	GIBCO	cat#16000044
Xanthurenic acid	Sigma-Aldrich	cat#D120804
Matrigel	BD	cat#356234
Nycodenz	Axis-shield	cat#66108-95-0
Giemsa solution	Sigma-Aldrich	cat#GS80
Trypsin	Sigma-Aldrich	cat#T1426
Hoechst 33342	ThermoFisher Scientific	cat#23491-52-3
Protease inhibitor cocktail	Medchem Express	cat#HY-K0010

(*Continued on next page*)

Continued		
REAGENT or RESOURCE	SOURCE	IDENTIFIER
Western Bright ECL	Advansta	cat#K12045-D10
RIPA	Solaribio	cat#R0010
ACK lysing buffer	ThermoFisher Scientific	cat#A1049201
Pyrimethamine	Sigma-Aldrich	cat#46706
Sulfadiazine	Sigma-Aldrich	cat#S8626
5-Fluorouracil (5FC)	Sigma-Aldrich	cat# F6627
2-BMP	Sigma-Aldrich	cat# 21604
Zaprinast	Sigma-Aldrich	cat#Z0878
Compound 2 (C2)	PI: Oliver Billker [7]	N/A
Protein A/G affinity argrose beads	Pierce	cat#20423
Thiopropyl Sepharose 6B	GE healthcare	cat#17-0402-01
ExpressPlus PAGE Gel,10 × 8, 4-12%, 10 wells	Genescript	cat#M41210
Low gelling temperature Agarose	Sigma-Aldrich	cat#A9414
Critical Commercial Assays		
Pierce BCA Protein Assay Kit	ThermoFisher Scientific	cat#23225
Annexin V-FITC assay kit	Abcam	cat#ab14085
Nucleofector Kit	Lonza	cat#VVMI-1011
cDNA and gDNA Resource		
P.yoelii 17XNL cDNA	Our lab	N/A
P.falciparum 3D7 genomic DNA	Our lab	N/A
Oligonucleotides		
Oligonucleotides and primers listed in Table S2	Genewiz	https://www.genewiz.com.cn/
Software and Algorithms		
ZiFiT	[40]	http://zifit.partners.org/ZiFiT/ChoiceMenu.aspx
TMHMM	[41]	http://topcons.cbr.su.se/
Mega5.0	[42]	http://macdownload.informer.com/mega-5/5.0/
Fiji-ImageJ	[43]	http://imagej.net/Fiji
Prism GraphPad	[44]	https://www.graphpad.com/scientific-software/prism/

CONTACT FOR REAGENT AND RESOURCE SHARING

Further information and requests for resources and reagents should be directed to and will be fulfilled by the Lead Contact, Jing Yuan (yuanjing@xmu.edu.cn).

EXPERIMENTAL MODEL AND SUBJECT DETAILS

Mouse usage and ethics statement

All animal experiments were performed in accordance with approved protocols (XMULAC20140004) by the Committee for Care and Use of Laboratory Animals of Xiamen University. The ICR mice (female, 5 to 6 weeks old) were purchased from the Animal Care Center of Xiamen University and used for parasite propagation, drug selection, parasite cloning, and mosquito feedings.

Genotypic analysis of transgenic parasites

All transgenic parasites were generated from *P. yoelii* 17XNL strain and are listed in Table S1. Parasite infected blood samples from infected mice were collected from the mouse orbital sinus, and mouse blood cells were lysed using 1% saponin in PBS. Parasite genomic DNAs were isolated from transfected blood stage parasite populations using DNeasy Blood kits (QIAGEN) after washing off hemoglobin and subjected to diagnostic PCR. For each modification, both the 5′ and 3′ homologous recombination was detected by diagnostic genotype PCR (see Data S1), confirming successful integration of the homologous templates. All the primers used in this study are listed in Table S2. Parasite clones with targeted modifications were obtained after limiting dilution. At least two clones of each gene-modified parasite were used for phenotype analysis.

Housing conditions of mosquitos

The *Anopheles stephensi* mosquito (strain Hor) was reared at 28°C, 80% relative humidity and at a 12h light/dark cycle in the standard insect facility. Mosquito adults were maintained on a 10% sucrose solution.

Culture conditions for *in vitro* systems

Parasite ookinetes were prepared using *in vitro* culture. 100 μL of infected blood containing gametocytes was obtained from the orbital sinus of infected mouse and mixed immediately with 1 mL ookinete culture medium (RPMI 1640 medium containing 25 mM HEPES, 10% FCS, 100 μM xanthurenic acid, and pH 8.0). The mixture was incubated at 22°C for 12–24 h to allow gametogenesis, fertilization, and ookinete differentiation. Ookinetes formation was monitored by Giemsa staining of smears of the cultured cells.

METHOD DETAILS

Plasmid construction and parasite transfection

CRISPR/Cas9 plasmid pYCm was used for parasite genomic modification. To construct the vectors for gene deleting, we amplified the 5′- and 3′- genomic sequence (400 to 700 bp) of target genes as left and right homologous arms using specific primers (Table S2) and inserted into the restriction sites in pYCm. Oligonucleotides for guide RNAs (sgRNAs) were annealed and ligated into pYCm. For each gene, two sgRNAs were designed to target the coding region of gene (Table S2) using the online program ZiFit [40]. To construct the vectors for gene tagging and T2A insertion, we first amplified the C- or N-terminal segments (400 to 800 bp) of the coding regions as left or right arm and 400 to 800 bp from 5′UTR or 3′ UTR following the translation stop codon as left and right arm, respectively. A DNA fragment (encoding mCherry, mScarlet, 6HA, 4Myc, or 3V5 tag) was inserted between the left and right arms in frame with the gene of interest. For each gene, two sgRNAs were designed to target sites close to the C- or N-terminal part of the coding region. To construct vectors for site-directed nucleotide mutations, the substitution sites were designed with a restriction site for modification detection and placed in the middle of the homologous arms. Parasite-infected red blood cells (RBC) were electroporated with 5 μg purified circular plasmid DNA using the Lonza Nucleotector. Transfected parasites were immediately intravenously injected into a new mouse and placed under pyrimethamine pressure (provided in drinking water at concentration 6 μg/ml) from day 2 post-transfection. Parasites with transfected plasmids usually appear 5 to 7 days during drug selection.

Parasite negative selection with 5-Fluorouracil

Modified parasites subject for sequential modification were negatively selected to remove episomal pYCm plasmid. 5-Fluorouracil (5FC, Sigma, F6627) was prepared in water at a final concentration of 2.0 mg/ml and was provided to the mice in a dark drinking bottle. A naive mouse receiving parasites with residual plasmid from previous pyrimethamine selection was subjected to 5FC pressure for 8 days, with a change of drug at day 4. To estimate the amount of plasmid in the parasite populations, we used two independent primer pairs from the plasmid backbone to amplify the DNAs. All PCR primers used are listed in Table S2.

Gametocyte induction in mouse

ICR mice were treated with phenylhydrazine (80 μg /g mouse body weight) through intraperitoneal injection. Three days post treatment, the mice were infected with 2.0×10^6 parasites through tail vein injection. Peaks of gametocytemia usually were observed three days post infection. Male and female gametocytes were counted via Giemsa staining of thin blood smears. Gametocytemia was calculated as the ratio of male or female gametocyte over parasitized erythrocyte. All experiments were repeated three times independently.

In vitro ookinete culture and purification

In vitro culture for ookinete development was prepared as described previously [45]. Briefly, mouse blood with 4%–6% gametocytemia was collected in heparin tubes and immediately added to ookinete culture medium. Parasites were cultured in the medium with a blood/medium volume ratio of 1:10 at 22°C. After 12–24 h culture, the ookinete culture was Giemsa-stained and analyzed for ookinetes morphology. Ookinete conversion rate was calculated as the number of ookinetes (both normal and abnormal morphology) per 100 female gametocytes. Ookinetes were purified using ACK lysing method as described previously [46]. Briefly, the cultured ookinetes were collected by centrifugation and transferred into ACK lysing buffer (ThermoFisher Scientific, A1049201) on ice for 8 min. After erythrocytes lysis, the remaining ookinetes were isolated via centrifugation and washed twice with PBS. The ookinetes were examined on the hemocytometer under 40 × objective lens for purity and counted. Only the samples with > 80% ookinete purity were used for further biochemical analysis.

Mosquito feeding and transmission assay

For mosquito transmission, thirty female *Anopheles stephensi* mosquitoes were allowed to feed on an anesthetized mouse carrying 4%–6% gametocytemia for 30 min. For oocyst formation assay, mosquito midguts were dissected on day 7 or 8 post blood-feeding and stained with 0.1% mercurochrome for oocyst counting. For salivary gland sporozoite counting, salivary glands from 20–30 mosquitoes were dissected on day 14 post blood-feeding, and the number of sporozoites per mosquito was calculated.

For sporozoite infection of mice, 15–20 infected mosquitoes were allowed to bite one anesthetized naive mouse for 30 min. The time for parasite emerging in mouse peripheral blood circulation after the bite was considered as prepatent time.

Ookinete motility assay

Ookinete gliding motility was evaluated as previously described [8]. All procedures were performed in a temperature-controlled room with 22°C. Briefly, 20 μL of the suspended ookinete cultures were mixed with 20 μL of Matrigel (BD, #356234) on ice. The mixtures were transferred onto a slide, covered with a coverslip, and sealed with nail varnish. The slide was placed at 22°C for 30 min before observation under microscope. After tracking a gliding ookinete under microscopic field, time-lapse videos (1 frame per 20 s, for 20 min) were taken to monitor ookinete movement using a 40 × objective lens on a Nikon ECLIPSEE100 microscope fitted with an ISH500 digital camera controlled by *ISCapture v3.6.9.3N* software (Tucsen). Time-lapse movies were analyzed with Fiji software and the Manual Tracking plugin. Motility speed was calculated by dividing the distance an ookinete moved by the time it took. All experiments were repeated three times independently.

Chemical treatment of ookinetes and gliding motility

To evaluate the effects of chemical treatment on ookinete development and GCβ protein localization, chemicals were added to developing ookinete cultures at variable times, and the cultures were collected for Giemsa staining or IFA analysis. Compound 2 (5 μM C2) targeting *Plasmodium* PKG [7], 2-BMP (100 μM) inhibiting *Plasmodium* DHHCs, or 0.1% saponin were used in this study. For the effects of chemical treatment on ookinete gliding motility, 5 μM C2 or 100 μM zaprinast (zap) inhibiting *Plasmodium* PDEs were added to the mixture containing both ookinete culture and Matrigel before gliding motility assay. All experiments were repeated three times independently.

Plasmid transfection for protein transient expression in ookinetes

Transient expression of proteins in ookinetes via plasmid episome was as described with minor modifications [45]. Coding sequence of target proteins with appropriate 5′- and 3′-UTR regulatory regions were inserted into the pL0019-derived vector with human *dhfr* marker for pyrimethamine selection. Briefly, blood stage parasites were electroporated with 10 μg plasmid DNA and selected with pyrimethamine (70 μg/ml) for 7 days. Meanwhile, another group of ICR mice were treated with phenylhydrazine for 3 days through intraperitoneal injection. The phenylhydrazine-treated mice were infected with 2.0×10^6 drug-selected parasites through intravenous injection and further selected for another 3–4 days until peak gametocytemia was reached. The high-level gametocytemia blood was collected for ookinete culture and further tests.

Antibodies and antiserum

The primary antibodies used were: rabbit anti-HA (western, 1:1000 dilution, IFA, 1:500 dilution), mouse anti-HA(IFA, 1:500), rabbit anti-Myc (western, 1:1000), and mouse anti-Myc (IFA, 1:500) from Cell Signaling Technology, mouse anti-αTubulin II (Sigma-Aldrich) (IFA, 1:1000), mouse anti-V5 (Genescript)(western, 1:1000, IFA, 1:500), rabbit anti-mCherry (Abcam) (western, 1:1000, IFA, 1:500), Rabbit anti-Flag (Sigma-Aldrich,) (western, 1:1000). The secondary antibodies used were: goat anti-rabbit IgG HRP-conjugated and goat anti-mouse IgG HRP-conjugated secondary antibody from Abcam (1:5000), the Alexa 555 goat anti-rabbit IgG, Alexa 488 goat anti-rabbit IgG, Alexa 555 goat anti-mouse IgG, Alexa 488 goat anti-mouse IgG, and Alexa 555 goat anti-rat IgG secondary antibody from ThermoFisher Scientific(1:500). The anti-serums, including the rabbit anti-Hep17(western, 1:1000), rabbit anti-P28(western, 1:1000, IFA, 1:1000), rabbit anti-BiP(western, 1:1000, IFA, 1:500), rat anti-ACP(IFA, 1:100), and rabbit anti-ERD2(IFA, 1:500) were prepared in the Lab.

Immunofluorescence assays

Purified parasites were fixed using 4% paraformaldehyde and transferred to a Poly-L-Lysine pre-treated coverslip. The fixed cells were permeabilized with 0.1% Triton X-100 PBS solution for 7 min, blocked in 5% BSA solution for 60 min at room temperature, and incubated with the primary antibodies diluted in 3% BSA-PBS at 4°C for 12 h. The coverslip was incubated with fluorescent conjugated secondary antibodies for 1 h. Cells were stained with Hoechst 33342, mounted in 90% glycerol solution, and sealed with nail polish. All images were captured and processed using identical settings on a Zeiss LSM 780 confocal microscope. Stochastic optical reconstruction microscopy (STORM) imaging was acquired using a Nikon N-STORM 5.0 Super-Resolution Microscope System.

Imaging of live ookinetes using confocal fluorescence microscopy

Developing ookinetes (20 μl) of *gcβ::mScarlet* parasite from 8 to 12 hr cultures were mixed with 20 μL of Matrigel thoroughly. The mixtures were transferred onto a slide, covered with a coverslip, and sealed with nail varnish. The developing ookinetes were monitored under a Zeiss LSM 780 confocal microscope. Stage IV live ookinetes were monitored and fluorescent signals were tracked and recorded.

Cellular cGMP detection in ookinetes

Cellular cGMP detection was conducted using the Green-cGull probe as described previously [21] with minor modifications. The coding region of Green-cGull protein driven by 1.5 kb *Pysoap* 5′-UTR and 1.0 kb *Pbdhfr* 3′-UTR was inserted to pL0019-derived plasmid containing human *dhfr* marker for pyrimethamine selection. Briefly, blood stage parasites were electroporated with 10 μg

plasmid DNA and selected with pyrimethamine (70 μg/ml) for 7 days. Ookinetes from 12 to 24 hr *in vitro* cultures were enriched by centrifugation and resuspended in 1% low-melting agarose (Sigma-Aldrich, A9414) to avoid cell movement during detection. The mixtures were transferred to the bottom of 15 mm glass-bottom cell culture dish (Corning, #801002) and overlaid with RPMI 1640 medium. Using a Zeiss LSM 780 confocal microscope, the fluorescent signals of Green-cGull were monitored in 30 randomly chosen ookinetes for their basal fluorescence (F_0) (collected before treatment) and enhanced fluorescence (F) collected 20 min post zaprinast treatment respectively. cGMP response was calculated as the ratio of F/F_0.

Cellular phosphatidylserine detection in ookinetes

To detect the phosphatidylserine (PS) on the outer leaflet of plasma membrane of ookinetes, Annexin V-FITC assay kit (Abcam, ab14085) was used according to the manufacturer's instructions. To detect the PS on the inner leaflet of plasma membrane of ookinetes, a sequence encoding human Annexin V tagged with mScarlet driven by 1.5 kb *Pysoap* 5′-UTR and 1.0 kb *Pbdhfr* 3′-UTR was inserted to pL0019-derived plasmid containing human *dhfr* marker for pyrimethamine selection. Briefly, blood stage parasites were electroporated with 10 μg plasmid DNA and selected with pyrimethamine (70 μg/ml) for 7 days. Ookinetes from transfected parasites were prepared from *in vitro* culture. Both Annexin V-mScarlet and mScarlet expressed ookinetes were treated with 1 μM A23187, and the cytoplasmic distribution and intensity of the fluorescent signal was monitored using a Zeiss LSM 780 confocal microscope.

Protein extraction and western blotting

Protein extraction from asexual blood parasites, gametocytes, zygotes, retorts, and ookinetes was performed using buffer A (0.1% SDS, 1mM DTT, 50 mM NaCl, 20 mM Tris-HCl; pH8.0) containing protease inhibitor cocktail and PMSF. After ultrasonication, the protein solution was incubated on ice for 30 min before centrifugation at 12,000 g for 10 min at 4°C. The supernatant was lysed in Laemmli sample buffer. GCβ was separated in 4.5% SDS-PAGE and transferred to PVDF membrane (Millipore, IPVH00010). The membrane was blocked in 5% skim milk TBST buffer and incubated with primary antibodies. After incubation, the membrane was washed three times with TBST and incubated with HRP-conjugated secondary antibodies. The membrane was washed four times in TBST before enhanced chemiluminescence detection.

Cellular fractionation

Cellular fractionation was conducted as described previously with minor modifications [47]. The purified retorts and ookinetes were ruptured in the hypotonic buffer (10 mM HEPES, 10 mM KCl, pH 7.4) after passing through a 1 mL syringe needle gently ten times. Total cell lysate were centrifuged for 15 min at 1,000 g, and the supernatant (light fraction, including cytoplasm and cytosol vesicles) and the pellet (heavy fraction, including plasma membrane, IMC, and cytoskeleton) were collected respectively and solubilized in Laemmli buffer for 10min on ice. The solubilized protein samples were analyzed by western blotting.

Immunoprecipitation

For immunoprecipitation analysis, 1.0-2.0 × 10^6 ookinetes were lysed in 1 mL protein extraction buffer A plus (0.01% SDS, 1 mM DTT, 50 mM NaCl, 20 mM Tris-HCl; pH 8.0) and centrifuged at 12,000 g for 10 min at 4°C before collecting the supernatant solution. Rabbit anti-HA antibody (1 μg, CST, #3724S) was added to the protein solution and incubated at 4°C for 12 h on a vertical mixer. After incubation, 20 μL buffer A plus pre-balanced protein A/G beads (Pierce, #20423) was added and incubated for 2 h. The beads were washed three times with buffer A plus before elution with Laemmli buffer.

Detection of protein palmitoylation

The palmitoylation modification of ISP1 protein was performed using Acyl-RAC assay described previously [48]. Ookinetes were lysed in DHHC Buffer B (2.5% SDS, 1 mM EDTA, 100 mM HEPES, pH 7.5) containing protease inhibitor cocktail and PMSF and incubated on ice for 30 min. After centrifugation at 12,000 g for 10 min, supernatant was collected and treated with 0.1% methyl methanethiosulfonate (MMTS) at 42°C for 15 min. MMTS was removed by acetone precipitation followed by washing with 70% acetone three times. Protein samples were solubilized in DHHC Buffer C (1% SDS, 1 mM EDTA, 100 mM HEPES, pH 7.5 and were captured on thiopropyl Sepharose 6B (GE Healthcare, 17-0402-01) in the presence of 2 M hydroxylamine or 2 M NaCl (negative control) by agitating for 3 h at room temperature. Loading controls (Input) were collected before addition of thiopropyl Sepharose 6B beads. After five times washing with urea DHHC Buffer (1% SDS, 1 mM EDTA, 100 mM HEPES, 8 M urea, pH 7.5), the captured proteins were eluted from thiopropyl Sepharose 6B beads in 60μl urea DHHC Buffer supplemented with 50mM DTT, and mixed with Laemmli sample buffer for further western blot analysis.

Bioinformatic searches and tools

The genomic sequences of target genes were downloaded from PlasmoDB database. The transmembrane domains of proteins were identified using the TMHMM Server (http://www.cbs.dtu.dk/services/TMHMM/) [41]. The phylogeny tree and protein amino acid sequence alignment was analyzed using MEGA5.0 [42].

QUANTIFICATION AND STATISTICAL ANALYSIS

For quantification of protein expression in western blot, protein band intensity was quantified using Fiji software from three independent experiments. The signals of target proteins were normalized with that of control proteins. For quantification of protein expression in IFA, confocal fluorescence microscopy images were acquired under identical parameters. Fluorescent signals were quantified using Fiji software [43]. More than 30 cells were randomly chosen in each group. Protein expression was expressed as the relative percentage compared to control group. Protein polarization rate was calculated as the ratio of the protein fluorescent signal at OES over the fluorescent signal from the whole cell. Statistical analysis was performed using GraphPad Software 5.0 [44]. Two-tailed Student's t test or Whiney Mann test was used to compare differences between treated groups and their paired controls. n represents the number of mosquitos or parasite cells tested in each group, or experimental replication. The exact value of n was indicated within the figures. p value in each statistical analysis was also indicated within the figures.

Current Biology, Volume *28*

Supplemental Information

ISP1-Anchored Polarization of GCβ/CDC50A Complex Initiates Malaria Ookinete Gliding Motility

Han Gao, Zhenke Yang, Xu Wang, Pengge Qian, Renjie Hong, Xin Chen, Xin-zhuan Su, Huiting Cui, and Jing Yuan

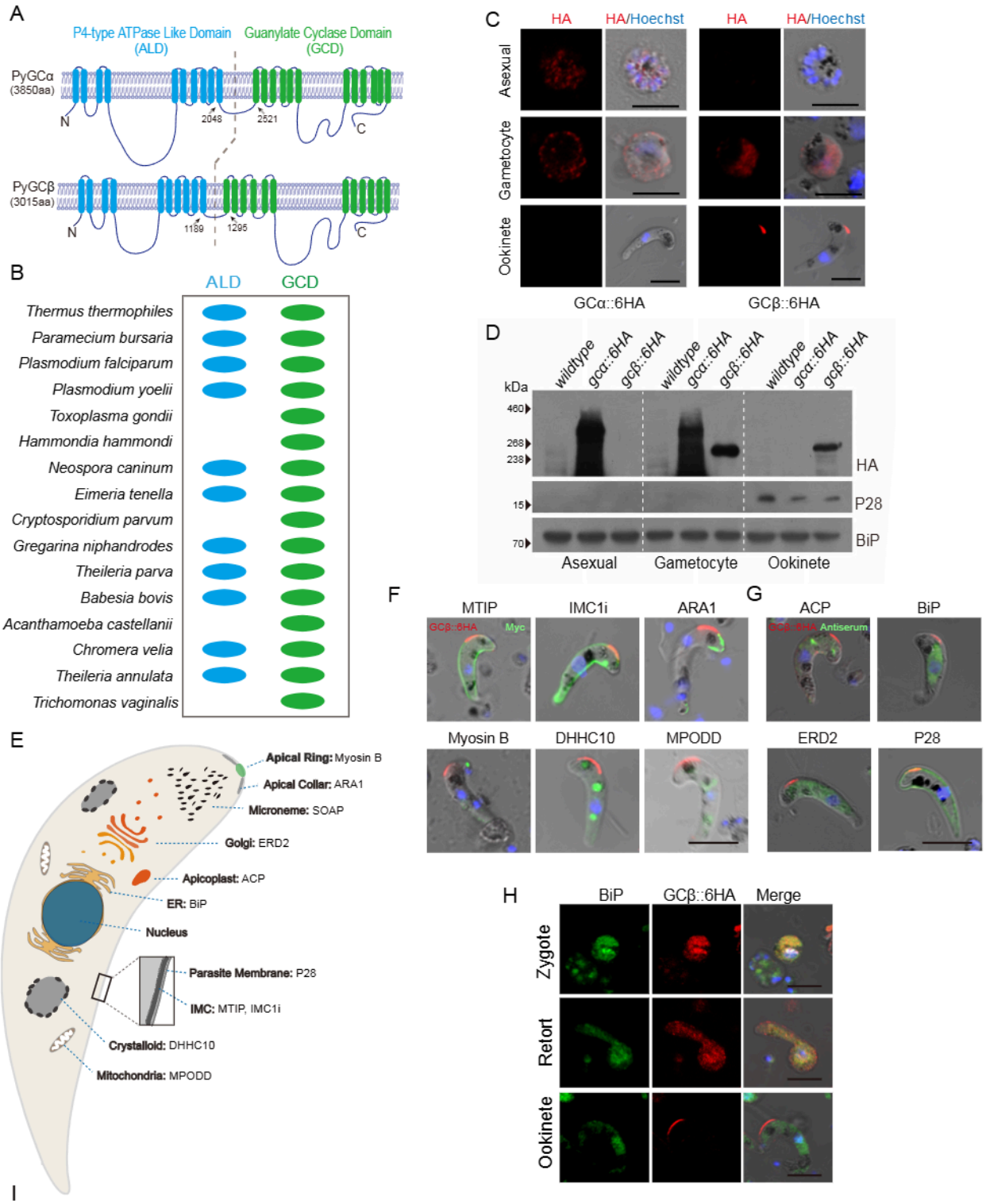
A
P4-type ATPase Like Domain (ALD)
Guanylate Cyclase Domain (GCD)
PyGCα (3850aa)
N
2048
2521
C
PyGCβ (3015aa)
1189
1295
B
ALD
GCD
Thermus thermophiles
Paramecium bursaria
Plasmodium falciparum
Plasmodium yoelii
Toxoplasma gondii
Hammondia hammondi
Neospora caninum
Eimeria tenella
Cryptosporidium parvum
Gregarina niphandrodes
Theileria parva
Babesia bovis
Acanthamoeba castellanii
Chromera velia
Theileria annulata
Trichomonas vaginalis
C
HA
HA/Hoechst
Asexual
Gametocyte
Ookinete
GCα::6HA
GCβ::6HA
D
wildtype
gcα::6HA
gcβ::6HA
kDa
460
268
238
15
70
HA
P28
BiP
Asexual
Gametocyte
Ookinete
E
Apical Ring: Myosin B
Apical Collar: ARA1
Microneme: SOAP
Golgi: ERD2
Apicoplast: ACP
ER: BiP
Nucleus
Parasite Membrane: P28
IMC: MTIP, IMC1i
Crystalloid: DHHC10
Mitochondria: MPODD
F
MTIP
GCβ::6HA
Myc
IMC1i
ARA1
Myosin B
DHHC10
MPODD
G
ACP
GCβ::6HA
Antiserum
BiP
ERD2
P28
H
BiP
GCβ::6HA
Merge
Zygote
Retort
Ookinete
I
Stage II
III
IV
V
ookinete extrados site (OES)
Protein polarization rate in OES (%) =
Fluorescence in OES
Fluorescence of whole cell area
X 100%

Figure S1. Stage expression, cellular localization, and co-localization analysis of GCα and GCβ of rodent malaria parasite *Plasmodium yoelii*, Related to Figure 1.

(A) Predicted topologies and structures of GCα and GCβ, both possessing a ten-transmembrane P4-ATPase-like domain (ALD, green) in the N-terminal and a twelve-transmembrane guanylate cyclase domain (GCD, blue) in the C-terminal.

(B) The guanylate cyclases possessing the bi-functional ALD/GCD structure are observed in many protozoan species.

(C) IFA analysis of GCα and GCβ proteins in asexual blood stage, gametocytes, and ookinetes. Scale bar = 5 μm.

(D) Western blot analysis of GCα and GCβ proteins in asexual blood stage, gametocytes, and ookinetes. P28 is an ookinete-specific protein. BiP is used as a loading control for western blot.

(E) Diagram of a mature ookinete indicating subcellular organelles and their protein markers.

(F) Co-localization analysis of GCβ with MTIP (glideosome component), IMC1i (IMC protein), ARA1 (apical collar), Myosin B (apical ring), DHHC10 (crystalloid body), MPODD (mitochondria) using anti-HA and anti-Myc antibodies in the double-tagged parasites derived from *gcβ::6HAc*. Scale bar = 5 μm. All the double-tagged parasites information are indicated in Supplementary Table 1.

(G) Co-localization analysis of GCβ with ACP (apicoplast), BiP (ER), ERD2 (Golgi), and P28 (parasite plasma membrane) using anti-HA antibody and protein-specific antisera as indicated. Scale bar = 5 μm.

(H) IFA analysis of GCβ and BiP (ER) during zygote to ookinete development of the parasite *gcβ::6HA* using both anti-HA antibody and anti-BiP antiserum. Scale bar = 5 μm.

(I) Definition of protein polarization rate (PR) at OES during ookinete development. PR is the percentage of fluorescent signal at OES over that of whole ookinete cell. More than 30 cells were randomly chosen for quantification.

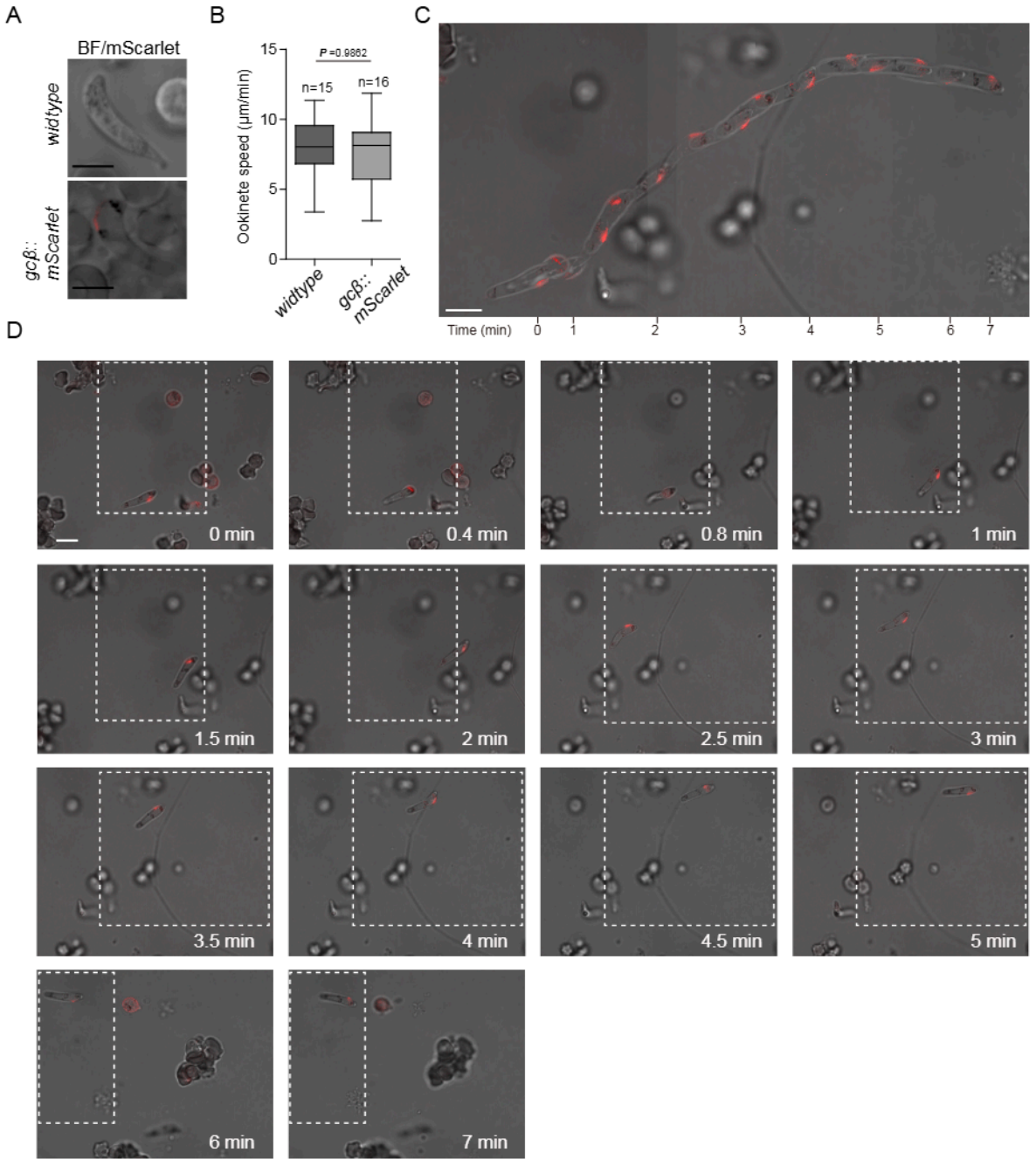
A
BF/mScarlet
widtype
gcβ::
mScarlet
B
P =0.9862
n=15
n=16
Ookinete speed (µm/min)
15
10
5
0
widtype
gcβ::
mScarlet
C
Time (min)
0
1
2
3
4
5
6
7
D
0 min
0.4 min
0.8 min
1 min
1.5 min
2 min
2.5 min
3 min
3.5 min
4 min
4.5 min
5 min
6 min
7 min

Figure S2. GCβ polarization at OES of mature ookinete of the *gcβ::mScarlet* parasites, Related to Figure 1 and Video S1.

(A) Confocal microscopy observation of GCβ tagged with mScarlet. GCβ::mScarlet protein is detected (red) at OES of mature ookinete. Scale bar = 5 μm.

(B) Ookinetes gliding motility of the wildtype and *gcβ::mScarlet* parasites. n is the number of ookinetes tested in each group. Two-tailed *t* test was used for statistical analysis.

(C) Real-time capturing of fluorescent signals with mScarlet-tagged GCβ in a mature gliding ookinete. The composite time-lapse picture shows the spiral gliding movement of the ookinete. The time points (minute) for signal capturing are indicated. Scale bar = 5 μm. Signal in each time point is indicated in the white dash line box of the figures in (**D**).

(D) Fluorescent microscopy observation of a gliding *gcβ::mScarlet* ookinetes over time. GCβ::mScarlet protein is detected (red) at OES of the ookinetes in all time. Scale bar = 5 μm.

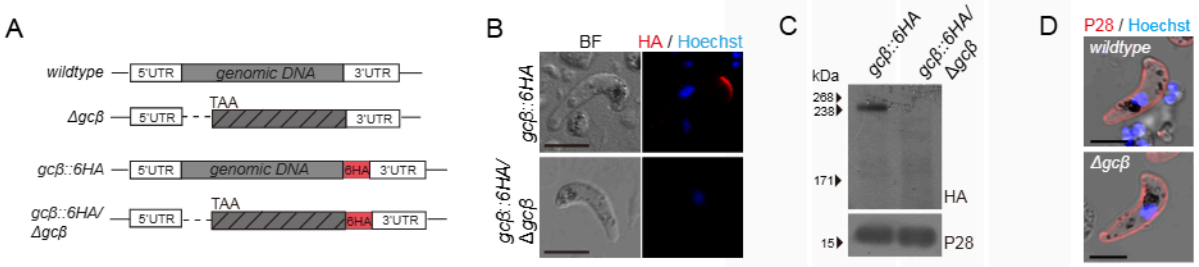

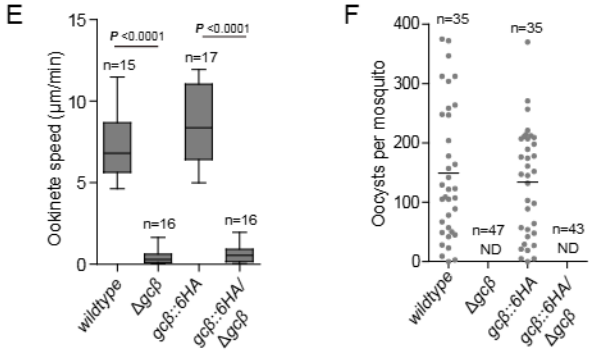

G

Parasite	No.of Mosquito dissected	Salivary gland sporozoite/ mosquito Average±SD	Transmission to naïve mice Mouse bitten/ Mouse infected	Prepatency time (days)
Wildtype	55	6,750±854	3/3	4
Δgcβ	57	0	3/0	/
gcβ::6HA	58	6,625±747	3/3	4
gcβ::6HA/Δgcβ	54	0	3/0	/

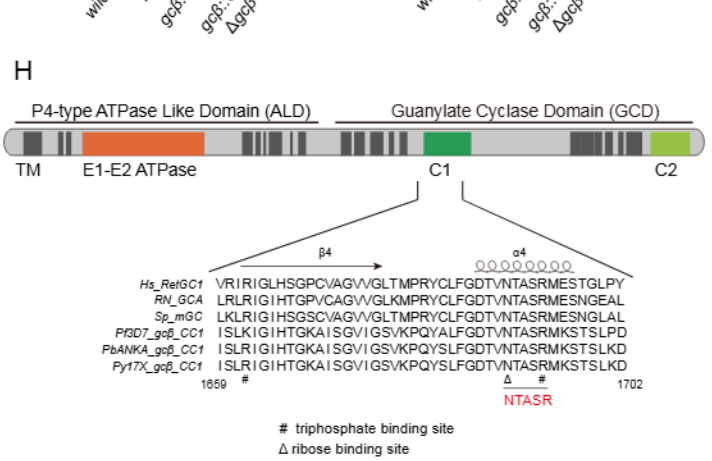

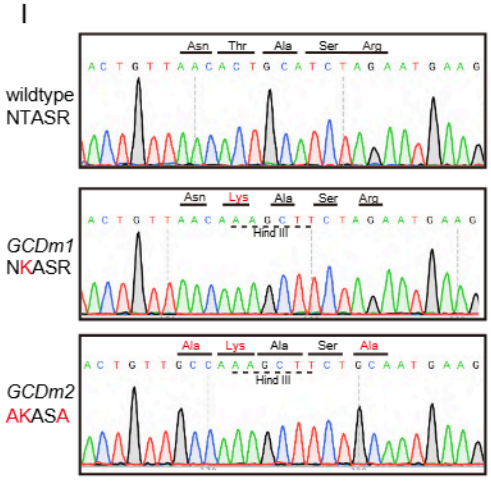

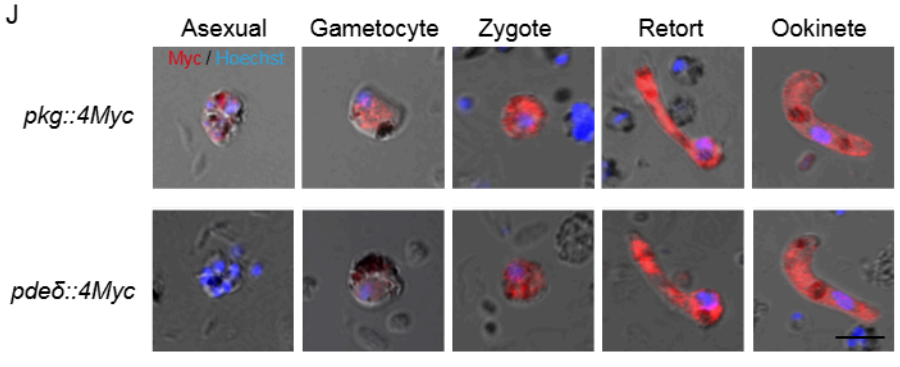

Figure S3. Effects of disruption or mutation of GCβ on ookinete motility and parasite mosquito transmission, and expression of PKG and PDEδ during ookinete development, Related to Figure 2.

(A) Diagram showing *gcβ* gene deletion in wildtype and *gcβ::6HA* parasites using CRISPR/Cas9 method. An N-terminal segment of genomic sequence (including 516 bp exon1 and 348bp intron1) was deleted and a stop codon was inserted upstream of the remaining region to stop translation.

(B) IFA analysis of GCβ protein in *gcβ::6HA*/Δ*gcβ* ookinetes. Scale bar = 5 μm.

(C) Western blot of GCβ protein in *gcβ::6HA*/Δ*gcβ* ookinetes.

(D) IFA analysis of P28 proteins in wildtype and Δ*gcβ* ookinetes. Loss of GCβ had no effect on ookinete maturation. Scale bar = 5 μm.

(E) Gliding motility of the Δ*gcβ* and *gcβ::6HA*/Δ*gcβ* ookinetes. n is the number of ookinetes tested in each group. Two-tailed *t* test was used for statistical analysis.

(F) Number of midgut oocysts 7 days post blood feeding. n is the number of mosquitoes tested in each group. The horizontal line shows the mean value of each group. ND: not detected.

(G) Formation and infectivity to mouse of salivary gland sporozoites from parasites as indicated. Mosquitoes were dissected 14 days post blood feeding, and salivary gland sporozoites per mosquito were counted. In each group of mouse infection, ten mosquitoes were fed on one mouse and the pre-patent time was measured.

(H) GCβ domain structure and alignment of amino acid sequences of guanylate cyclase catalytic domain (C1) from six GC proteins revealed potential conserved motif sequence NTASR in the C1 domain. Human RetGC1 (GenBank Q02846), *Rattus norvegicus* GCA (P18910), *Strongylocentrotus purpuratus* mGC (P16065)，*P. falciparum* GCβ, *P. berghei* GCβ, and *P. yoelii* GCβ were included.

(I) DNA sequencing confirming substitutions at the C1 domain of GCβ from the *GCDm1* and *GCDm2* parasites.

(J) IFA analysis of PKG and PDEδ proteins expression in asexual blood stage, gametocyte, zygote, retort, and ookinete of the *pkg::4Myc* and *pdeδ::4Myc* parasites, respectively. Scale bar = 5 μm.

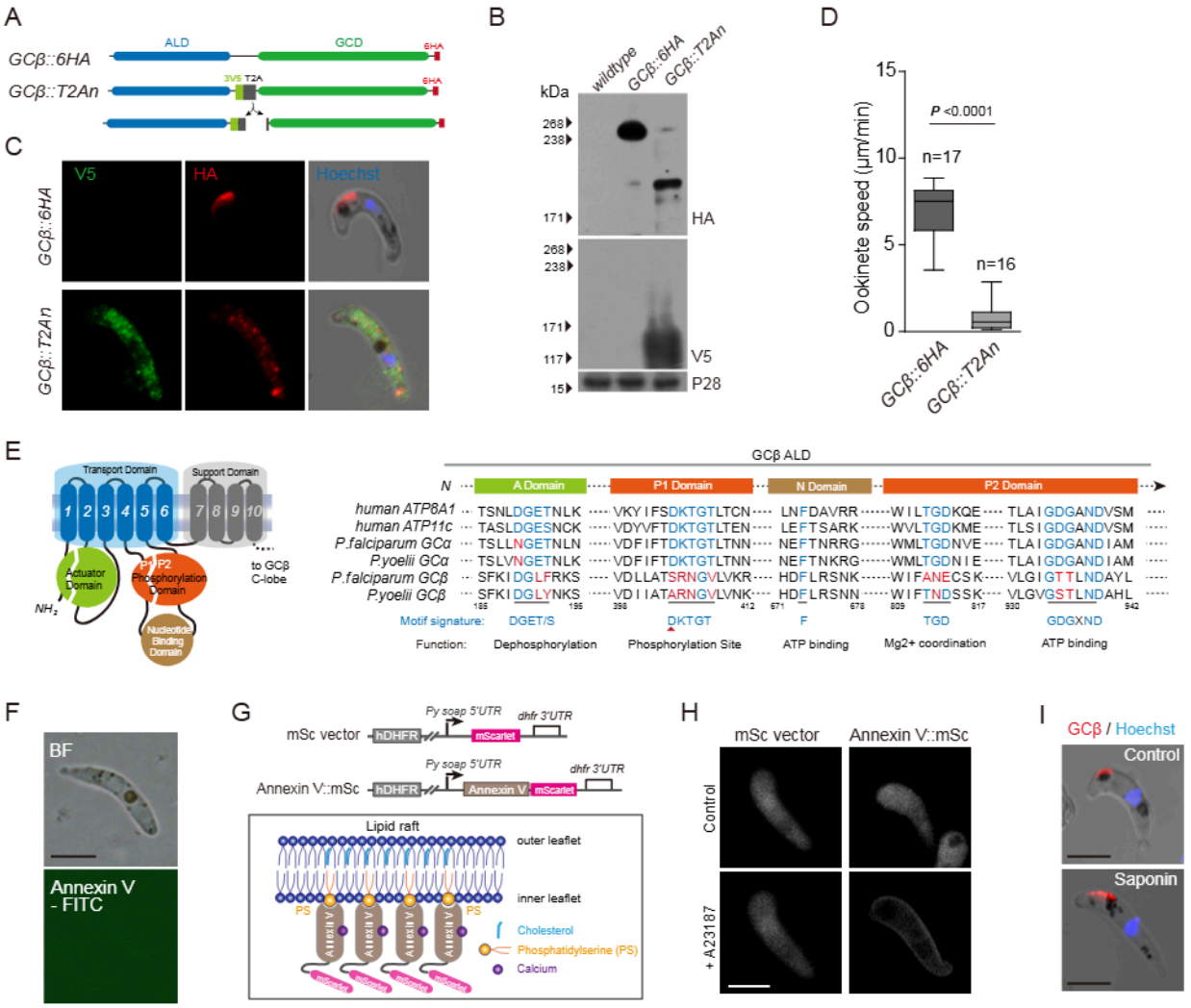
A
ALD
GCD
6HA
GCβ::6HA
3V5 T2A
GCβ::T2An
B
kDa
wildtype
GCβ::6HA
GCβ::T2An
268
238
171
HA
V5
117
15
P28
D
P <0.0001
n=17
n=16
Ookinete speed (μm/min)
15
10
5
0
GCβ::6HA
GCβ::T2An
C
V5
HA
Hoechst
GCβ::6HA
GCβ::T2An
E
Transport Domain
Support Domain
1 2 3 4 5 6
7 8 9 10
Actuator Domain
P1 P2 Phosphorylation Domain
Nucleotide Binding Domain
NH2
to GCβ C-lobe
GCβ ALD
N
A Domain
P1 Domain
N Domain
P2 Domain
human ATP8A1 TSNLDGETNLK VKYIFSDKTGTLTCN LNFDAVRR WILTGDKQE TLAIGDGANDVSM
human ATP11c TASLDGESNCK VDYVFTDKTGTLTEN LEFTSARK WVLTGDKME TLSIGDGANDVSM
P.falciparum GCα TSLLNGETNLN VDFIFTDKTGTLTNN NEFTNRRG WMLTGDNVE TLAIGDGANDIAM
P.yoelii GCα TSLVNGETNLK VDFIFTDKTGTLTNN NEFTNKRG WMLTGDNIE TLAIGDGANDIAM
P.falciparum GCβ SFKIDGLFRKS VDLLATSRNGVLVKR HDFLRSNK WIFANECSK VLGIGTTLNDAYL
P.yoelii GCβ SFKIDGLYNKS VDIIATARNGVLVNK HDFLRSNN WIFTNDSSK VLGVGSTLNDAHL
185 195 398 412 671 678 809 817 930 942
Motif signature: DGET/S DKTGT F TGD GDGXND
Function: Dephosphorylation Phosphorylation Site ATP binding Mg2+ coordination ATP binding
F
BF
Annexin V - FITC
G
Py soap 5'UTR
dhfr 3'UTR
mSc vector
hDHFR
mScarlet
Annexin V::mSc
Annexin V
Lipid raft
outer leaflet
inner leaflet
PS
Cholesterol
Phosphatidylserine (PS)
Calcium
H
mSc vector
Annexin V::mSc
Control
+ A23187
I
GCβ / Hoechst
Control
Saponin

Figure S4. Functional analysis of N-terminal ALD domain in GCβ polarization and ookinete motility, and detection of phosphatidylserine (PS) in ookinete using Annexin V-FITC probe, Related to Figure 3.

(A) Diagram of T2A-mediated separate expression of ALD and GCD of GCβ in the modified strain *GCβ*::*T2An*. T2A peptide was inserted into the region between ALD and GCD in the *gcβ::6HAc* parasite, leading to separation of ALD::3V5::T2A and GCD::6HA parts.

(B) Western blot of ALD::3V5::T2A and GCD::6HA expression in *GCβ*::*T2An* ookinetes.

(C) IFA analysis of ALD::3V5::T2A and GCD::6HA expression and localization in *GCβ*::*T2An* ookinetes.

(D) Ookinete gliding motility of the *GCβ*::*T2An* parasite.

(E) Predicted topology of the GCβ N-terminal ALD. The actuator domain (green), phosphorylation domain (orange), and nucleotide binding domain (brown) are indicated. Sequence alignment of conserved amino acids in catalytic domain of six P4-type ATPase proteins (human ATP8A1, human ATP11c, *P. falciparum* GCα, PyGCα, *P. falciparum* GCβ, and PyGCβ). Mutations at multiple signature motifs of ALD in *P. falciparum* GCβ and PyGCβ are indicated in red.

(F) Detection of phosphatidylserine (PS) at exofacial leaflet of plasma membrane of living ookinete through Annexin V-FITC direct staining.

(G) Construction of a plasmid for episomal expression of human Annexin V::mScarlet to detect intracellular PS in ookinetes. Annexin V is capable of binding to PS in the presence of calcium. Sequence of 1.5 kb 5'UTR of *Pysoap* gene was used to drive transcription of *Annexin V::mScarlet* in ookinetes.

(H) Fluorescence microscopy detection of PS in living ookinetes transfected with Annexin V::mScarlet. mScarlet alone serves as a control. Both mScarlet and Annexin V::mScarlet distribute in cytosol of the ookinete, while Annexin V::mScarlet relocates to plasma membrane periphery after treating with 1 μM calcium ionophore A23187.

(I) IFA detecting GCβ in *gcβ::6HA* ookinetes treated with 0.1% saponin. Saponin is a cholesterol scavenger that breaks the PS-rich lipid rafts of plasma membrane.

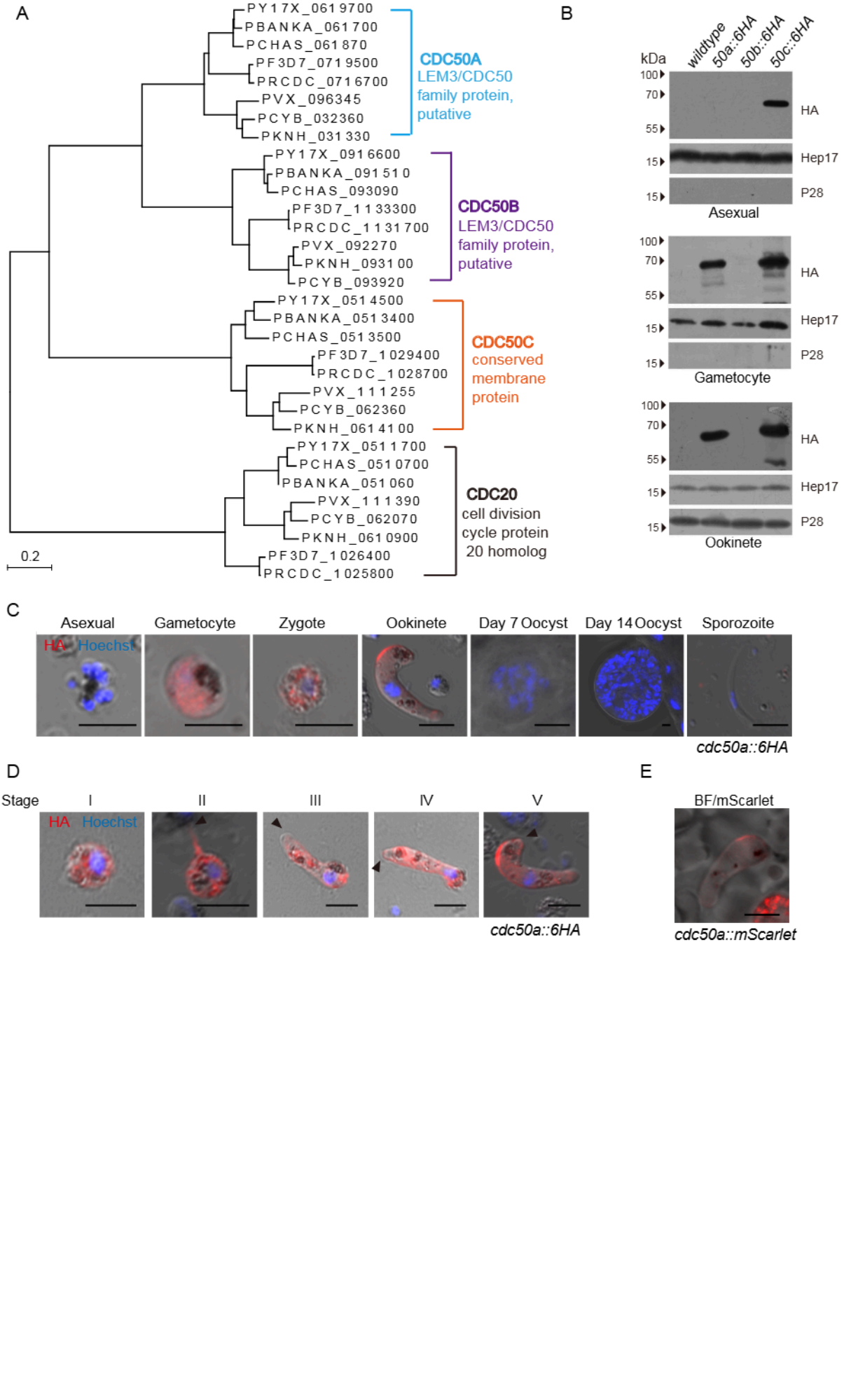
A
PY17X_061 9700
PBANKA_061 700
PCHAS_061 870
PF3D7_071 9500
PRCDC_071 6700
PVX_096345
PCYB_032360
PKNH_031 330
CDC50A
LEM3/CDC50
family protein,
putative
PY17X_091 6600
PBANKA_091 510
PCHAS_093090
PF3D7_1 133300
PRCDC_1 131 700
PVX_092270
PKNH_0931 00
PCYB_093920
CDC50B
LEM3/CDC50
family protein,
putative
PY17X_051 4500
PBANKA_051 3400
PCHAS_051 3500
PF3D7_1 029400
PRCDC_1 028700
PVX_1 11 255
PCYB_062360
PKNH_061 41 00
CDC50C
conserved
membrane
protein
PY17X_051 1700
PCHAS_051 0700
PBANKA_051 060
PVX_1 11 390
PCYB_062070
PKNH_061 0900
PF3D7_1 026400
PRCDC_1 025800
CDC20
cell division
cycle protein
20 homolog
0.2
B
kDa
wildtype
50a::6HA
50b::6HA
50c::6HA
100
70
55
15
HA
Hep17
P28
Asexual
Gametocyte
Ookinete
C
Asexual
Gametocyte
Zygote
Ookinete
Day 7 Oocyst
Day 14 Oocyst
Sporozoite
HA Hoechst
cdc50a::6HA
D
Stage
I
II
III
IV
V
HA Hoechst
cdc50a::6HA
E
BF/mScarlet
cdc50a::mScarlet

Figure S5. **Phylogenetic analysis of CDC50 proteins, stage expression and cellular localization of CDC50A proteins, Related to Figure 4.**

(A) All CDC50 proteins are clustered to three paralogs (CDC50A, CDC50B, and CDC50C) from eight *Plasmodium* species, including *P. yoelii*, *P. berghei*, *P. chabaudi*, *P. falciparum*, *P. reichenowi*, *P. vivax*, *P. cynomolgi*, and *P. knowlesi*. *Plasmodium* CDC20 (cell division cycle protein 20 homolog protein) serves as a control not related to CDC50.

(B) Western blot detecting protein expression of the three CDC50s in asexual mouse blood stages, gametocytes, and ookinetes.

(C) IFA analysis of CDC50A protein during *in vitro* ookinete development of the *cdc50a::6HA* parasite. Black arrows indicate the apical end of the developing ookinetes. Scale bar = 5 μm.

(D) Fluorescent microscopy indicating the CDC50A protein polarization at OES of the *cdc50a::mScarlet* parasite. Scale bar = 5 μm.

(E) IFA detection of CDC50A during the life cycle of the *cdc50a::6HA* parasite. Scale bar = 5 μm.

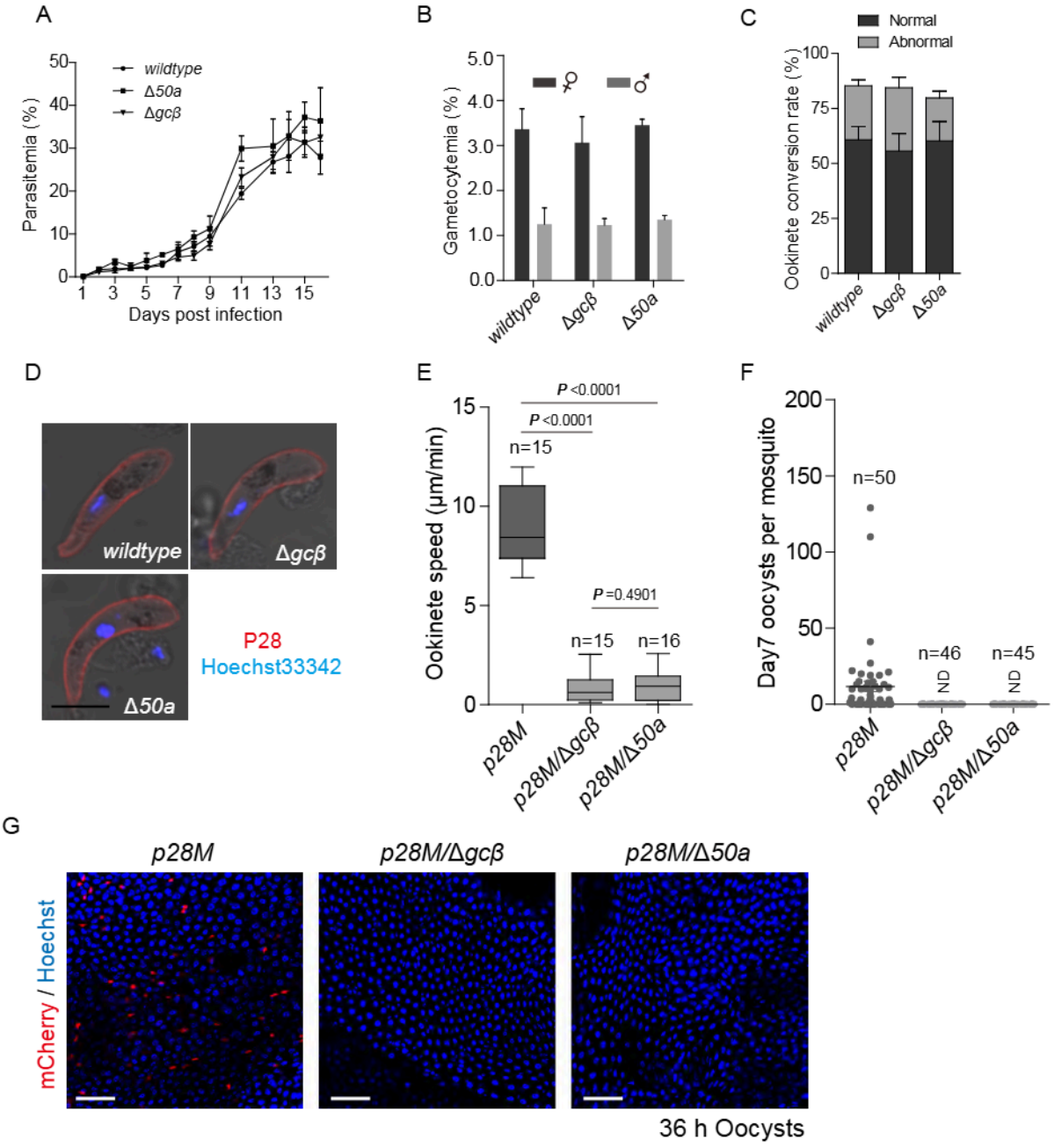
A
wildtype
Δ50a
Δgcβ
Parasitemia (%)
Days post infection
B
♀
♂
Gametocytemia (%)
wildtype
Δgcβ
Δ50a
C
Normal
Abnormal
Ookinete conversion rate (%)
wildtype
Δgcβ
Δ50a
D
wildtype
Δgcβ
Δ50a
P28
Hoechst33342
E
P <0.0001
P <0.0001
P =0.4901
n=15
n=15
n=16
Ookinete speed (μm/min)
p28M
p28M/Δgcβ
p28M/Δ50a
F
n=50
n=46
n=45
ND
ND
Day7 oocysts per mosquito
p28M
p28M/Δgcβ
p28M/Δ50a
G
p28M
p28M/Δgcβ
p28M/Δ50a
mCherry / Hoechst
36 h Oocysts

Figure S6. Genetic deletion and phenotype analysis of wildtype, Δ*50a*, and Δ*gcβ* parasites, Related to Figure 4.

(A) Asexual blood stage proliferation of wildtype, Δ*50a*, and Δ*gcβ* parasites.

(B) Male and female gametocyte formation in mouse blood of wildtype, Δ*50a*, and Δ*gcβ* parasites.

(C) *In vitro* ookinete differentiation of wildtype, Δ*50a*, and Δ*gcβ* parasites.

(D) IFA analysis of P28 proteins in ookinetes of wildtype, Δ*50a*, and Δ*gcβ* parasites. Scale bar = 5 μm.

(E) Ookinete gliding motility of the modified parasites *p28M*, *p28M*/Δ*50a*, and *p28M*/Δ*gcβ*. Each *50a* and *gcβ* was deleted in 17XNL P28mCh reporter strain expressing P28::mCherry fusion protein, generating *p28M*/Δ*gcβ* and *p28M*/Δ*50a* strain, respectively.

(F) Midgut oocyst counts in mosquitoes 7 days post blood feeding.

(G) Fluorescence microscopy observation of mosquito midguts 36 h post blood feeding, indicating early oocysts formation of the parasites tested. Scale bar = 50 μm.

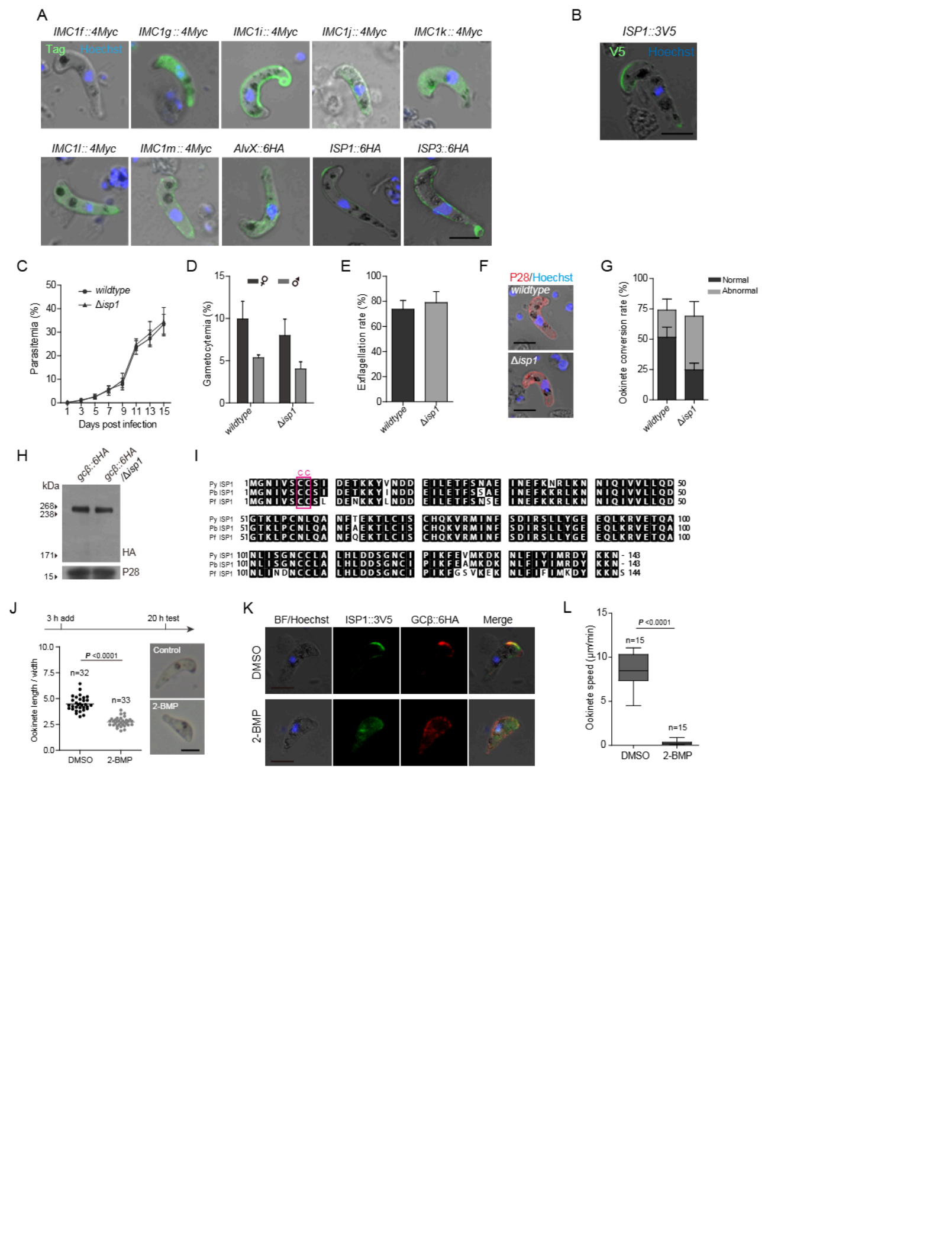
A
IMC1f::4Myc
IMC1g::4Myc
IMC1i::4Myc
IMC1j::4Myc
IMC1k::4Myc
Tag
Hoechst
IMC1l::4Myc
IMC1m::4Myc
AlvX::6HA
ISP1::6HA
ISP3::6HA
B
ISP1::3V5
V5
Hoechst
C
wildtype
Δisp1
Parasitemia (%)
Days post infection
D
♀
♂
Gametocytemia (%)
wildtype
Δisp1
E
Exflagellation rate (%)
wildtype
Δisp1
F
P28/Hoechst
wildtype
Δisp1
G
Normal
Abnormal
Ookinete conversion rate (%)
wildtype
Δisp1
H
gcβ::6HA
gcβ::6HA /Δisp1
kDa
268
238
171
15
HA
P28
I
Py ISP1
Pb ISP1
Pf ISP1
J
3 h add
20 h test
P <0.0001
n=32
n=33
Ookinete length / width
DMSO
2-BMP
Control
2-BMP
K
BF/Hoechst
ISP1::3V5
GCβ::6HA
Merge
DMSO
2-BMP
L
P <0.0001
n=15
n=15
Ookinete speed (μm/min)
DMSO
2-BMP

Figure S7. Screening and identification of IMC-residing protein ISP1 critical for anchoring GCβ at OES of mature ookinete, Related to Figure 6 and 7.

(A) IFA analysis of IMC-related proteins in ookinetes tagged with HA or Myc tags. Scale bar = 5 μm.

(B) IFA analysis of ISP1 in ookinetes of the *isp1::3V5* parasite. Scale bar = 5 μm.

(C) Parasitemia of wildtype and Δ*isp1* parasites in mouse. The data is indicated as means ±SEM from three mice.

(D) Gametocyte formation in mouse blood of wildtype and Δ*isp1* parasites. The data is indicated as means ±SEM from three mice.

(E) Male gametocyte activation *in vitro* of wildtype and Δ*isp1* parasites. The data is indicated as means ±SEM of three independent tests.

(F) IFA analysis of P28 proteins in ookinetes of wildtype and Δ*isp1* parasites. Scale bar = 5 μm.

(G) *In vitro* ookinete differentiation of wildtype and Δ*isp1* parasites. The data is indicated as means ±SEM of three independent tests.

(H) Western blot of GCβ expression in ookinetes of *gcβ::6HA* and *gcβ::6HA/*Δ*isp1* parasites. P28 as the loading control.

(I) Alignment of ISP1 protein sequences from *P. yoelii* (PY17X_1212600), *P. berghei* (PBANKA_1209400), and *P. falciparum* (PF3D7_1011000). The red box highlights the N-terminal cysteine residues for potential palmitoylation.

(J) Morphology of wildtype ookinetes treated with 2-BMP, a potent inhibitor of palmitoyl transferase for protein palmitoylation. Ookinete cultures were treated with 100 μM 2-BMP or DMSO at 3 h point and were observed under a microscope at 20 h. n is the number of ookinetes tested in each group. The horizontal line shows the mean value of each group. Two-tailed *t* test was used for statistical analysis.

(K) IFA analysis of ISP1 and GCβ proteins in ookinetes of *gcβ::6HA/isp1::3V5* parasite treated with DMSO or 100 μM 2-BMP. Scale bar = 5 μm.

(L) Gliding motility of ookinetes treated with 2-BMP. n is the number of ookinetes tested in each group. The horizontal line shows the mean value of each group. Two-tailed *t* test was used for statistical analysis.

Table S1. List of genetically modified parasite strains in this study

Strain	Parental strain	Discription	Resource	Asexual growth in mouse	Gametocytemia in mouse (% wildtype)	Ookinete conversion (Average ± SD)	Ookinete morphology	Day 7 oocyst per mosquito (% wildtype)	Day 14 salivary gland sporozoite per mosquito (% wildtype)	Infection to naïve mice (Mouse bitten/Mouse infected)
17XNL	/	The wildtype strain	NIH	normal	/	69.43 ± 3.85	normal	/	/	3/3
Parasites with gene tagging										
gcβ::6HAc	17XNL	gcβ C-terminally tagged with 6HA	Data S1	normal	115.45	72.97±3.54	normal	99.56	101.36	3/3
gcβ::6HAm	17XNL	gcβ tagged with 6HA between ALD and GCD	Data S1	normal	96.33	63.93±5.81	normal	118.77	nt	3/3
gcβ::6HAn	17XNL	gcβ N-terminally tagged with 6HA	Data S1	normal	91.21	65.13±5.19	normal	94.87	nt	3/3
gcβ::mScarlet	17XNL	gcβ C-terminally tagged with red fluorencence protein mScarlet	Data S1	normal	118.36	74.40±6.71	normal	90.54	93.86	3/3
gcα::6HAc	17XNL	gcα C-terminally tagged with 6HA	Data S1	normal	92.61	65.63±4.06	normal	89.67	91.62	3/3
gcβ::6HA/mtip::4Myc	gcβ::6HAc	mtip C-terminally tagged with 4Myc	Data S1	normal	nt	nt	normal	nt	nt	nt
gcβ::6HA/imc1i::4Myc	gcβ::6HAc	imc1i C-terminally tagged with 4Myc	Data S1	normal	nt	nt	normal	nt	nt	nt
gcβ::6HA/ara1::4Myc	gcβ::6HAc	ara1 C-terminally tagged with 4Myc	Data S1	normal	nt	nt	normal	nt	nt	nt
gcβ::6HA/myosinb::4Myc	gcβ::6HAc	myosinb C-terminally tagged with 4Myc	Data S1	normal	nt	nt	normal	nt	nt	nt
gcβ::6HA/dhhc10::4Myc	gcβ::6HAc	dhhc10 C-terminally tagged with 4Myc	Data S1	normal	nt	nt	normal	nt	nt	nt
gcβ::6HA/mpodd::4Myc	gcβ::6HAc	mpodd C-terminally tagged with 4Myc	Data S1	normal	nt	nt	normal	nt	nt	nt
gcβ::6HA/pdeδ::4Myc	gcβ::6HAc	pdeδ N-terminally tagged with 4Myc	Data S1	normal	nt	nt	normal	nt	nt	nt
gcβ::6HA/pkg::4Myc	gcβ::6HAc	pkg N-terminally tagged with 4Myc	Data S1	normal	nt	nt	normal	nt	nt	nt
pdeδ::4Myc	17XNL	pdeδ N-terminally tagged with 4Myc	Data S1	normal	100.82	65.07±5.96	normal	103.59	nt	3/3
pkg::4Myc	17XNL	pkg N-terminally tagged with 4Myc	Data S1	normal	86.11	80.30±3.45	normal	114.45	108.66	3/3
cdc50a::6HA	17XNL	cdc50a C-terminally tagged with 6HA	Data S1	normal	97.07	71.20±2.44	normal	90.16	95.34	3/3
cdc50b::6HA	17XNL	cdc50b C-terminally tagged with 6HA	Data S1	normal	84.38	71.07±7.13	normal	90.44	nt	3/3
cdc50c::6HA	17XNL	cdc50c C-terminally tagged with 6HA	Data S1	normal	76.29	72.07±8.13	normal	88.15	nt	3/3
cdc50a::mScarlet	17XNL	cdc50a C-terminally tagged with mScarlet	Data S1	normal	80.06	72.00±1.47	normal	nt	nt	nt
gcβ::6HA/cdc50A::mCherry	gcβ::6HAc	cdc50a C-terminally tagged with mCherry	Data S1	normal	104.4	69.67±3.51	normal	95.13	98.91	3/3
gcβ::6HA/cdc50A::3V5	gcβ::6HAc	cdc50a C-terminally tagged with 3V5	Data S1	normal	120.58	65.13±5.15	normal	93.42	nt	3/3
Δcdc50a/gcβ::6HA	Δcdc50a	gcβ C-terminally tagged with 6HA	Data S1	normal	93.45	63.90±6.95	normal	0	nt	nt
imc1f::4Myc	17XNL	imc1f C-terminally tagged with 4Myc	Data S1	normal	nt	nt	normal	nt	nt	nt
imc1g::4Myc	17XNL	imc1g C-terminally tagged with 4Myc	Data S1	normal	nt	nt	normal	nt	nt	nt
imc1i::4Myc	17XNL	imc1i C-terminally tagged with 4Myc	Data S1	normal	nt	nt	normal	nt	nt	nt
imc1j::4Myc	17XNL	imc1j C-terminally tagged with 4Myc	Data S1	normal	nt	nt	normal	nt	nt	nt
imc1k::4Myc	17XNL	imc1k C-terminally tagged with 4Myc	Data S1	normal	nt	nt	normal	nt	nt	nt
imc1l::4Myc	17XNL	imc1l C-terminally tagged with 4Myc	Data S1	normal	nt	nt	normal	nt	nt	nt
imc1m::4Myc	17XNL	imc1m C-terminally tagged with 4Myc	Data S1	normal	nt	nt	normal	nt	nt	nt
alvx::6HA	17XNL	alvx C-terminally tagged with 6HA	Data S1	normal	nt	nt	normal	nt	nt	nt
isp1::6HA	17XNL	isp1 C-terminally tagged with 6HA	Data S1	normal	84.04	80.53±3.11	normal	95.18	96.23	3/3
isp3::6HA	17XNL	isp3 C-terminally tagged with 6HA	Data S1	normal	79.22	58.50±6.14	normal	95.34	90.74	3/3
isp1::3V5	17XNL	isp1 C-terminally tagged with 3V5	Data S1	normal	130.5	65.23±3.90	normal	117.33	109.16	3/3

gcβ::6HA/isp1::3V5	gcβ::6HAc	isp1 C-terminally tagged with 3V5	Data S1	normal	108.73	66.57±5.25	normal	104.35	95.72	3/3
Parasites with gene knockout										
Δgcβ	17XNL	Deleted the first three exons of gc β causing frame shift mutation	Data S1	normal	92.83	69.87±3.82	normal	0	0	3/0
P28M/Δgcβ	P28M	Deleted the first three exons of gc β causing frame shift mutation	Data S1	normal	73.51	69.53±4.58	normal	0	0	3/0
gcβ::6HA/Δgcβ	gcβ::6HAc	Deleted the first three exons of gc β causing frame shift mutation	Data S1	normal	107.95	74.53±4.49	normal	0	0	3/0
Δcdpk3	17XNL	Deleted the whole coding sequences of cdpk3	Zhang et al 2016	normal	80.9	65.47±4.49	normal	3.56	nt	nt
Δpdeδ	17XNL	Deleted the kinase domain sequences of pdeδ	Data S1	normal	79.26	75.50±2.71	Stum and round	2.49	nt	nt
gcβ::6HAΔpdeδ	gcβ::6HAc	Deleted the kinase domain sequences of pdeδ	Data S1	normal	93.98	72.68±3.76	Stum and round	3.87	nt	nt
Δcdc50a	17XNL	Deleted the whole coding sequences of cdc50a	Data S1	normal	103.78	63.13±6.41	normal	0	0	3/0
P28M/Δcdc50a	P28M	Deleted the whole coding sequences of cdc50a	Data S1	normal	109.17	70.33±3.36	normal	0	0	3/0
gcβ::6HA/Δcdc50a	gcβ::6HAc	Deleted the whole coding sequences of cdc50a	Data S1	normal	86.34	67.07±3.04	normal	0	nt	3/0
cdc50a::6HA/Δgcβ	cdc50a::6HA	Deleted the first three exons of gc β causing frame shift	Data S1	normal	90.77	71.73±3.06	normal	0	nt	nt
Δcdc50a/Δgcβ	Δcdc50a	Deleted the first three exons of gc β causing frame shift	Data S1	normal	83.11	70.80±2.50	normal	0	nt	3/0
Δcdpk3/Δgcβ	Δcdpk3	Deleted the first three exons of gc β causing frame shift	Data S1	normal	76.29	65.83±6.55	normal	0	nt	nt
Δcdpk3/Δcdc50a	Δcdpk3	Deleted the whole coding sequences of cdc50a	Data S1	normal	88.93	63.60±5.42	normal	0	nt	nt
Δpdeδ/Δgcβ	Δpdeδ	Deleted the first three exons of gc β causing frame shift	Data S1	normal	68.24	62.03±4.76	normal	nt	nt	nt
Δpdeδ/Δcdc50a	Δpdeδ	Deleted the whole coding sequences of cdc50a	Data S1	normal	74.61	71.67±4.60	normal	nt	nt	nt
Δisp1	17XNL	Deleted the whole coding sequences of isp1	Data S1	normal	88.3	69.00± 12.12	Normal form reduced	8.43	nt	nt
isp1::3V5/Δgcβ	isp1::3V5	Deleted the first three exons of gc β causing frame shift	Data S1	normal	114.3	65.97±5.64	normal	0	nt	nt
gcβ::6HA/Δisp1	gcβ::6HAc	Deleted the whole coding sequences of isp1	Data S1	normal	122.06	74.00±4.72	Normal form reduced	2.64	nt	nt
Parasites with gene compelementation										
Δcdc50a/Flag::50a	Δcdc50a	Complementation of flag tagged cdc50a sequence	Data S1	normal	111.84	57.8±2.82	normal	82.95	86.49	3/3
gcβ::6HA/Δcdc50a/cdc50a::3V5	gcβ::6HA/ Δcdc50a	Plasmid based complemtation of 3V5 tagged Pycdc50a sequence	/	normal	73.59	62.73±6.94	normal	nt	nt	nt
gc β::6HA/Δcdc50a/Pfcdc50a::3V5	gcβ::6HA/ Δcdc50a	Plasmid based complemtation of 3V5 tagged Pfcdc50a sequence	/	normal	84.07	69.1±5.1	normal	nt	nt	nt
gcβ::6HA/Δisp1/Pyisp1::3V5	gcβ::6HA/ Δisp1	Plasmid-based complemtation of 3V5 tagged-Pyisp1	/	normal	83.43	64.8±6.11	normal	nt	nt	nt
gcβ::6HA/Δisp1/Pfisp1::3V5	gcβ::6HA/ Δisp1	Plasmid-based complemtation of 3V5 tagged-Pfisp1	/	normal	99.02	70.8±3.13	normal	nt	nt	nt
Parasite with modification in GCβ										
gcβT2A	gcβ::6HAc	Inserting T2A sequence between ALD and GCD of GCβ	Data S1	normal	103.07	66.47±5.79	normal	0	0	3/0
gcβT2Am	gcβ::6HAc	Inserting an mutated T2A sequence (T2Am) between ALD and GCD of GCβ	Data S1	normal	88.39	63.97±3.74	normal	94.63	95.82	3/3
gcβT2An	gcβ::6HAc	Inserting T2A sequence between ALD and GCD of GCβ with a 3V5 tag on 5' side of T2A sequence.	Data S1	normal	92.44	61.43±7.48	normal	0	nt	nt
GCDm1	gcβ::6HAc	The NTASR residue in C1 of GCβ are replaced with NKASR	Data S1	normal	76.59	72.03±3.88	normal	nt	nt	nt
GCDm2	gcβ::6HAc	The NTASR residues in C1 of GC β are replaced with AKASA	Data S1	normal	83.55	67.57±6	normal	0	nt	nt

nt: not tested

Table S2. Primers and oligonucleotides used in this study

Oligo sequence for gene knockout plasmid construction

Gene name	Gene ID	Gene size (bp)/ deleted gene size (bp)	Left homologous arm		Right homologous arm		Target site of sgRNA	
			Forward primer	Reverse primer	Forward primer	Reverse primer	Oligo (Forward)	Oligo (Reverse)
gcβ	PY17X_1138200	11182 / 864	CGGGGTACCCATTTAATAC ACACACTTGTATGT	CATGCCATGGACCTCGCT CTTTATTTTATCTG	CCGCTCGAGTGATTCGT TTAAAATCGATGGAT	CCGGAATTCATGCAATA ATAATAGTTCAATCA	TATTGTAGCAATTAGAT GGGAAAA	AAACTTTTCCCATCTAATT GCTAC
odc50a	PY17X_0619700	1397 / 1397	CGGGGTACCTACGAAATAA ATACATGCTAAT	CATGCCATGGACTATGTAC ATTTTTTTATGACCCA	CATGCCATGGGCTCCAA AAAAGGGGGGAAAAG	CCGGAATTCCGAATTTT TATTTATTTTAAAATATG	TATTGGAATTTTATATTT AATAAT	AAACATTATTAAATATAAA ATTCC
odc50b	PY17X_0916600	1122 / 1122	CGGGGTACCAGATCGAAC AAGTTGAGCATT	CATGCCATGGATATATTAT TAACATTTATCAGAAC	CATGCCATGGGACGAAT AAATTAACATAATATA	CCGCTCGAGTCACTAT GCAAATTGTACACTC	TATTGGTAATGGGCTTG GAAATGG	AAACCCATTTCCAAGCCC ATTACC
isp1	PY17X_1212600	1021 / 1021	CATGCCATGGGAAATATAT GATACATTAGCATAACATG A	CCGGAATTCCCCATTTTGT CGTTATCTGAT	CCGGAATTCGCCAAATTA ATAAATATTTGCTTTATC	CCCCTTAAGTGTTTCTA TAGACATATTCTCCTAT T	TATTGCGTTACATTTAG ATGATAG	AAACCTATCATCTAAATGT AACGC
odpk3	PY17X_0410700	1671 / 1099	CGGGGTACCACTATGTGA TTTACCAATGATT	CATGCCATGGGTTCTACAC ACAACTGATTCAT	CCGCTCGAGAGTAAATT CGTAATGTGGGTACA	CCGGAATTCTGCTTTCT GTCTAATGCTGCC	TATTGCAGTAGCAGTAG ATATGTT	AAACAACATATCTACTGC TACTGC
pdeδ	PY17X_1338400	3069 / 649	CGGGGTACCACTTATTAGT ATGTATATTTTAAGCG	CATGCCATGGACGAATAAT CCCAATTTCTTCCT	CCGCTCGAGGAGAGATC ATGCTAAGTGGACA	CCGGAATTCCCATGTTT TTAAATTTACATTTAAAT TG	TATTCGTTTATAGATTCT GAGTA	AAACTACTCAGAATCTAT AAACGA

Primers for PCR-genotyping parasite with gene knockout

Gene name	Gene ID	P1	P2	P3	P4	P5	P6	
gcβ	PY17X_1138200	GTCTACACCTGACTGGA CATA	ATGCAATAATAATAGTTCAA TCA	ATGGAGGCTTAATATTGGG T	TAATTCTTAATGTATATAA AAGTATAGACA	GTCTACACCTGACTGG ACATA	TGCGTCGAGTGATATCA AC	
odc50a	PY17X_0619700	GGTCATTCTAATGTTATA AGA	GAAATGTTATTGCATATCC ACC	CAAGACGATTCCTCTATAT GTATGC	TCTACATAATAAAAGCAT CGC	CACATTGTGTCTTATTT ACAACC	TCTACATAATAAAAGCA TCGC	
odc50b	PY17X_0916600	AATTTCCCTTTGGGGTTT CAC	ACATGTTAATATTTATCCGA ATGGA	TGTGTGATTATACAATTGC TTATGA	GGAAATATATTACAAAAC ATAGTG	GGAAATATATTACAAAA CATAGTG	TGGATGATACCATCACC ATTTAG	
isp1	PY17X_1212600	AATAATATTATAGAGCAA TTTAAAATAG	ATAATAGTAGTAGTAGTAG TAATAGCA	CAGATAACGACAAAATGG GG	GTGCTTATTCTTTTGGAG TTAGTCA	AATAATATTATAGAGCA ATTTAAAATAG	AAACCATATTATCTACTA ATATAC	
odpk3	PY17X_0410700	AGGGAAGTAACCTAATT TGC	GTCAATAGTGAGACATCGC T	TGATTTTACATCCTTTAGTT CGT	AAACTCATTGTTCTTGTC AACTTC	AGGGAAGTAACCTAAT TTGC	TATTGCAGTAGCAGTAG ATATGTT	
pdeδ	PY17X_1338400	GGTACTACCATACTAATT CTGCTAA	CTAAATTCTTGTAATAATCT GTTC	CTAAATTCTTGTAATAATCT GTTC	CATTTTGCAAATAGCTTA TGAAGCAG	GGTACTACCATACTAAT TCTGCTAA	TAAATGACAGACTGTTG CTCCA	

Oligo sequences for gene tagging plasmid construction

Gene name	Tag	Gene ID	Left homologous arm		Right homologous arm		Target site of sgRNA	
			Forward primer	Rerverse primer	Forward primer	Reverse primer	Oligo (Forward)	Oligo (Reverse)
gcβ	C-terminal 6HA	PY17X_1138200	CGGGGTACCTGGATGTAT TGATAGCAAATCA	CATGCCATGGACACATTTA CTTTATTTTTTTCTCGA	CCGGAATTCATTTCATTG ATATATTACATAACAT	CCCCTTAAGGTTGTGTT GGAATATTAAGAACAT	TATTGTCTCGTAGTTTAT AATTTT	AAACAAAATTATAAACTAC GAGAC
gcβ	inter-domain 6HA/	PY17X_1138200	CGGGGTACCATCGAATCG ATATTTGCTTCA	CATGCCATGGTTCTCTTAT TATATAACTTTTGGGGA	CCGCTCGAGGACAATGC ATATTATGGGAAATC	CCCCTTAAGTCTGCTGT TTACATATACACG	TATTTATAACTTTTGGG GACAGGA	AAACTCCTGTCCCCAAAA GTTATA
gcβ	N-terminal 6HA	PY17X_1138200	CGCGGATCCATTTAATACA CACACTTGTATGTTTAAG	CTAGCTAGCTTTTGTATTT AGCCATTAACAAAAAATAT AATATTCAAAATTATG	CCGCTCGAGAAGGAAAC AGATAAAATAAAGAGCG AG	CCCCTTAAGCAAAAGC GAAATAGCTGTATCT	TATTAATATTATATTTTTT GTTAA	AAACTTAACAAAAAATATA ATATT
gcβ	C-terminal mScarl	PY17X_1138200	CGGGGTACCTGGATGTAT TGATAGCAAATCA	CATGCCATGGACACATTTA CTTTATTTTTTTCTCGA	CCGGAATTCATTTCATTG ATATATTACATAACAT	CCCCTTAAGGTTGTGTT GGAATATTAAGAACAT	TATTGTCTCGTAGTTTAT AATTTT	AAACAAAATTATAAACTAC GAGAC
gcα	C-terminal 6HA	PY17X_0911700	CGGGGTACCGTGTATACC AAATTTAAATATGAGA	CATGCCATGGGCAAAATTG AACTTGTGTCTTTGGA	CCGCTCGAGTACTTTTA GAACTTTCTAATTTATG	CCGGAATTCCCATGTA CTGTGAACATATCA	TATTATAGTTTTCTAAAT GTTGGA	AAACTCCAACATTTAGAA AACTAT
pdeδ	N-terminal 4Myc	PY17X_1338400	CGGGGTACCAGACCCAA ATAATTTCAATGGA	CATGCCATGGTCGCTTATT TTTCTTTTCTTTTTTTTTTT TTCA	CCGCTCGAGTTTGTTTAT AATATCTTTGTATACAT	CCGGAATTCTATTCTAC AGTATTATTGAGGCGT	TATTGAAAAACAACAATT GCTAAG	AAACCTTAGCAATTGTTG TTTTTC
pkg	N-terminal 4Myc	PY17X_1009800	CGCGGATCCAGAAATAAAA TTACAACATAATGATAGAT	CTAGCTAGCTTTTATTATCT TCCAATCTCGTTAACTTTA	CCGCTCGAGGATGATGA TGAAATAATTCCAAAGA	CCGGAATTCATCCCTC AATTCTAGGTGGT	TATTACATAAAGTATGTT TTTGAG	AAACCTCAAAAACATACT TTATGT
mtip	C-terminal 4Myc	PY17X_1462100	CGGGGTACCGTCAAATATC AGGAGAAGAT	CATGCCATGGTTGCAATAT ATCCTCGCAAA	CCGCTCGAGGCAATTGT GATTTAATATGTG	CCCCTTAAGCAAATATG TGCATATACCATG	TATTGAATCAGAAGAAT CTGAACA	AAACTGTTCAGATTCTTC TGATTC
ara1	C-terminal 4Myc	PY17X_1412750	CGGGGTACCTGTAGGTAG CTATTTAGTT	CATGCCATGGTATTATTAT GGTTTTTCCTCCTATTGG	CCGCTCGAGAACATTGA AAATTTACAGTT	CCCCTTAAGGCTCATAT TCATCCACGATA	TATTGTTTTTATTTCTAA TCCAAT	AAACATTGGATTAGAAAT AAAAAC
myosinb	C-terminal 4Myc	PY17X_0931400	CGGGGTACCGGTTTTTCCT CAGCTTTTTTC	CATGCCATGGTTCGAGCT CTTTCATATATTTG	CCGCTCGAGGTAAGAAA CTGATATTTTG	CCCCTTAAGCAATTAAC CTTTACTCCACTC	TATTGAAATTAACAGATA AGGAAA	AAACTTTCCTTATCTGTTA ATTTC
soap	C-terminal 4Myc	PY17X_1040200	CGGGGTACCGAAATGTAG TAAGCGCATATC	CATGCCATGGACAATAACA TGAACAGCTAC	CCGCTCGAGTTATGCAT AAACACTGTAT	CCCCTTAAGTGCTCCA AAAATATGAATGC	TATTGATAATAATGACAT TGATAA	AAACTTATCAATGTCATTA TTATC
dhhc10	C-terminal 4Myc	PY17X_0513100	CGGGGTACCGTATGCCCA TTTAATAGCTAGC	CATGCCATGGTAATGTTTT ATAAAATAGTCCATTCCC	CCGCTCGAGATCACATTT TTGTGTTGGA	CCCCTTAAGACAAGTT GCATATGCAGTT	TATTGGAAAACTTTAAG CAAGTTT	AAACAAACTTGCTTAAAG TTTTCC
mpodd	C-terminal 4Myc	PY17X_1225400	CCCAAGCTTGGAGAAATG CTCTAAACACA	CATGCCATGGTATCAGGG ATACGGTATATA	CCGGAATTCAAAATGGA CAAAATGATGAA	CCCCTTAAGTGGAATG GTAAAGGAGTCTC	TATTTTGTTGGTTCAAT GCTGTAA	AAACTTACGCATTGAACC AACAA
odc50a	C-terminal 6HA	PY17X_0619700	CGGGGTACCAACCCAAAC GACGTTTC	CATGCCATGGGTATGTGG CCCATGATCCGAG	CCGCTCGAGCTCCAAAA AAGGGGGGAAAAGAGG	CCGGAATTCGAAAAGG AAATACCAAATTGGGT	TATTGGAATTTTATATTT AATAAT	AAACATTTATTAAAATAAA AATTCC
odc50a	C-terminal mCher	PY17X_0619700	CCCAAGCTTACGAACCCAA ACGACGTTTC	CGCGGATCCTATGTGGCC CATGATCCGAG	CCGCTCGAGCTCCAAAA AAGGGGGGAAAAGAGG	CCGGAATTCGAAAAGG AAATACCAAATTGGGT	TATTGGAATTTTATATTT AATAAT	AAACATTATTAAATATAAA ATTCC
odc50a	C-terminal 3V5	PY17X_0619700	CGGGGTACCAACCCAAAC GACGTTTC	CATGCCATGGGTATGTGG CCCATGATCCGAG	CCGCTCGAGCTCCAAAA AAGGGGGGAAAAGAGG	CCGGAATTCGAAAAGG AAATACCAAATTGGGT	TATTGGAATTTTATATTT TAATAAAT	AAACATTTATTAAAATAAA AATTCC
odc50a	C-terminal mScarl	PY17X_0619700	CGGGGTACCAACCCAAAC GACGTTTC	CATGCCATGGGTATGTGG CCCATGATCCGAG	CCGCTCGAGCTCCAAAA AAGGGGGGAAAAGAGG	CCGGAATTCGAAAAGG AAATACCAAATTGGGT	TATTGGAATTTTATATTT TAATAAAT	AAACATTTATTAAAATAAA AATTCC
odc50b	C-terminal 6HA	PY17X_0916600	CGGGGTACCTTAGGAGGG AAAATAGTTGTATC	CATGCCATGGTTCGTCAAC TTGTCGCATAAAT	CCGCTCGAGATTAACATA ATATATAATTTATACATTA TTCC	CCGGAATTCGATAAAT GATTAAACATTTTATG	TATTGTTTATAGAATTGC TCTTAG	AAACCTAAGAGCAATTCT ATAAAC
odc50c	C-terminal 6HA	PY17X_0514500	CGGGGTACCGGTTAAATAT GTTTTCTCCTGAAT	CATGCCATGGATGCAGTG GGCAAATGCACA	CCGGAATTCCCAAATAA GCATGCACACCCAA	CCCCTTAAGGCATTCTT TTTGCATTTAAAATTG	TATTGCTTATTTGGTCA ATGCAGT	AAACACTGCATTGACCAA ATAAGC
imc1f	C-terminal 4Myc	PY17X_1370200	CGGGGTACCTAAATGAAAT TATTGTCAAAGGCAGA	CATGCCATGGTGTACACAT ATCACCACTAAAAGAATAA T	CCGGAATTCGGAAATGA ATGATTTTTTAGTTCATG	CCCCTTAAGTAATTGAG TGTATACACATATTATT ATCT	TATTGGTAGCAATTATT CTTTTAG	AAACCTAAAAGAATAATT GCTACC
imc1g	C-terminal 4Myc	PY17X_1243800	CGGGGTACCACAAAGAAC GAATTGTTCATGTAC	CATGCCATGGGTTACAGTA AAAACCTCTATTAACTAC	CCGGAATTCATTTAAGAA GGTAATCATGATGTTATA T	CCCCTTAAGTGCACAC ACAAAAAATAGCGTA	TATTGTTTTGGAAATTCT TATTTT	AAACAAAATAAGAATTTC CAAAAC
imc1i	C-terminal 4Myc	PY17X_0707400	CGGGGTACCTGCAAATATT TCTCATGATAATAACA	CATGCCATGGTTCACCACC ACAACATTTATTCAT	CCGGAATTCTCATATATT AAGTAAATAAATAACTAT	CCCCTTAAGTGCAAAG TTCTATTACATATTTCAA	TATTGATTTGAATTTTCT TGGCTT	AAACAAGCCAAGAAAATT CAAATC
imc1j	C-terminal 4Myc	PY17X_1121700	CGGGGTACCATGAATAAAT GTATGAATATATAACT	CTAGCCATGGTGCATTGTT TATTTTCCATTGTCT	CCGCTCGAGACAAGTAG ATATAGTAAAGTATGAAT G	CCGGAATTCGGTCAAT ATCGTCAGATCCACT	TATTGATCATATGGGTT ATGAAAA	AAACTTTTCATAACCCATA TGATC
imc1k	C-terminal 4Myc	PY17X_1360600	CGGGGTACCAAATACCAAA ATATGTAGATGAAGT	CATGCCATGGAGAATTTAC GCCAATGAGCA	CCGGAATTCAAAATACAC ATACACATATATGTGC	CCCCTTAAGACTGTGC AAATTAACAAAAATATTT C	TATTGATATGCTATTACA TGGATA	AAACTATCCATGTAATAG CATATC

imc1l	C-terminal 4Myc	PY17X_1028100	CGGGGTACCACCCTAATATATATCAATGAAGGT	CATGCCATGGTTTCTTTTTTTTAACAATAAGTTCTGC	CCGGAATTCATATGTTTAATTAAATTTTAGTTAATATATGC	CCCCTTAAGTGAAGACCTTACATACATATAATGA	TATTATTATTATTGGAGTTATAAT	AAACATTATAACTCCAATAATAAT
imc1m	C-terminal 4Myc	PY17X_0514100	CGGGGTACCTGCATCAAATGATAGAAGAAC	CATGCCATGGTATTTTTTCGTCTGCCTTGTTAAGGT	CCGGAATTCTTTAAATAAGGGGAAACATAGTTCG	CCCCTTAAGGATAATAAGACCTTTACTATGTG	TATTGCAGGTAAATTGGGTATATA	AAACTATATACCCAATTTACCTGC
alvx	C-terminal 4Myc	PY17X_1240600	CGGGGTACCGAGGAGACGCAACTCTTGTAG	CATGCCATGGAAAAACGTAGGTGTTTTCAACACTATT	CCGGAATTCCAGTGATCATTGAAATAATATAACA	CCCCTTAAGCATTAAAACACATGGATAGTGCA	TATTGTTGTTCCTAACAATGACAT	AAACATGTCATTGTTAGGAACAAC
isp1	C-terminal 6HA	PY17X_1212600	CGGGGTACCCAACAGAATAATGATAACAT	CATGCCATGGATTTTTTTTATAATCTCTCAT	CCGGAATTCGCCAAATTAATAAATATTTGCTTTATC	CCCCTTAAGTGTTTCTATAGACATATTCTCCTATT	TATTCCATTCCATTAAATTATATA	AAACTATATAATTTAATGGAATGG
isp1	C-terminal 3V5	PY17X_1212600	CGGGGTACCCAACAGAATAATGATAACAT	CATGCCATGGATTTTTTTTATAATCTCTCAT	CCGGAATTCGCCAAATTAATAAATATTTGCTTTATC	CCCCTTAAGTGTTTCTATAGACATATTCTCCTATT	TATTCCATTCCATTAAATTATATA	AAACTATATAATTTAATGGAATGG
isp3	C-terminal 6HA	PY17X_1328100	CGGGGTACCTGGGAAACAGCTTGTGCTGC	CATGCCATGGAGCAGTTAAGCAATATTTGT	CCGCTCGAGGCACAGAAAATAATAATTCACAC	CCGGAATTCGACAAATAATAAGGATAGGA	TATTTGGATAGATAAATATAAGAA	AAACGGCTTATATTTATCTATCC
Primer sequence for PCR-genotyping parasite with gene tagging								
Gene name	**Tag**	**Gene ID**	**P7**	**P8**	**P9**	**P10**		
gcβ	C-terminal 6HA	PY17X_1138200	CGTGTGTTGGAGGAATTATAGGA	TTCCTCATGCCGATGAATATGT	GGTAAAGCTTATAAAATAGTGAT	TCCAAAAATTATAAACTACGAGAC		
gcβ	Inter-domain 6HA	PY17X_1138200	GAGAAGAAAATATTATCTTAACAACAC	AGATTTCCCATAATATGCATTG	TTCATAAATAGACAAATTAATGTAAAACT	GGTTCCTGTCCCCAAAAG		
gcβ	N-terminal 6HA	PY17X_1138200	CACTGGTCTACACCTGACTGGAC	ATTTAAAACCTCGCTCTTTATTTTTATC	TAATTCTTAATGTATATAAAAGTATAGAC	ATTTAAGCTCAAAAAGACTTTCTATAAC		
gcβ	C-terminal mScarl	PY17X_1138200	CGTGTGTTGGAGGAATTATAGGA	TTCCTCATGCCGATGAATATGT	GGTAAAGCTTATAAAATAGTGAT	TCCAAAAATTATAAACTACGAGAC		
gcα	C-terminal 6HA	PY17X_0911700	TTAGAAATGGCATATTCAATG	CCATGTACTGTGAACATATCA	GTGTATACCAAATTTAAATATGAGA	ATGAAATTAATTTCCAAAATGGA		
pdeδ	N-terminal 4Myc	PY17X_1338400	TGAAAGGAACAGATTATTACAAGA	AGTTCAAAATAAAAAGGAGAAACA	GACACTGGTAAGTCTCGTTTTTGG	CCCCTTTCCTGGTATCTCTTTTC		
pkg	N-terminal 4Myc	PY17X_1009800	CTTTGTATACATTTTTTGTAATCCTGT	ATACATGTGCATATGTAGCAA	GTGACGATATCTTCTGCTAA	GAAAAACTTTATTAAAGGATTTAATTGTGC		
mtip	C-terminal 4Myc	PY17X_1462100	GGGGACCCGGTTTTGAATGG	CAAATATGTGCATATACCATG	GTCAAATATCAGGAGAAGAT	CCTATTCATTCTTTTTAATTCG		
ara1	C-terminal 4Myc	PY17X_1412750	GGAAAAAATGTATGCACAAAC	GCTCATATTCATCCACGATA	TGTAGGTAGCTATTTAGTT	ATCCATTTGAAAACCGTAG		
myosinb	C-terminal 4Myc	PY17X_0931400	CGGACAACAAGTTAGTGAAAAG	CAATTAACCTTTACTCCACTC	GGTTTTTCCTCAGCTTTTTTC	GCGGCAAAAATATATATGCAC		
soap	C-terminal 4Myc	PY17X_1040200	CATTGTCTACATATTCCTCTCT	TGCTCCAAAAATATGAATGC	GAAATGTAGTAAGCGCATATC	TGCTATTTTATCGTAGGGCGT		
dhhc10	C-terminal 4Myc	PY17X_0513100	CCTAGAAATTGTTTTATCGGCTG	ACAAGTTGCATATGCAGTT	GCCTTGGATATATGTATATGC	GCCTTGGATATATGTATATGC		
mpodd	C-terminal 6HA	PY17X_1225400	GAAGAGAGAAATTTGGAAT	CTATGAACTAGTAGTAATTG	CCTATGCTTAATGATAGTTC	GTTAACTAAGGATAACATCG		
odc50a	C-terminal mCherr	PY17X_0619700	TACCACTTCAACATGTCTGCATC	GAAATGTTATTGCATATCCACC	CACATTGTGTCTTATTTACAACC	TCTACATAATAAAAGCATCGC		
odc50a	C-terminal 3V5	PY17X_0619700	TACCACTTCAACATGTCTGCATC	GAAATGTTATTGCATATCCACC	CACATTGTGTCTTATTTACAACC	TCTACATAATAAAAGCATCGC		
odc50a	C-terminal mScarl	PY17X_0619700	TACCACTTCAACATGTCTGCATC	GAAATGTTATTGCATATCCACC	CACATTGTGTCTTATTTACAACC	TCTACATAATAAAAGCATCGC		
odc50a	C-terminal 6HA	PY17X_0619700	TACCACTTCAACATGTCTGCATC	GAAATGTTATTGCATATCCACC	CACATTGTGTCTTATTTACAACC	TCTACATAATAAAAGCATCGC		
odc50b	C-terminal 6HA	PY17X_0916600	GTCTATACTTTATTATATGAG	TCCGTCTATATTGCAACCACA	GAATGGAATAATGTATAAAT	TATGGAGTACAACAAAATCATTAT		
odc50c	C-terminal 4Myc	PY17X_0514500	CAACATTCTACAATATTTAAGTGA	GATATTTATTAATTATGATGTATGTGAAG	TGTATGCATAGAGATGGGTAATGAT	CTTATATTGTACATAAATATAATGTGCA		
imc1f	C-terminal 4Myc	PY17X_1370200	AAGGCAGCAATAACAATGGCA	ACCACTTAACATATTATAATATTTCTGA	ACATATGTTGTTGAATATTTAGGAGA	ATGTAAAAATGTTTGAATATCTCAGT		
imc1g	C-terminal 4Myc	PY17X_1243800	TAAAACTATTGAAAAGGTTGTCGA	ATATATAACATCATGATTACCTTCT	GAATTTCCAAAACCCCAAACGT	GCACACACCTTAAAATTATATAGGT		
imc1i	C-terminal 4Myc	PY17X_0707400	AAGTCTCTCATGAATCCGTTGA	TATTCTATATGCATACATTCATATAGT	ATCTAGATTTTGCAACATAATGA	TTAGATAAAAATACTTATAAAAGTCTCT		
imc1j	C-terminal 4Myc	PY17X_1121700	GTTAATTTTATAGATTGTATAATAG	AATGTACTTCAGGATATGGTACT	TTCAATAGTTGGACTAACTGGAC	CATACACCCTTTTGTAAGCACG		
imc1k	C-terminal 4Myc	PY17X_1360600	GTTGAAAGAGAAGTTGTTGTTGA	GTGCAATATGCACATATATGT	TAAGTACTGATCCCAGCTCT	TATTTTAAATTTATGGCATATTTATGA		
imc1l	C-terminal 4Myc	PY17X_1028100	GCCTGATCAAAATATTATTAATCCT	AAAGGGTGTATATGCATATATTAACT	ATAACTCCAATAATAATAGTGTAGCA	TAAGAGCATGTGTGATTTAATTAGT		
imc1m	C-terminal 4Myc	PY17X_0514100	GCATATACAAGAGAATTACCACT	GTGCGTTGTTTACATGATTC	GGACATAAAGAAATGAACAAG	CGTTCAACTGTGTACTTATCT		
alvX	C-terminal 4Myc	PY17X_1240600	CATATATATAAAACCCCATTACCACAT	ACATGCTGCAATAGTAGCATATG	GGCATATATAACGAATGCGTGA	ATATAATGCTTATACATTACCTTATGA		
isp1	C-terminal 6HA	PY17X_1212600	GCATACGTTACAATTTTGAG	CGAAATTGAGCATGTAAAATA	CGTTACATTTAGATGATAGT	GTGCTTATTCTTTTGGAGTTA		
isp1	C-terminal 3V5	PY17X_1212600	GCATACGTTACAATTTTGAG	CGAAATTGAGCATGTAAAATA	CGTTACATTTAGATGATAGT	GTGCTTATTCTTTTGGAGTTA		
isp3	C-terminal 6HA	PY17X_1328100	TTCGATACGCACTTTACACAC	CACCACTTGGACACCATTGTAA	CCTGGAGAGGAAAGAATGTT	ATTGGATATAATACATGCTG		
Oligo sequences for gcβ modification plasmid construction								
Modification	**Discription**	**Left homologous arm**		**Right homologous arm**		**Target site of sgRNA**		
		Forward primer	**Reverse primer**	**Forward primer**	**Reverse primer**	**Oligo (Forward)**	**Oligo (Reverse)**	
gcβT2A	T2A inserted between 1248E/1249D	CGGGGTACCATCGAATCGATATTTGCTTCA	CATGCCATGGTTCTCTTATTATATAACTTTTGGGGA	CCGCTCGAGGACAATGCATATTATGGGAAATC	CCCCTTAAGTCTGCTGTTTACATATACACG	TATTTATAACTTTTGGGGACAGGA	AAACTCCTGTCCCCAAAAGTTATA	
gcβT2Am	T2Am inserted between1248E/1249D	CGGGGTACCATCGAATCGATATTTGCTTCA	CATGCCATGGTTCTCTTATTATATAACTTTTGGGGA	CCGCTCGAGGACAATGCATATTATGGGAAATC	CCCCTTAAGTCTGCTGTTTACATATACACG	TATTTATAACTTTTGGGGACAGGA	AAACTCCTGTCCCCAAAAGTTATA	
gcβT2An	T2An inserted between1248E/1249D	CGGGGTACCATCGAATCGATATTTGCTTCA	CATGCCATGGTTCTCTTATTATATAACTTTTGGGGA	CCGCTCGAGGACAATGCATATTATGGGAAATC	CCCCTTAAGTCTGCTGTTTACATATACACG	TATTTATAACTTTTGGGGACAGGA	AAACTCCTGTCCCCAAAAGTTATA	
Oligo sequences for gcβ nucleotide replacement plasmid construction								
Modification	**Discription**	**Homologous arm**		**Target site of sgRNA**		**site mutation**		
		Forward primer	**Reverse primer**	**Oligo (Forward)**	**Oligo (Reverse)**	**Forward primer**	**Reverse primer**	
GCDm1	NTASR(1690-1694) replaced with NKASR	CGGGGTACCGTGACAATCCATATACTATCCT	CATGCCATGGGGCGAGGTAAAGAAATCATCAG	TATTGAATCATATTTAGCTGCATC	AAACGATGCAGCTAAATATGATTC	ACCACAATATTCGCTGTTTGGTGATACTGTTAACAAAGCTTCTAGAATGAAGTCTACTTCGTTAAAG	TCCTTTAACGAAGTAGACTTCATTCTAGAAGCTTTGTTAACAGTATCACCAAACAG	
GCDm2	AKASA(1690-1694) replaced with NKASR	CGGGGTACCGTGACAATCCATATACTATCCT	CATGCCATGGGGCGAGGTAAAGAAATCATCAG	TATTGAATCATATTTAGCTGCATC	AAACGATGCAGCTAAATATGATTC	ACCACAATATTCGCTGTTTGGTGATACTGTTGCCAAAGCTTCTGCAATGAAGTCTACTTCGTTAAAG	TCCTTTAACGAAGTAGACTTCATTGCAGAAGCTTTGGCAACAGTATCACCAAACAGCGA	
Primer sequence for PCR-genotyping prarsite with gcβ modification								

Modification	P7	P8	P9	P10			
gcβT2A	GAGAAGAAAATATTATCTTAACAACAC	AGATTTCCCATAATATGCATTG	TTCATAAATAGACAAATTAATGTAAAACT	GGTTCCTGTCCCCAAAAG			
gcβT2Am	GAGAAGAAAATATTATCTTAACAACAC	AGATTTCCCATAATATGCATTG	TTCATAAATAGACAAATTAATGTAAAACT	GGTTCCTGTCCCCAAAAG			
gcβT2An	GAGAAGAAAATATTATCTTAACAACAC	AGATTTCCCATAATATGCATTG	TTCATAAATAGACAAATTAATGTAAAACT	GGTTCCTGTCCCCAAAAG			
gcβGCDm1	AATGAGCCTAATTATTTTATCCATAG			GTATGTCTTGTTTGATGTATCAC			
gcβGCDm2	AATGAGCCTAATTATTTTATCCATAG			GTATGTCTTGTTTGATGTATCAC			
Primers for RT-PCR							
Gene name	**Gene ID**	**Forward Primer**	**Reverse Primer**				
18s Rrna	PY17X_0522400	GGTTTTATAATTGGAATGATGGGAAT	ACGCTATTGGAGCTGGAATTACC				
cdc50a	PY17X_0619700	ATGCTTCTTGCTACTAATCCAC	AAGGTCCTAAAAGGCCAT				
gcβ	PY17X_1138200	ATTAGGGTATTTCAAGGTGAAG	AGGCAATTCACATTTGATAACA				
Primers for plasmid complementation							
Gene name	**Gene ID**	**CDS**		**5'UTR**		**3'UTR**	
		Forward Primer	**Reverse Primer**	**Forward Primer**	**Reverse Primer**	**Forward Primer**	**Reverse Primer**
Pycdc50a	PY17X_0619700	CATGCCATGGATGGAAGGAAAAAAAGAAAAAAAAG	CATGCCATGGCTATATGTGGCCCATGATCCG	CGGGGTACCCATAAGGTAACAAAAGAAGATG	CATGCCATGGACTATGTACATTTTTTTATGACC	CCGCTCGAGCTCCAAAAAAGGGGGGAAAAG	CCCCTTAAGGATGTAAAACTGTGGATTTCGCG
Pfcdc50a	PF3D7_0719500	CATGCCATGGTGAAAGAAACGATGA	CATGCCATGGCAAAAAAAAGAAAATATATATG	CGGGGTACCCATAAGGTAACAAAAGAAGATG	CATGCCATGGACTATGTACATTTTTTTATGACC	CCGCTCGAGCTCCAAAAAAGGGGGGAAAAG	CCCCTTAAGGATGTAAAACTGTGGATTTCGCG
Pyisp1	PY17X_1212600	CATGCCATGGATGGGGAATATTGTATCCTG	CTAGCTAGCATTTTTTTTATAATCTCTCA	GCGGGATCCTGTCTAAAGGAAGAGCTTGT	CATGCCATGGTTTGTCGTTATCTGATTATCTT	CTAGCTAGCAAAATTGATAAGTTAACAGC	CCCCTTAAGCGACGAATGTATGGCCCTACAT
Pfisp1	PF3D7_1011000	CATGCCATGGATGGGGAATATTGTATCATG	CTAGCTAGCCGAATTTTTTTTATAATCTT	GCGGGATCCTGTCTAAAGGAAGAGCTTGT	CATGCCATGGTTTGTCGTTATCTGATTATCTT	CTAGCTAGCAAAATTGATAAGTTAACAGC	CCCCTTAAGCGACGAATGTATGGCCCTACAT
Peimers for gene in situ complementation							
Gene name	**Tag**	**Gene ID**	**CDS**		**Left homologous arm**		**Right homologous arm**	
			Forward primer	**Rerverse primer**	**Forward primer**	**Reverse primer**	**Forward primer**	**Reverse primer**
Pycdc50a	N-terminal Flag	PY17X_0619700	CATGCCATGGCTACTTATCGTCGTCATCCTTGTAATCTATGTGGCCCATGATCCGA	CATGCCATGGATGGAAGGAAAAAAAGAAAAAA	CGGGGTACCTACGAAATAAATACATGCTAAT	CATGCCATGGACTATGTACATTTTTTTATGACCCA	CATGCCATGGGCTCCAAAAAAAGGGGGGAAAAG	CCGGAATTCCGAATTTTTATTTATTTTAAAATATG

Data S1 Genotyping data of the genetic modified parasite strains in this study

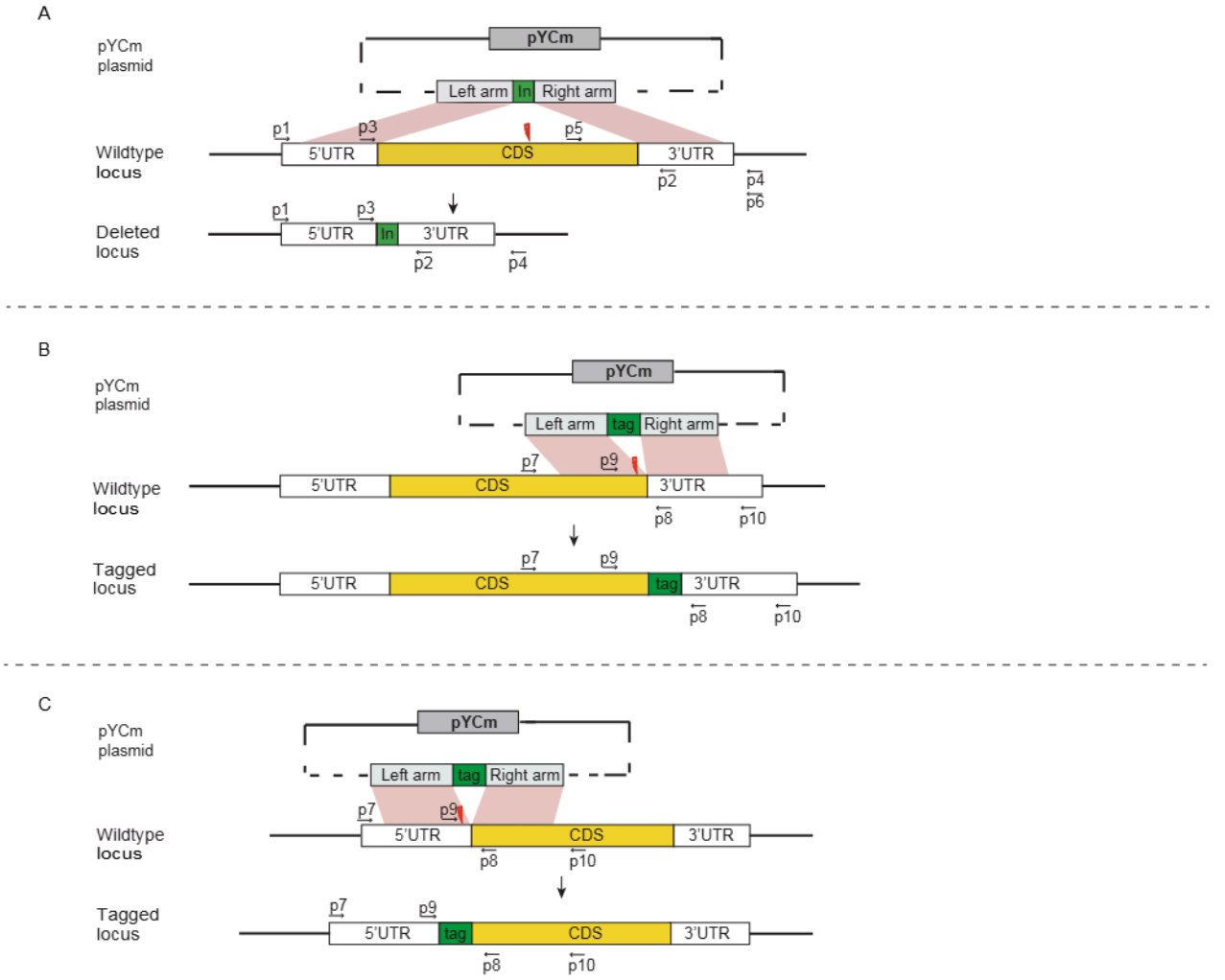

D Parasite clones with modification in *gcβ, gcα, pkg, and pdeδ* loci

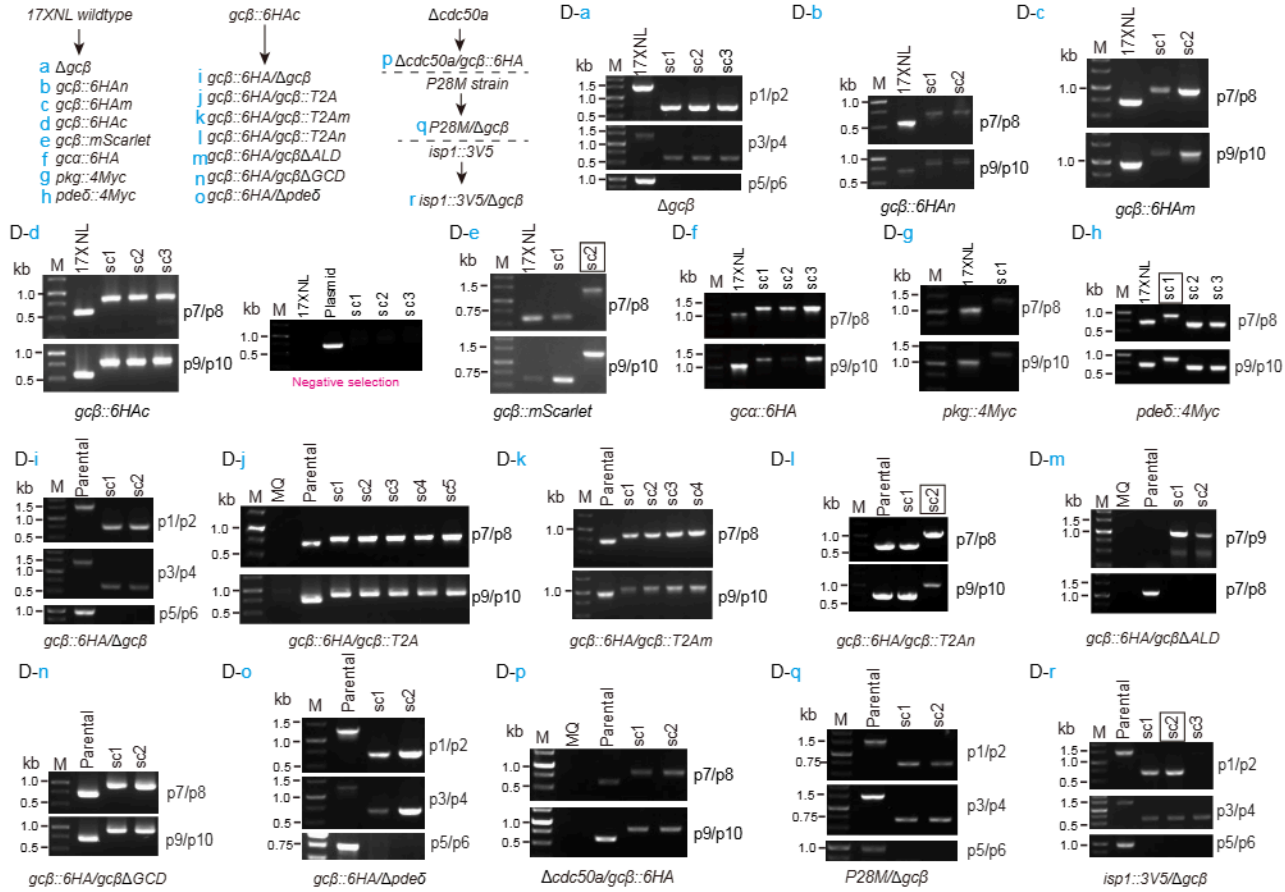

Data S1. Genotyping results of the genetic modified parasite strains in this study

(A) Schematic representation for CRISPR/Cas9 mediated gene deletion via double cross homologous recombination. **(B and C)** Schematic representation for CRISPR/Cas9 mediated N-terminal **(B)** or C-terminal **(C)** tagging of endogenous genes with epitope tag or fluorescence protein via double cross homologous recombination. Primers used for diagnostic PCR are indicated and listed in the SI Table S2. **(D to J)** For each modification, both the 5' and 3' homologous recombination was detected by diagnostic PCR, confirming successful integration of the homologous templates. For most modification, at least two single clones (sc) with targeted modifications were obtained after limiting dilution and were used for phenotype analysis.

H Parasite clones with double gene deletion among either *gcβ*, *50a*, *pdeδ*, and *cdpk3*

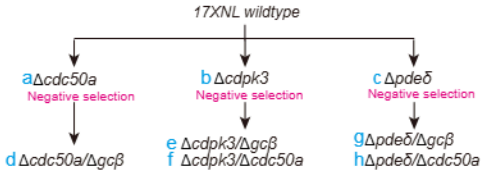

H-a

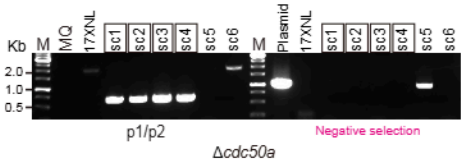

H-b

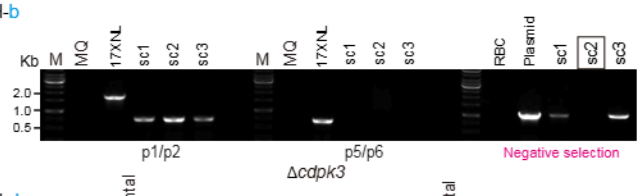

H-c

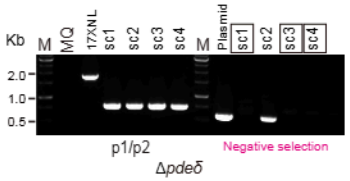

H-d

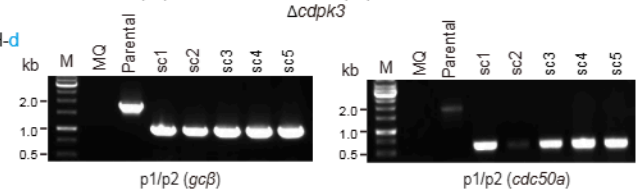

H-e

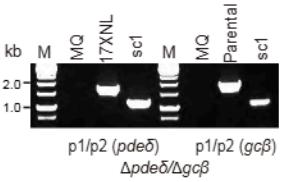

H-f

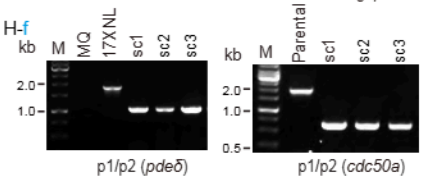

H-g

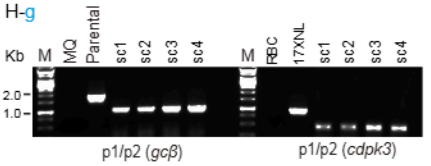

H-h

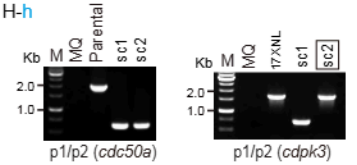

I Parasite clones with gene tagging of IMC proteins

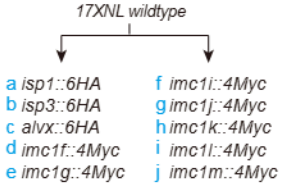

I-a

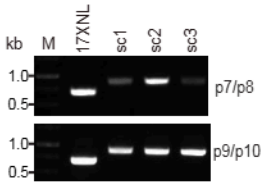

I-b

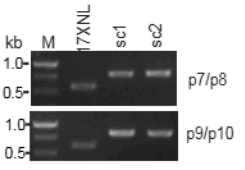

I-c

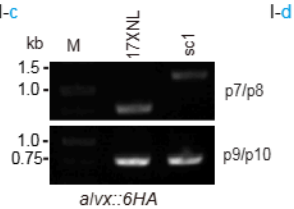

I-d

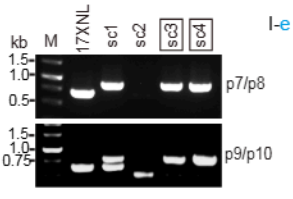

I-e

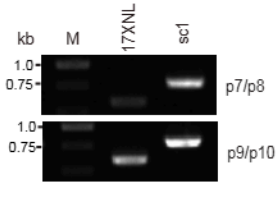

I-f

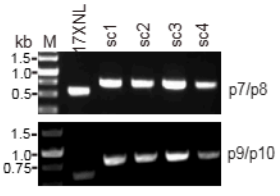

I-g

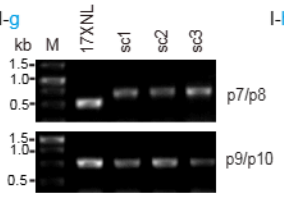

I-h

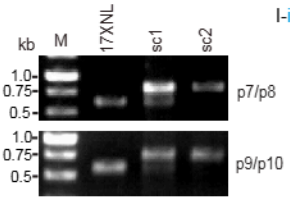

I-i

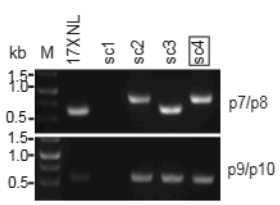

I-j

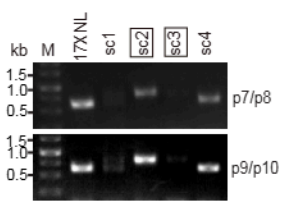

J Parasite clones with modification in *isp1* locus

J-a

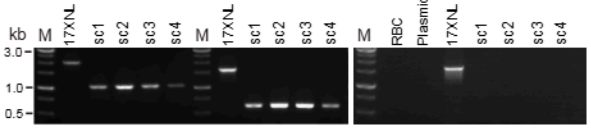

J-b

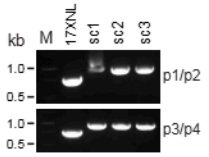

J-c